



Interestuarine comparison: Hydro-geomorphology

Hydro- and geomorphodynamics of the TIDE estuaries Scheldt,
Elbe, Weser and Humber

Vandenbruwaene, W.; Plancke, Y.; Verwaest, T.; Mostaert, F.

February 2013

WL2013_770_62b_rev4_0



European Union



The European Regional Development Fund

This publication must be cited as follows:

Vandenbruwaene, W.; Plancke, Y.; Verwaest, T.; Mostaert, F. (2013). Interestuarine comparison: Hydro-geomorphology: Hydro- and geomorphodynamics of the TIDE estuaries Scheldt, Elbe, Weser and Humber. Version 4. WL Rapporten, 770_62b. Flanders Hydraulics Research: Antwerp, Belgium.



Waterbouwkundig Laboratorium

Flanders Hydraulics Research

B-2140 Antwerp

Tel. +32 (0)3 224 60 35

Fax +32 (0)3 224 60 36

E-mail: waterbouwkundiglabo@vlaanderen.be

www.watlab.be

Nothing from this publication may be duplicated and/or published by means of print, photocopy, microfilm or otherwise, without the written consent of the publisher. The authors are solely responsible for the content of this report. Material included herein does not represent the opinion of the European Community, and the European Community is not responsible for any use that might be made of it.

Documentidentification

Title:	Interestuarine comparison: Hydro-geomorphology: Hydro- and geomorphodynamics of the TIDE estuaries Scheldt, Elbe, Weser and Humber		
Customer:	Antwerp Port Authority	Ref.:	WL2013_770_62b_rev4_0
Keywords (3-5):	estuary; hydrodynamics; geomorphology; interestuarine comparison		
Text (p.):	63	Appendices (p.):	14
Confidentiality:	<input checked="" type="checkbox"/> Yes	Exceptions	<input checked="" type="checkbox"/> Customer
	<input type="checkbox"/> No		<input type="checkbox"/> Internal
		<input type="checkbox"/> Available online	<input type="checkbox"/> Flemish government
		Released as from	

Approval

Author Dr. W. Vandenbruwaene	Reviser Ir. Y. Plancke	Project Leader Ir. Y. Plancke	S&A Director Ir. T. Verwaest	Division Head Dr. F. Mostaert
---------------------------------	---------------------------	----------------------------------	---------------------------------	----------------------------------

Revisions

Nr.	Date	Definition	Author
1_0	07/06/2012	Preliminary concept version	Vandenbruwaene, W.
1_1	07/06/2012	Preliminary revision	Plancke, Y.
2_0	26/10/2012	Concept version	Vandenbruwaene, W.
2_1	08/11/2012	New concept version	Vandenbruwaene, W.
2_2	07/12/2012	Revision concept version	Plancke, Y.; Ides, S.; Roose, F.; Taal, M.
3_0	19/12/2012	Final concept	Vandenbruwaene, W.
3_1	15/01/2012	Revision by TIDE partners	Wolfstein, K.; Whitehead, P.
3_2	20/02/2012	Final concept	Vandenbruwaene, W.; Plancke, Y.
4_0	21/02/2013	Final version	Vandenbruwaene, W.

Abstract

Within the scope of the INTERREG IVb project TIDE (**T**idal river **D**evelopment), an interestuarine comparison of 4 partner estuaries (Scheldt, Elbe, Weser and Humber) was performed. Different aspects of the estuaries were handled within the interestuarine comparison: hydrodynamics, geomorphology, ecology, birds, historical changes and monitoring. This study reports on the hydro- and geomorphodynamics of the TIDE estuaries.

Five research topics were handled within the hydro-geomorphology study: (1) tidal damping/amplification, (2) relation between habitats and the tide, (3) suspended sediments, (4) residence times, and (5) tidal marshes. For each topic a number of specific research questions were listed (see §2). To be able to answer these questions several main parameters (i.e. directly measured in the estuary) were collected (topo-bathymetry data, tide, salinity, SPM, freshwater discharges and tidal marsh data). Furthermore some additional parameters were derived (e.g., flow velocities, tidal energy, tidal damping scale) using some specific techniques (e.g., cubage technique, Dalrymple energy concept).

We found that tidal damping in an estuary becomes important once the estuary depth (i.e. cross-section averaged depth at low water) becomes lower than 4.2 – 7.7 m, depending on the estuary-convergence. Similar results were found for the habitat analysis: once the area of the deep subtidal habitat (> 5 m below low water) becomes smaller than 20 %, and the area of the shallow subtidal habitat (< 5 m below low water) becomes larger than 35 %, tidal damping in an estuary prevails. Concerning SPM, turbidity maxima are associated with maxima in tidal energy. We further found that these high SPM values force tidal marshes to faster attain a high climax vegetation state with less plant diversity.

Contents

1	Introduction.....	1
1.1	Introduction.....	1
1.2	Outline.....	1
2	Objectives.....	2
3	Methodology.....	3
3.1	Main parameters.....	3
3.1.1	Topo-bathymetry.....	3
3.1.2	Tide.....	3
3.1.3	Salinity.....	4
3.1.4	Suspended particle matter (SPM).....	6
3.1.5	Freshwater discharge.....	6
3.1.6	Tidal marshes.....	7
3.2	Derived parameters.....	8
3.2.1	Flow velocity, tidal discharge and tidal volume (“Cubage” technique).....	8
3.2.2	Tidal damping scale.....	11
3.2.3	Sediment fluxes.....	14
3.2.4	Tidal and fluvial energy (Dalrymple concept).....	16
3.2.5	Residence time.....	17
3.3	Habitats.....	17
3.3.1	Classification.....	17
3.3.2	Habitat mapping and quantification.....	17
3.4	Mouth definition.....	18
4	TIDE estuaries.....	20
4.1	Scheldt.....	20
4.2	Elbe.....	22
4.3	Weser.....	23
4.4	Humber.....	25
4.5	Parameters of the 4 estuaries (TIDE km).....	27
5	Interestuarine comparison.....	36
5.1	TOPIC 1 – Tidal amplification.....	36
5.1.1	Tidal range.....	36
5.1.2	Damping or amplification?.....	38
5.1.3	Critical threshold values for depth and estuary convergence.....	39
5.1.4	Conclusions.....	42
5.2	TOPIC 2 – Habitats.....	43
5.2.1	Quantification.....	43
5.2.2	Relation between flow velocity and habitats.....	46
5.2.3	Relation between habitats and tidal damping/amplification.....	47
5.2.4	Conclusions.....	49
5.3	TOPIC 3 – Relation between sediment load and tidal/riverine characteristics.....	50
5.3.1	Suspended particle matter (SPM).....	50
5.3.2	Sediment fluxes.....	54
5.3.3	Relation between tidal energy and SPM.....	55

5.3.4	Relation between salinity and SPM	57
5.3.5	Conclusions	58
5.4	TOPIC 4 – Residence time.....	59
5.4.1	Parameters determining residence time	59
5.4.2	Residence time for low, mean and high river discharges	61
5.4.3	Conclusions	63
5.5	TOPIC 5 – Impact of increasing MHWL on tidal marsh ecosystems.....	64
5.5.1	Change in marsh platform elevation	64
5.5.2	Conclusions	65
6	General conclusions	67
6.1.1	Geometrical characteristics.....	67
6.1.2	The important role of morphology on tidal amplification/damping.....	68
6.1.3	Indirect effects of morphology on SPM and tidal marsh evolution	69
7	References	70
	Appendix A – Estuary convergence.....	A1
	Appendix B – Habitat maps	A3
	Appendix C – Habitat widths.....	A12
	Appendix D – Tidal marsh sites	A14

List of tables

Table 1 – Overview of the data collected (main parameters) for each estuary, indicating the time periods and number of stations (in between brackets).....	3
Table 2 – Overview of the available SPM datasets and sampling methodology	6
Table 3 – Input data used for the cubage calculations of each estuary	11
Table 4 – Overview of the parameters used to calculate $1/\beta$	14
Table 5 – Overview of the input parameters used to calculate sediment fluxes. (R = riverine discharge)	15
Table 6 – Relationship between the tide kilometers and kilometers to mouth _{geo} and mouth _{sal} . For the Scheldt, the distance to Vlissingen is also provided.....	19
Table 7 – R^2 and $D-LW_{cr}$ for the logarithmic regression lines in Figure 35 and Figure 37. All found trendlines are significant. $D-LW_{cr}$ is the critical D-LW value for tidal damping/amplification. Below this value tidal damping occurs, above this value tidal amplification occurs	42
Table 8 – Residence time (in days) from up-estuary boundary to mouth _{geo} under conditions of mean, low and high freshwater discharge (river flow), calculated according to the fractal freshwater method	63
Table 9 – Residence time (in days) for each salinity zone (definition of salinity zones see Geerts et al., 2011) under conditions of mean freshwater discharge (= river discharge = R), calculated according to the fractal freshwater method	63

List of figures

Figure 1 – Salinity variation (3 stations in the Elbe) over a single tidal cycle when riverine discharge is high (15 feb 2004). Stations are located at TIDE km 108 (low salinity values), TIDE km 133 (intermediate PSU values) and TIDE km 162 (high salinity values) (see Figure 10 for locations).....	5
Figure 2 – Salinity variation (3 stations in the Elbe) over a single tidal cycle when riverine discharge is low (20 oct 2004). Stations are located at TIDE km 108 (low salinity values), TIDE km 133 (intermediate PSU values) and TIDE km 162 (high salinity values) (see Figure 10 for locations). Same stations as presented in Figure 1.....	5
Figure 3 – Topo-bathymetry (2006), water levels (2001-2010) and cross-section used for the cubage calculation of the Elbe.....	8
Figure 4 – Schematisation of cubage technique in a segment of the estuary (opwaarts = up-estuary afwaarts = down estuary)	9
Figure 5 – Sensitivity analysis on the tidal damping scale for the Scheldt estuary.....	13
Figure 6 – Variation of flow velocity and SPM (turbidity) over tidal cycle for station Oosterweel (Scheldt estuary).....	15
Figure 7 – Dalrymple energy-concept – equations used to calculate tidal and fluvial energy	16
Figure 8 – Definition of the mouth _{geo} based on changes in estuary width	19
Figure 9 – Topo-bathymetry of the Scheldt estuary (2001) with indication of the different parameter locations, TIDE kilometers (i.e. distance to up-estuary boundary), and the most downstream cubage cross-section	21
Figure 10 – Topo-bathymetry of the Elbe estuary (2006) with indication of the different parameter locations, TIDE kilometers (i.e. distance to up-estuary boundary), and the most downstream cubage cross-section ..	23
Figure 11 – Topo-bathymetry of the Weser estuary (2009) with indication of the different parameter locations, TIDE kilometers (i.e. distance to up-estuary boundary), and the most downstream cubage cross-section	24
Figure 12 – Topo-bathymetry of the Humber estuary (2005) with indication of the different parameter locations, TIDE kilometers (i.e. distance to up-estuary boundary), and the most downstream cubage cross-section	26
Figure 13 – Width at MHWL and MLWL for the Scheldt, Elbe, Weser and Humber-Ouse.....	27
Figure 14 – Thalweg depth for the Scheldt (blue), Elbe (red), Weser (green) and Humber-Ouse (yellow), relative to low water level at mouth _{geo}	27
Figure 15 – Cross-section averaged depth at MHWL and MLWL for the Scheldt (blue), Elbe (red), Weser (green) and Humber-Ouse (yellow)	28
Figure 16 – Wet section at MHWL and MLWL for the Scheldt (blue), Elbe (red), Weser (green) and Humber-Ouse (yellow).....	28
Figure 17 – Mean high water level (MHWL), mean low water level (MLWL) and thalweg depth along the Scheldt (blue), Elbe (red), Weser (green), Humber-Ouse and Trent (yellow); (m TAW = Belgian ordnance level; m NN = German ordnance level; OD Newlyn = British ordnance level).....	29
Figure 18 – Mean tidal range along the Scheldt (blue), Elbe (red), Weser (green), Humber-Ouse and Trent (yellow)	29
Figure 19 – Gradient (averaged over 5 km blocks) for the tidal range, MHWL and MLWL, for the Scheldt (blue), Elbe (red), Weser (green) and Humber-Ouse (yellow).....	30
Figure 20 – Tidal asymmetry for the present situation along the Scheldt (blue), Elbe (red) and Weser (green). Tidal asymmetry presented by the ratio between mean tidal fall and mean tidal rise	30
Figure 21 – Freshwater discharge at Schelle (Scheldt), Neu Darchau (Elbe), and Intschede (Weser). For the Humber, the freshwater discharge is presented at North Muskam (Trent up-estuary boundary) and Skelton (Ouse up-estuary boundary). Total Q in the Humber is sum of the discharges at North Muskam and Skelton, and the mean discharges of the other tributaries (Wharfe, Derwent, Aire and Don)	31

Figure 22 – Mean flood (+) and ebb (-) flow velocities (cross-section averaged) (v_{mean}) along the Scheldt (blue), Elbe (red), Weser (green) and Humber-Ouse (yellow), under high (winter) and low (summer) freshwater discharge conditions. For the Scheldt, flow velocities are only calculated under mean freshwater discharge conditions..... 32

Figure 23 – Maximum flood (+) and ebb (-) flow velocities (cross-section averaged) (v_{max}) along the Scheldt (blue), Elbe (red), Weser (green) and Humber-Ouse (yellow), under high (winter) and low (summer) freshwater discharge conditions. For the Scheldt, flow velocities are only calculated under mean freshwater discharge conditions..... 32

Figure 24 – Tidal damping ($1/\beta$) (averaged over 5 km blocks) for the Scheldt (blue), Elbe (red), Weser (green) and Humber-Ouse (yellow) 33

Figure 25 – Energy fluxes (tidal = $E_{tij,tot}$, fluvial = $E_{q,tot}$ and total = E_{tot} , averaged over 5 km blocks) along the Scheldt (blue), Elbe (red), Weser (green) and Humber-Ouse (yellow), under high (winter) and low (summer) freshwater discharge conditions. For the Scheldt, energy fluxes are only calculated under mean freshwater discharge conditions 33

Figure 26 – Longitudinal mean (grey), winter (blue) and summer (orange) salinity profiles along the 4 TIDE estuaries, with indication of the low and high water envelopes for winter (P0.2 and P30) and summer (P70 and P99). Humber = Humber-Ouse..... 34

Figure 27 – Difference in salinity between the summer and winter profiles (grey), and between the high and low water envelopes (blue for winter, orange for summer) of Figure 26. Humber = Humber-Ouse 34

Figure 28 – SPM data for the 4 TIDE estuaries. For the Scheldt (blue): 3 different datasets are presented: (1) surface SPM for the period 2001-2010 (mean values over a tidal cycle), (2) depth-averaged SPM for the period 2001-2010 (mean values over a tidal cycle), and (3) depth-averaged SPM for the year 2009 at half tide conditions. For the Elbe (red): surface SPM at low water conditions. For the Weser (green): surface SPM at low water conditions. For the Humber-Ouse (yellow): surface SPM averaged over a tidal cycle. Error bars represent the P5 and P95 values. 35

Figure 29 – 10-yearly averages for the tidal range (2001-2010) along the different estuaries. For the Humber, data are averaged over a time period of 1 year (2005)..... 36

Figure 30 – Dimensionless presentation of the tidal range defined by TR_x/TR_0 (with TR_x = tidal range at distance x in the estuary; TR_0 = tidal range at mouth_{geo}, mouth_{geo} see Figure 9, Figure 10, Figure 11 and Figure 12). 37

Figure 31 – Dimensionless presentation of the tidal range and distance along the estuary..... 37

Figure 32 – Tidal range gradient along the 4 estuaries calculated over 5 km blocks 38

Figure 33 – Tidal range gradient along the 4 estuaries (dimensionless) 38

Figure 34 – Theoretical tidal damping ($1/\beta$) versus the observed tidal range gradient (∇TR). Humber = Humber-Ouse 39

Figure 35 – The cross-section averaged depth at MLWL versus tidal damping ($1/\beta$). For $1/\beta < 0$ tidal damping, for $1/\beta > 0$ amplification..... 40

Figure 36 – Relationship between the estuary convergence and the cross-section averaged depth, based on the calculated tidal damping scale. The threshold between amplification/damping is based on the intersections of the regression lines at $1/\beta = 0$ (see Figure 35)..... 40

Figure 37 – The cross-section averaged depth at MLWL versus the observed gradient in tidal range (∇TR). For $\nabla TR < 0$ tidal damping, for $\nabla TR > 0$ amplification..... 41

Figure 38 – Relationship between the estuary convergence and the cross-section averaged depth, based on the observed gradient in tidal range. The threshold between amplification/damping is based on the intersections of the regression lines at $\nabla TR = 0$ (see Figure 37) 41

Figure 39 – Total estuary surface area (in hectares, calculated from mouth_{geo} to up-estuary boundary)..... 43

Figure 40 – Absolute habitat areas (in hectares) for the 4 estuaries (calculated from mouth_{geo} to up-estuary boundary, Sd = subtidal deep, Sm = subtidal moderately deep, Ss = subtidal shallow, If = intertidal flat, Is = intertidal steep, M = marsh) 44

Figure 41 – Relative presentation of the habitat areas (percentages) for the 4 estuaries (from mouth_{geo} to up-estuary boundary)..... 44

Figure 42 – Relative presentation of the subtidal and intertidal habitat areas (percentages) for the 4 estuaries (from mouth_{geo} to up-estuary boundary)..... 45

Figure 43 – Habitat width (%) and tidal range along the 4 estuaries (for the Humber along Humber-Ouse), averaged over 5 km blocks. Habitat legend: Sd = subtidal deep, Sm = subtidal moderately deep, Ss = subtidal shallow, If = intertidal flat, Is = intertidal steep, M = marsh. 46

Figure 44 – Maximum flood flow velocity versus the width of the moderately deep and shallow subtidal habitat (%) 46

Figure 45 – Maximum flood flow velocity versus the width of the intertidal habitat (%)..... 47

Figure 46 – Width of the deep subtidal habitat (%) versus the tidal range gradient 47

Figure 47 – Width of the moderately deep and shallow subtidal habitat (%) versus the tidal range gradient..... 48

Figure 48 – Width of the intertidal habitat (%) versus the tidal range gradient..... 48

Figure 49 – Width of the marsh habitat (%) versus the tidal range gradient..... 49

Figure 50 – Mean surface SPM values along the four TIDE estuaries. Error bars represent the P5 and P95 values 50

Figure 51 – Surface SPM (averaged over a tidal cycle) relative to the maximum observed surface SPM in the Scheldt estuary. Under mean tidal conditions, sediment fluxes are directed in the flood direction from TIDE km 125-160, and in the ebb direction from TIDE km 0 -125. The maximum tidal energy occurs around TIDE km 69..... 51

Figure 52 – Depth-averaged SPM (averaged over a tidal cycle) relative to the maximum observed depth-averaged SPM in the Scheldt estuary. Under mean tidal conditions, sediment fluxes are directed in the flood direction from TIDE km 125-160, and in the ebb direction from TIDE km 0 -125. The maximum tidal energy occurs around TIDE km 69..... 51

Figure 53 – Surface SPM (at low water conditions) relative to the maximum observed surface SPM in the Elbe estuary. Under mean tidal conditions, sediment fluxes are directed in the flood direction from TIDE km 138-150, and in the ebb direction from TIDE km 0-138. The maximum tidal energy occurs around TIDE km 110..... 52

Figure 54 – Surface SPM (at low water conditions) relative to the maximum observed surface SPM in the Weser estuary. Under mean tidal conditions, sediment fluxes are directed in the ebb direction for the entire estuary. The maximum tidal energy occurs around TIDE km 74..... 52

Figure 55 – Surface SPM (averaged over a tidal cycle) relative to the maximum observed surface SPM along the Humber-Ouse tributary. Under mean tidal conditions, sediment fluxes are directed in the flood direction from TIDE km 84-130, and in the ebb direction from TIDE km 0-84. The maximum tidal energy occurs around TIDE km 84..... 53

Figure 56 – Relation between surface SPM and depth-averaged SPM in the Scheldt estuary 53

Figure 57 – Sediment fluxes for the four TIDE estuaries, under conditions of mean tidal range and mean riverine discharge. Positive values represent sediment transport in the flood direction, negative values represent transport in the ebb direction. Sediment fluxes are calculated based on the surface SPM values, for the Scheldt flux values are also calculated based on the depth-averaged SPM values (see §3.2.3). Error bars are calculated based on the P5 and P95 values of the SPM values (see Figure 28)..... 54

Figure 58 – Sediment fluxes for 3 TIDE estuaries, under conditions of mean tidal range and low and high riverine discharge. Positive values represent sediment transport in the flood direction, negative values represent transport in the ebb direction. Sediment fluxes under mean riverine discharge are presented in Figure 57..... 55

Figure 59 – Relative presentation of the mean salinity (grey line, compared to 30 PSU), mean tidal energy (light green line, compared to maximum tidal energy) and SPM data (compared to maximum SPM) for the different estuaries. Salinity zones (relatively to 30 PSU) – freshwater: < 0.017, oligohaline: 0.017-0.17, mesohaline: 0.17-0.6, polyhaline: 0.6-1. (a) surface SPM 2001-2010 for the Scheldt, (b) depth-averaged SPM 2001-2010 for the Scheldt, (c) surface SPM 2009 for the Scheldt, (d) surface SPM 2004-2009 for the Elbe, (e) surface SPM 2005, 2009-2010 for the Weser, (f) surface SPM 2004-2009 for the Humber..... 56

Figure 60 – Relationship between the tidal energy and the SPM for the Scheldt (blue), Elbe (red), Weser (green) and Humber (yellow). Data averaged over 5 km blocks and presented relatively by dividing with the maximum value..... 57

Figure 61 – Relationship between the salinity and the SPM for the four TIDE estuaries. Data averaged over 5 km blocks and presented relatively by dividing with the maximum value (for SPM) and by 30 (for salinity). Data for the freshwater zone are excluded..... 57

Figure 62 – Estuary volume V (over 5 km) and fractional freshwater concentration f for the four estuaries . 59

Figure 63 – The total volume of fresh water ($V_f = V \cdot f$) in each estuary segment (over 5 km), calculated according to the fractional freshwater method (Dyer, 1973)..... 60

Figure 64 – Mean freshwater discharges for the 4 estuaries. Error bars are representative for typical high (P95) and low (P5) freshwater discharge values..... 60

Figure 65 – Residence times for each estuary segment of 5 km along the different estuaries. Solid lines represent the residence time under mean freshwater discharge conditions, envelopes (dashed lines) represent high and low freshwater discharges (respectively P95 and P5 values)..... 61

Figure 66 – Cumulative residence times along the different estuaries. Solid lines represent the residence time under mean freshwater discharge conditions, envelopes (dashed lines) represent high and low freshwater discharges (respectively P95 and P5 values) 62

Figure 67 – Total residence time (from up-estuary boundary to $mouth_{geo}$) under mean freshwater discharge conditions (bar), and for high and low freshwater discharges (P95 and P5) 62

Figure 68 – Change in marsh platform elevation, MHWL, and MHWLS for the Scheldt marsh site (Saefthinghe) (location, see Figure 9 and Figure D 1)..... 64

Figure 69 – Change in marsh platform elevation and MHWL for the Elbe marsh site (Kehdingen area) (location, see Figure 10 and Figure D 2) 65

Figure 70 – Convergence (based on $1/b$ value, see estuary convergence in §3.2.2) and friction (based on the cross-section averaged depth at low water) for the four TIDE estuaries. 67

Figure 71 – Cross-section averaged depth at low water along the four TIDE estuaries, with indication of the major ports..... 68

Abbreviations

D =	depth
DA =	depth-averaged
HO =	Humber-Ouse
HT =	half tide
HW =	high water
If =	intertidal flat habitat
Is =	intertidal steep habitat
LW =	low water
M =	marsh habitat
MHWL =	mean high water level
MHWLS =	mean high water level at spring tide
MLWL =	mean low water level
NN =	German ordnance level
OD Newlyn =	British ordnance level
P5 =	5 th percentile
P95 =	95 th percentile
PSU =	practical salinity unit
S =	surface
Sd =	subtidal deep habitat
SF =	sediment flux
Sm =	subtidal moderately deep habitat
Ss =	subtidal shallow habitat
SPM =	suspended particle matter
T =	Trent
TAW =	Belgian ordnance level
TR =	tidal range
TR ₀ =	tidal range at mouth _{geo}
TR _x =	tidal range at distance x in the estuary
W =	watercolumn

1 Introduction

1.1 Introduction

Within the scope of the European project (INTERREG IVb) TIDE (Tidal River Development) an interestuarine comparison of the 4 partner estuaries (Elbe, Weser, Scheldt and Humber) takes place. This comparison will be made for hydrodynamics, geomorphology, ecology, birds, monitoring and historical changes.

This report describes the results of the hydro- and geomorphological comparison of the 4 estuaries. The comparison is executed based on the 5 research topics formulated in the note of Ides et al. (2011) (see also §2). Increasing our knowledge on the hydrology and geomorphology, together with other estuary functions (historical changes, ecology, monitoring), will lead to increased estuarine knowledge. A better understanding of these estuarine functions will result in recommendations for integrated management strategy. These recommendations can be considered as one of the main objectives of the TIDE project.

1.2 Outline

In chapter 2 the five research topics are described. The processing of the parameters that were collected in order to answer the five research topics, and a description of some specific applied techniques (cubage technique, tidal damping, habitat classification, Dalrymple energy-concept, residence time) is given in the methodology section (chapter 3).

Chapter 4 presents some general characteristics of each tide estuary (Scheldt, Elbe, Weser, Humber). Parameters are presented along the length axis of each estuary (§4.5), with the origin at the up-estuary boundary (the so-called TIDE kilometers)

Chapter 5 handles the interestuarine comparison by presenting specific graphs for the 5 research topics. These graphs are considered to be crucial to discuss the research topics (§5.1 - §5.5). At the end of each research topic, a brief conclusion section is added.

Chapter 6 contains the general conclusions of this report.

2 Objectives

5 research topics were developed by the TIDE project partners:

- 1) *Which factors influence the amplification of the tide in an estuary? How can the tidal amplification in an estuary be stopped or even be reduced?*
These questions are directly related to flood protection along estuaries and measures that could be introduced to improve the safety against flooding.
- 2) *Higher average flow velocities in an estuary result in less intertidal and shallow water area.*
This hypothesis looks at the effect of flow on habitat occurrence. The availability of different habitat areas is not only relevant within the hydro-geomorphology study, but is also important for the ecosystem services and bird studies performed within TIDE.
- 3) *What are the similarities and differences between the estuaries with regard to their suspended sediment loads in relation to their tidal and riverine characteristics? Which factors influence the position of the turbidity maximum?*
A high amount of sediment transport may lead to some important challenges for estuarine management, e.g. with regard to port accessibility. Moreover, suspended sediments play an important role in the primary production which is important for the ecology of estuaries.
- 4) *What are the differences in residence time in the different estuaries?*
Residence times influence the time that particles in the watercolumn, e.g. sediments, nutrients or phytoplankton, stay in a certain area of an estuary. Residence times are thus not only important for the hydro-geomorphology study but also for the ecology study within TIDE.
- 5) *What is the impact of increasing tidal range along all estuaries on the tidal marsh ecosystems? Did the increasing high water levels result in increased tidal flooding of the tidal marshes or was vertical sediment accretion in the marshes sufficiently high so that the elevation of the marshes could grow in accordance with the growing high water level? And moreover, if vertical sediment accretion was important, did this result in steepening of the intertidal area and hence in increased landward erosion of the tidal marsh shorelines?*

For each topic several relations between different parameters will be investigated for each estuary.

- Topic 1: relation between tidal (HW, LW, tidal range, tidal amplification), geometrical characteristics (width, wetted section, depth) and derived parameters (damping and amplification of the tide).
- Topic 2: relation between habitat occurrence (habitat width), and the horizontal tide (flow velocity) and vertical tide (tidal range)
- Topic 3: relation between salinity, turbidity maximum, and tidal energy.
- Topic 4: relation between residence time, tidal and fresh water characteristics.
- Topic 5: relation between salt marsh characteristics (e.g., increase in platform elevation), hydrodynamics and sediment characteristics.

After a first analysis of the data, research topic 2 and 5 were reformulated. For research topic 2 we did not find any relationship between flow velocities (horizontal tide) and habitat occurrence. Therefore we additionally related habitat occurrence to tidal damping/amplification (vertical tide). For research topic 5, historical data on tidal marsh edges are very scarce. As a consequence, we related the increase in MHWL only to changes in marsh platform elevation and not to changes in tidal marsh shoreline.

3 Methodology

3.1 Main parameters

Main parameters are parameters which are directly measured in the estuaries. In this study we focus on the present situation of each estuary and therefore we collected the most recent data, and if appropriate over a time period of several years. An overview of the collected main parameters for each estuary is given in Table 1. A description of each parameter is given in the following paragraphs (§3.1.1 - §3.1.6).

Table 1 – Overview of the data collected (main parameters) for each estuary, indicating the time periods and number of stations (in between brackets)

	Scheldt	Elbe	Weser	Humber
Topo-bathymetry	2001	2006	2009	2005
Tide	2001-2010 (17)	2001-2010 (17)	2001-2010 (12)	2005 (18)
Salinity	2000-2007 (19)	2004 (9)	2010 (9)	2004-2009 (10)
Suspended sediment	2001-2010 (34)	2004-2009 (27)	2005, 2009-2010 (10)	2004-2009 (12)
Freshwater discharge	2008-2009	2001-2010	2001-2010	2010
Tidal marshes	1931, 1951, 1963, 1992, 2004, 2010	1958, 1966, 1977, 1997, 2008	-	-

3.1.1 Topo-bathymetry

A topo-bathymetric grid of an estuary represents the elevation of the subtidal, intertidal and supratidal areas of the estuary, located within the dyke lines. In general, the bathymetry grids (based on multibeam or singlebeam measurements) cover the subtidal and lower intertidal parts of the estuary, while the topographic datasets (based on LIDAR data) cover the higher parts of the intertidal areas and tidal marsh areas (supratidal).

For the Scheldt and Elbe topo-bathymetric grids were directly available, respectively for the years 2001 and 2006. The Scheldt grid has a resolution varying between 5 x 5 m and 20 x 20 m, the Elbe grid has a resolution of 10 x 10 m. For the Weser and Humber, point datasets were delivered which still needed to be interpolated to grids. For the Weser the TopoToRaster interpolation method was used (ArcGIS software), while for the Humber (single beam data) the digipol methodology (Qinsy software) was applied, which is especially developed for single beam datasets. The input datasets were respectively from 2009 and 2005 for the Weser and Humber, and interpolation grids were created with a resolution of respectively 20 x 20 m and 10 x 10 m.

3.1.2 Tide

For each estuary the main water level parameters (mean high water level = MHWL, mean low water level = MLWL) were delivered for a number of stations. Table 1 gives an overview of the timespan and the number of stations used to present the MHWL and MLWL along the different estuaries. A 10-yearly average (2001-2010) was therefore used, except for the Humber where data from 2005 were used (Table 1). The

difference between MHWL and MLWL gives the tidal range. The change in tidal range along the length axis of the estuary returns the tidal range gradient (∇ TR). And the ratio between the mean tidal fall and the mean tidal rise returns the tidal asymmetry. An overview of the location of the water level stations is given in Figure 9 (Scheldt), Figure 10 (Elbe), Figure 11 (Weser) and Figure 12 (Humber).

3.1.3 Salinity

Salinity data were collected which cover the variation in salinity between high freshwater discharge (representative for a flushing event) and low freshwater discharge (representative for a dry event), and moreover the difference between different tides, and this for as many sampling stations as possible. For the Elbe and Weser continuous salinity data (respectively every 5 and 15 min) were collected over a period of one year, and this for in total 9 stations (Table 1). For the Scheldt and Humber continuous salinity datasets were only available for a limited number of stations and hence could not be used to cover the salinity gradient along the estuary. Therefore salinity data were collected that were measured along longitudinal transects at high water or low water slack. For the Scheldt these measurement campaigns are performed about every month since the 1970's (both at high and low water slack). For this study we only collected data for the present situation and this over a period of 8 years (Table 1). For the Humber less measurement campaigns were performed but still sufficiently enough to cover the variation in salinity between high and low freshwater discharge, and between high and low water slack.

To make salinity data comparable between the different estuaries all salinity data were converted to PSU/ppt¹ values. For the Scheldt chlorinity data were provided which were converted to ppt values according to (Forch et al., 1902):

$$\text{Salinity} = 0.03 + (1.805 \cdot \text{Chlorinity})$$

The Elbe dataset contained conductivity values. Based on the UNESCO formula (Fofonoff and Millard, 1983) conductivity values were converted to PSU values. For the Weser, data were directly provided as PSU values and for the Humber the dataset contained ppt conductivity values.

For every sampling station a mean value was calculated. By connecting the mean values of all stations a mean salinity profile was constructed for every estuary. To cover the variation in salinity caused by high and low freshwater discharges respectively the P(5%) (percentile 5%) and P(95%) (percentile 95%) values were calculated for every station. Connecting the P(5%) and P(95%) values results in a longitudinal salinity profile for respectively a flushing event and a dry event, which can be considered as representative for respectively a winter and summer situation.

Differences in salinity are not only explained by variations in riverine discharge, but are also influenced by the tidal intrusion in the estuary. As a consequence, measured salinity values at low water slack will be lower than during high water slack (Figure 1 and Figure 2). To cover this variation in salinity between low and high water slack two envelopes were created (one for a flushing and one for a dry event) where the lower limit of the envelopes represents low water slack and the upper limit high water slack. Comparable to the methodology for a flushing/dry event, percentile values were determined for the envelope limits. To determine the threshold values for the percentiles 3 salinity stations in the Elbe (continuous data available for all stations) were selected with one station close to the open sea, a station where the variation in salinity between P(5%) and P(95%) is the largest, and a station close to the freshwater zone. For these 3 stations two days (15/02/2004 and 20/10/2004) were selected for which the mean daily salinity is comparable with the P(5%) respectively the P(95%) value (Figure 1 and Figure 2). For each day the minimum and maximum values were selected which correspond with the salinity at respectively low and high water slack. Based on the continuous dataset over a period of one year the percentiles values were determined which correspond with the found minimum and maximum values for both days. Finally, for a flushing event the envelope

¹ PSU values represent the conductivity ratio of a water sample compared to a standard KCl solution whereas ppt values represent grams of salt per kilogram solution. Although the definition for both units is different, the difference in absolute values between PSU and ppt is small and negligible.

boundaries were found at P(0.2%) and P(30%), for a dry event at P(70%) and P(99%). The same threshold values were used to construct the envelopes for the other estuaries.

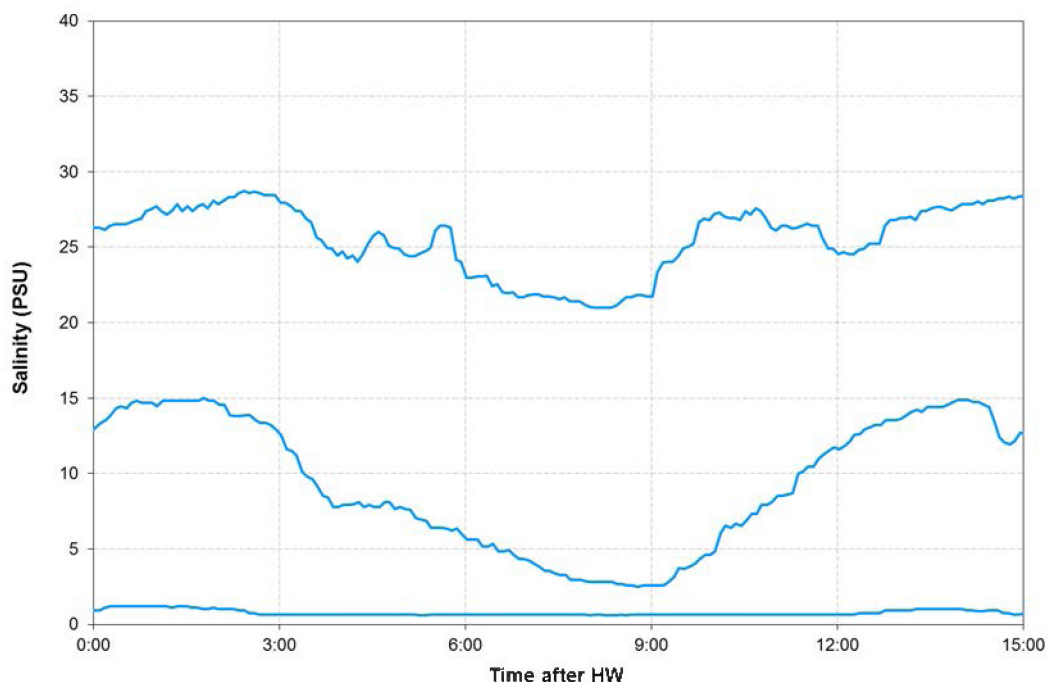


Figure 1 – Salinity variation (3 stations in the Elbe) over a single tidal cycle when riverine discharge is high (15 Feb 2004). Stations are located at TIDE km 108 (low salinity values), TIDE km 133 (intermediate PSU values) and TIDE km 162 (high salinity values) (see Figure 10 for locations)

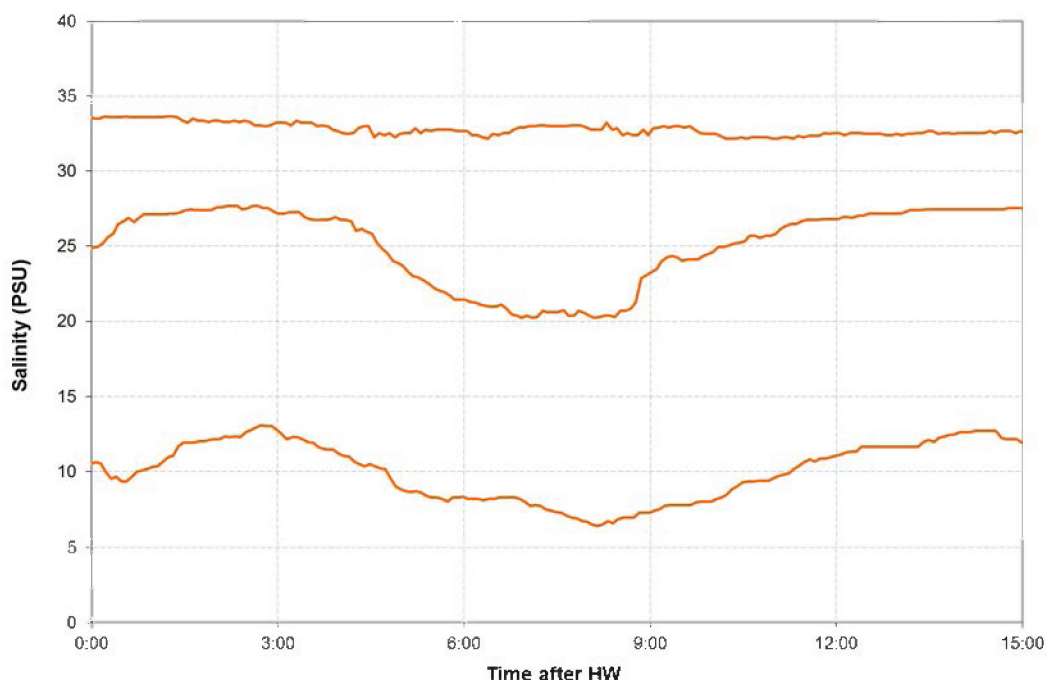


Figure 2 – Salinity variation (3 stations in the Elbe) over a single tidal cycle when riverine discharge is low (20 Oct 2004). Stations are located at TIDE km 108 (low salinity values), TIDE km 133 (intermediate PSU values) and TIDE km 162 (high salinity values) (see Figure 10 for locations). Same stations as presented in Figure 1

3.1.4 Suspended particle matter (SPM)

A large variability exists in the collected SPM data for the different estuaries. Variability is caused by differences in number of measuring campaigns, number of sampling locations, position of sampling (surface, watercolumn), and time of sampling (low water, high water, half tide). A detailed overview of the collected SPM data is given in Table 2.

Table 2 – Overview of the available SPM datasets and sampling methodology

	Scheldt1	Scheldt2	Scheldt3	Elbe	Weser	Humber
Time period	2001-2010	2001-2010	2009	2004-2009	2005, 2009-2010	2004-2009
Sampling position (S: surface; W: watercolumn)	S	W	W	S	S	S
Frequency campaigns	monthly	monthly	monthly	2-monthly	6-monthly	monthly
Number of sampling locations	34	27	17	29	10	12
Sampling time (Low Water, High Water, Half Tide)	LW, HW, HT	LW, HW, HT	HT	LW	LW	LW, HW, HT

Within this study, a mean SPM value is calculated for each location based on all available measuring campaigns. Only the sampling locations are included which were measured every campaign (or campaigns in the same time period of 2 weeks in case of the Humber). In this way, mean SPM values are comparable for each selected location. It is important to note that the mean SPM values for the datasets Scheldt1, Scheldt2 and Humber are based on SPM data sampled during various time steps within a tidal cycle, whereas for the datasets Scheldt 3 and Elbe/Weser sampling took place at a fixed time in the tidal cycle (respectively at half tide and low water, see Table 2). The variation on the calculated mean SPM value is presented by the standard deviation. Within the interestuarine comparison (§5), dataset Scheldt1 was used for the Scheldt as this dataset can be compared with the surface SPM datasets of the other estuaries (see Table 2).

3.1.5 Freshwater discharge

The total freshwater discharge of a river is the sum of the freshwater discharges of the main channel and all its tributaries. For the Elbe and Weser discharges were measured along the main channel in the more upstream parts of the river (respectively at Neu Darchau and Intschede, see Figure 10 and Figure 11). These measured discharges can be considered as the total freshwater discharge of the rivers since the tributary discharges are negligible compared to the discharge of the main channel (factor 100). For the Scheldt and Humber all tributaries have a significant contribution to the total river discharge. For the Scheldt discharge data are calculated at Schelle (Figure 9). The calculated discharge at Schelle is the sum of the freshwater discharges measured at each tributary, and thus representative for the total river discharge of the Scheldt. For the Humber discharge data are also available for each tributary. Summing up the tributary discharges returns the total river discharge for the Humber.

The discharges at the different stations are daily discharges. An overview of the time periods for which discharge data were available is given in Table 1. Based on the daily discharges a mean value was calculated for the total river discharge into each estuary. Moreover, the P(5%) and P(95%) values were calculated returning a low and high freshwater discharge value, representative for respectively a dry and a flushing event in the estuary. The calculated mean, P(5%) and P(95%) discharge values are input parameters for the cubage and residence time calculations (see respectively §3.2.1 and §3.2.5).

3.1.6 Tidal marshes

Historical data on marsh platform elevation are scarce. We received data on marsh platform elevation for the Scheldt and Elbe estuaries. To be able to analyse the historical changes in marsh platform elevation, the following conditions need to be fulfilled:

- The considered time period should be sufficiently long (± 50 year)
- There should be sufficient time steps with marsh elevation data (at least 3)
- There should be historical data on MHWL

Based on these conditions we were able to select one marsh site in the Scheldt estuary (Saeftinghe, see Figure 9 and Figure D 1) and one marsh site in the Elbe estuary (Kehdingen area, see Figure 10 and Figure D 2). Both selected marshes are brackish marshes.

Scheldt

For the selected marsh site in the Scheldt estuary, platform elevation data were available for the years 1931, 1951, 1963, 1992, 2004 and 2010. For the years 1931, 1951, 1963 and 1992 topographic surveys (in a grid) were carried out and data were provided as Digital Elevation Models (DEM) with a 20 x 20 m grid resolution. For the more recent time steps (2004 and 2010), DEMs with a 2 x 2 m resolution were available based on LIDAR data. The DEMs based on LIDAR data were corrected for vegetation.

All provided DEMs include the tidal channel network. To exclude grid cells located within the tidal channel network we delineated the tidal channel network for 1931 and 2010 based on aerial photographs. The channel network for 1931 and 2010 were merged and used as a mask to exclude grid cells located within the tidal channel network. As no significant changes occurred between the tidal channel networks in 1931 and 2010 we also used this mask for the intervening times steps. Besides the mean platform elevation of the selected site, additionally the standard deviation was calculated representing the spatial variation in marsh platform elevation.

Historical data on MHWL were derived from the nearby water level station at Bath. Besides the yearly MHWL also the yearly mean high water levels at spring tide (MHWLS) were available for this station.

From 1931 to 2010 the marsh evolved from a low elevated tidal marsh (mean platform elevation below MHWL) towards a high elevated tidal marsh (mean platform elevation above MHWL).

Elbe

For the Elbe marsh site, platform elevation data were available for 1958, 1966, 1977, 1997 and 2008. Elevation data were provided as point data (xyz), located along transects perpendicular to the Elbe main channel (same transects for every time step). To calculate mean platform elevations, DEM were built (1 x 1 m) for every time step using the TopoToRaster interpolation in ArcGIS 9.2. Based on the constructed DEM, mean values and standard deviations were calculated of the marsh platform, and this for every time step.

Historical data on MHWL were derived from the nearby water level station at Osteriff. No data on spring tide were available.

During the considered time period (1958 – 2008), the selected marsh site evolved from a low elevated tidal marsh (mean platform elevation below MHWL), towards a high elevated tidal marsh (mean platform elevation above MHWL)

3.2 Derived parameters

3.2.1 Flow velocity, tidal discharge and tidal volume (“Cubage” technique)

Introduction

The “cubage”-technique (“kubatuur” in Dutch) is a relatively simple technique to calculate the hydrodynamics in an estuary (Smets, 1996; Plancke et al., 2011). It requires only topo-bathymetric data and water levels at different stations to calculate discharges and cross-sectional averaged flow velocities (see Figure 3) starting from the conservation of mass formula. In contrast to numerical process models, this technique does not require any flow resistance (“roughness”) coefficients to calibrate the model. Where the cubage technique uses mass conservation (which is an exact relationship) the error of the method is solely related to the error in water level and topo-bathymetric data. Hereafter some mathematical background on this technique is given.

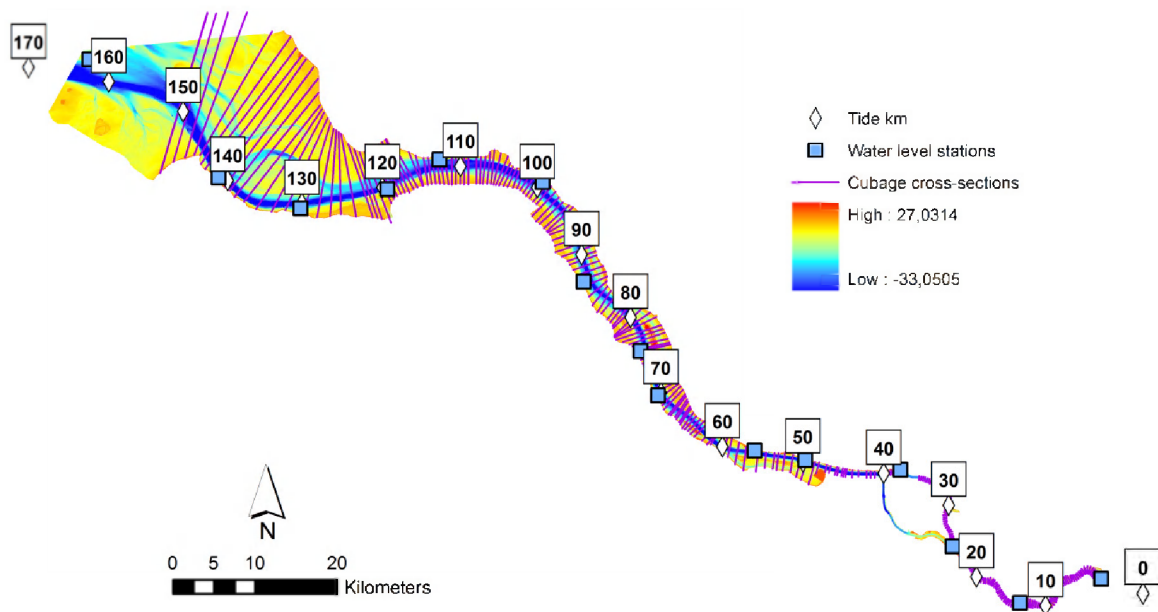


Figure 3 – Topo-bathymetry (2006), water levels (2001-2010) and cross-section used for the cubage calculation of the Elbe

The hydrodynamics in a river or estuary can be described in a one-dimensional way using following equations:

(1) Conservation of mass:
$$\frac{\partial Q}{\partial x} + B(x) \cdot \frac{\partial z}{\partial t} - f = 0$$

(2) Dynamic equation:
$$\frac{\partial z}{\partial x} + \frac{u}{g} \cdot \frac{\partial u}{\partial x} + \frac{1}{g} \cdot \frac{\partial u}{\partial t} + \frac{u \cdot |u|}{C^2 \cdot R} = 0$$

with: x: abscise of a cross-section in the estuary

z: water level to horizontal reference plain

t: time

Q: discharge, positive from up-estuary to down-estuary (ebb = + | flood = -)

A: area of wet section of cross-section x at water level z: $A(x,z)$

- B: width of a cross-section x at water level z: $B(x,z)$
- u: section-averaged flow velocity: $u = Q/A$
- g: gravitation constant ($9,81 \text{ m/s}^2$)
- C: Chézy roughness coefficient
- f: tributary discharge

The “cubage”-technique is based on the integration of the conservation of mass equation in a segment of the estuary between 2 consecutive cross-sections (Figure 4). Starting from a known discharge curve at one cross section (due to practical considerations this cross section is chosen at the up-estuary boundary), the discharges at the other cross sections can be calculated. Application of the trapezoidal rule leads to following equation:

$$Q_{n+1} - Q_n = -\frac{1}{2} \left[\frac{B_n^{t+1} + B_n^t}{2} \cdot \Delta z_n^{t,t+1} + \frac{B_{n+1}^{t+1} + B_{n+1}^t}{2} \cdot \Delta z_{n+1}^{t,t+1} \right] \cdot \Delta x \cdot \frac{1}{\Delta t}$$

- with:
- Q_n : discharge in cross-section n (up-estuary)
 - Q_{n+1} : discharge in cross-section n+1 (down-estuary)
 - B_n^t : width of cross-section n at time step t
 - $\Delta z_n^{t,t+1}$: change in water level for cross-section n, between time step t and t+1
 - Δx : distance between 2 consecutive cross-sections n en n+1 (500 m)
 - Δt : time interval between 2 time steps (i.e. temporal resolution of water level measurements; 10 to 15 minutes was chosen in this report)

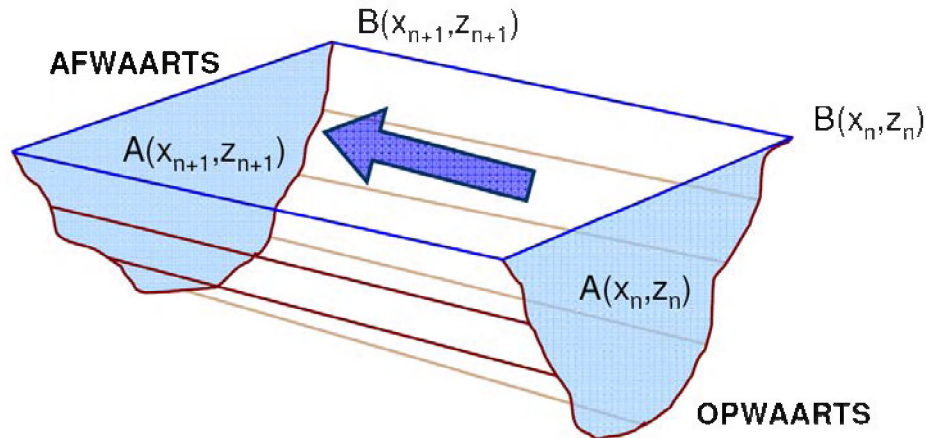


Figure 4 – Schematisation of cubage technique in a segment of the estuary (opwaarts = up-estuary | afwaarts = down estuary)

Output parameters

The “cubage”-technique calculates discharges in time between every 2 consecutive cross-sections in the estuary. From this parameter following additional parameters can be derived:

- (a) Maximum ebb and flood discharges

$$Q_{ebb}^{\max} = \max_{SHW < t < SLW} |Q(x, t)| \text{ and } Q_{flood}^{\max} = \max_{SLW < t < SHW2} |Q(x, t)|$$

- (b) Ebb and flood discharges averaged over one tidal cycle

$$\langle Q_{ebb} \rangle = \frac{\left| \int_{SHW}^{SLW} Q(x, t) . dt \right|}{SLW - SHW} \text{ and } \langle Q_{flood} \rangle = \frac{\left| \int_{SLW}^{SHW2} Q(x, t) . dt \right|}{SHW2 - SLW}$$

- (c) Ebb and flood tidal volumes

$$V_{ebb} = \left| \int_{SHW}^{SLW} Q(x, t) . dt \right| \text{ and } V_{flood} = \left| \int_{SLW}^{SHW2} Q(x, t) . dt \right|$$

- (d) Evolution in time of section-averaged velocity

$$v(x, t) = \frac{Q(x, t)}{A(x, z)}$$

- (e) Maximum ebb and flood velocity

$$v_{ebb}^{\max} = \max_{SHW < t < SLW} |v(x, t)| \text{ and } v_{flood}^{\max} = \max_{SLW < t < SHW2} |v(x, t)|$$

- (f) Ebb and flood velocities averaged over one tidal cycle

$$\langle v_{ebb} \rangle = \frac{\left| \int_{SHW}^{SLW} v(x, t) . dt \right|}{SLW - SHW} \text{ and } \langle v_{flood} \rangle = \frac{\left| \int_{SLW}^{SHW2} v(x, t) . dt \right|}{SHW2 - SLW}$$

Selected input data and implementation

Within the TIDE-project it was chosen to perform the cubage calculation for mean tidal conditions (only input data available for mean tidal conditions). In a first step the mean tidal parameters (HW, LW, time of rising and time of falling) were derived from measurements for the present situation for a station at the mouth, a station in the middle of the estuary, and a station at the upstream boundary of the estuary (see Table 3). Where the cubage technique requires a continuous time series of water levels, one period (or 2 periods for the Elbe and Humber) with several tidal cycles was chosen from the continuous measurements (see ‘selected tides’ Table 3) for which the low and high waters have the best agreement with the MHWL and MLWL values for the present situation for all 3 selected stations. For the Elbe and Humber 2 time periods were selected (one with low and one with high river discharge) because of the important differences in river discharge at the up-estuary boundary of these estuaries. From the selected time period, water level measurements for all tidal stations were selected as input for the cubage calculation (location of all tidal stations see Figure 9 (Scheldt), Figure 10 (Elbe), Figure 11 (Weser) and Figure 12 (Humber)) .

In a next step cross sections were defined perpendicular to the thalweg. The thalweg is defined as the longitudinal profile linking the deepest points of each cross section. The distance between two sections was chosen at about 500 m: this resolution was on the one hand sufficient to represent the topo-bathymetry, while on the other hand the number of cross section remained acceptable. These cross sections were exported in a MIKE11-format. Subsequently the different cross sections were imported in MIKE11 and the necessary parameters for each cross section were derived automatically within this software:

- Wet cross section area at different heights
- Width at different heights

At the up-estuarine boundaries the “cubage” technique requires the implementation of a fresh water discharge. Based on the daily values of the present situation, two characteristic fresh water discharges were calculated: P(5%) representing a “summer” condition and P(95%) representing a “winter” condition.

Cubage calculations with a winter/summer condition were within this study performed for 3 of the 4 estuaries (Elbe, Weser and Humber) (see Plancke et al., 2012a,b,c). For the calculation of the high/low discharge period of the Elbe and Humber, appropriate tides were selected in the high/low discharge period with implementation of respectively the P(95%) and P(5%) freshwater discharges. For the Weser, appropriate tides were selected only during one time period of the year. The high/low discharge variation was again simulated by implementation of respectively the P(95%) and P(5%) freshwater discharges. For the Scheldt, an earlier cubage calculation with implementation of a mean freshwater discharge (P(50%)) was used (Plancke et al., 2011). Here, no distinction was thus made between winter and summer condition, due to the limited effect of the discharge on the water level.

More detailed information on the cubage technique is given by Plancke et al. (2012a,b,c).

Table 3 – Input data used for the cubage calculations of each estuary

	Scheldt	Elbe	Weser	Humber
Topo-bathymetry	2001	2006	2009	2005
HW and LW	1991-2000	2001-2010	2001-2010	2005
Stations used for selection of mean tide	Vlissingen Antwerpen Sint-Amands	Großer Vogelsand Kollmar Wehr Geesthacht	LT Alte Weser Nordenham Grosse Weser-brücke	Spurn Point South Ferriby Naburn Lock (Ouse) Carlton on Trent (Trent)
Selected tides	21-22/06/2009	5/03/2006 (high Q) 25/05/2006 (low Q)	7-8/06/2010	5-6/01/2005 (high Q) 3-4/05/2005 (low Q)
Freshwater discharge	2000-2010 (P50)	2001-2010 (P95 and P5)	2001-2010 (P95 and P5)	2010 (P95 and P5)

3.2.2 Tidal damping scale

Introduction

The tidal penetration in an estuary is influenced by several factors, with the most important factors being the funnel shape of the estuary, leading to an amplification of the tidal range, and the friction within the estuary, leading to a decrease in tidal range. The relative importance of these 2 factors is presented in the tidal damping scale (β), which is a simple analytical expression to describe tidal amplification or damping (Savenije, 2001). Tidal damping ($1/\beta$) is defined as:

$$\frac{1}{\beta} = \frac{1}{b} - f' \cdot \frac{v \cdot \sin \epsilon}{c \cdot \bar{h}} \quad (1)$$

With: β = tidal damping scale [m]

b = width convergence length [m]; derived from following regression: $B = B_0 \cdot e^{-\frac{x}{b}}$

f' = adjusted friction factor = $\frac{g}{c^2} \cdot \left(1 - \left(\frac{\eta}{h}\right)^2\right)^{-1}$

v = amplitude of flow velocity (average of maximum ebb and maximum flood velocity at mean tidal conditions) [m/s]

ϵ = phase lag between HW and slack HW

c = celerity of tidal wave (= sqrt(g.h)) [m/s]

h = averaged water depth over tidal cycle (= $(h_{HW} + h_{LW})/2$) [m]

η = tidal amplitude (= tidal range/2) [m]

C = Chézy roughness coefficient [$m^{1/2}/s$]

g = gravitation constant (9,81 m/s^2)

In the case that the funneling of the estuary is more important than the friction in the estuary, $1/\beta$ will be positive, and tidal amplification can be expected. If friction becomes more important, $1/\beta$ will be negative and tidal damping can be expected.

Assumptions

To calculate $1/\beta$ the following assumptions were made:

- (1) Data were averaged over 5 km blocks along the thalweg
- (2) Only the estuary was regarded and not the mouth area (based on $mouth_{geo}$, for definition see §3.4)
- (3) Data with a ratio $TR/h > 0.80$ were excluded from the analysis (TR =tidal range, h = averaged water depth over tidal cycle). Above this threshold, tidal damping calculations become less accurate (Savenije, 1998). For the Scheldt, 5 data points were excluded (in total 25 km), for the Humber 11 datapoints (in total 55 km, a consequence of the shallowness of the estuary). For Elbe and Weser no data points were excluded.
- (4) Chézy roughness coefficient $C = 50$; phase lag difference $\epsilon = 50'$ (see sensitivity analysis below)

Estuary convergence

In the tidal damping equation (see Equation (1)), the estuary convergence is described by the width convergence length (b). This parameter is determined based on the following equation:

$$B = B_0 \cdot e^{-\frac{x}{b}} \quad (2)$$

With: B = the average cross-sectional and tidal-average width (m)

B_0 = the width at the estuary mouth (m)

x = the distance from the mouth

The slope of the relationship between $\ln(B)$ and x then returns $-1/b$ (see Appendix A). The larger $1/b$, the more convergent the estuary is. Classically, the b value is determined for the whole estuary (Savenije, 1998), however we observed some important breaks in $\ln(B)$ for 3 out of 4 estuaries (Scheldt, Elbe and Humber). The best example is the Humber-Ouse estuary where the Humber is clearly much more convergent than the Ouse tributary (see Figure A 4). When defining breaks, we assumed that estuary convergence has mainly an effect on tidal amplification/damping over a large distance along the estuary (>

20 km). Smaller, more local variations in $\ln(B)$ were not considered. The found $1/\beta$ values are listed in Table 4.

Sensitivity analysis

For the Scheldt estuary a sensitivity analysis was performed on the tidal damping scale (Figure 5) in relation to the following parameters:

- Chézy roughness coefficient: 40 – 50 – 60
- Phase lag HW – slack HW: 30' – 50' – 70'

These values were selected since they are common values in analysis for the Scheldt estuary (Savenije, 2001, 2005; van Rijn, 2011; Winterwerp, 2012)

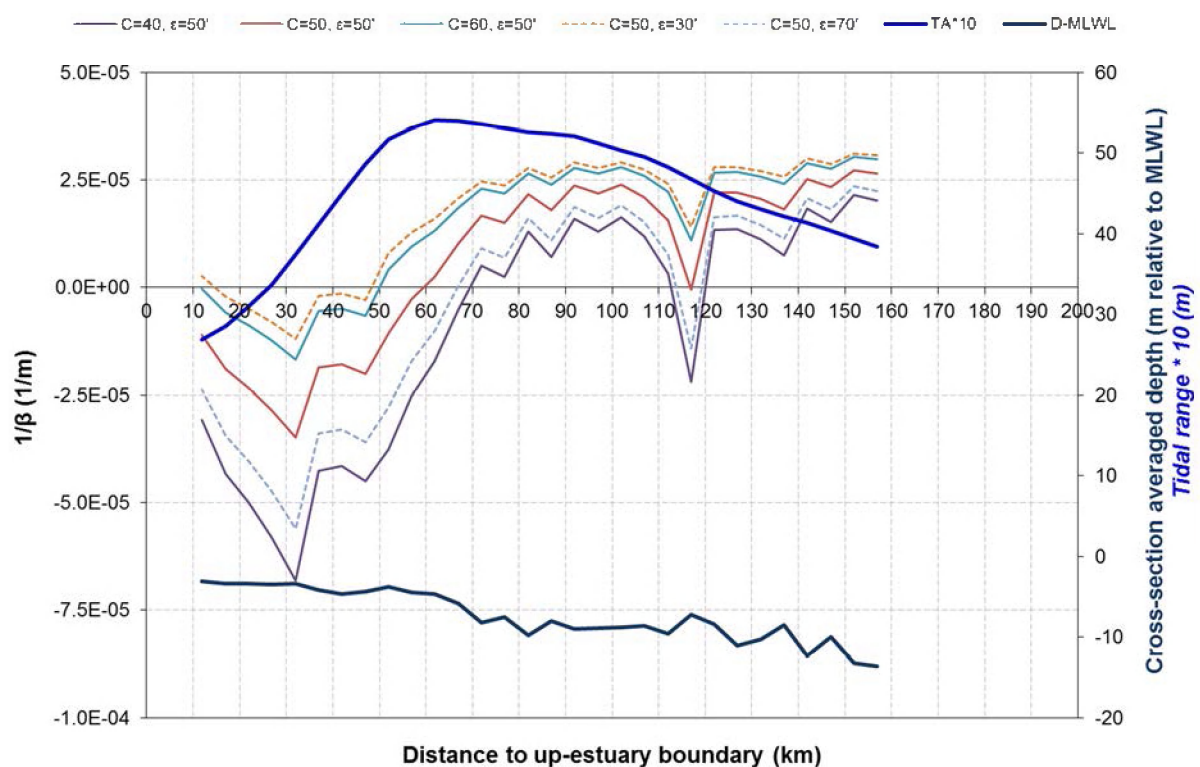


Figure 5 – Sensitivity analysis on the tidal damping scale for the Scheldt estuary

It was decided to use $C = 50$ and $\epsilon = 50'$ to calculate $1/\beta$ based on the following criteria:

- There should be a good agreement between $1/\beta$ and the change in tidal range: if $1/\beta > 0$ we can expect an increase in tidal range, if $1/\beta < 0$ we can expect a decrease in tidal range
- The selected values for C and ϵ should be realistic values. A Chézy coefficient of 50 is a commonly used value in estuarine modeling (Savenije, 2001, 2005; van Rijn, 2011; Winterwerp, 2012). However, it should be pointed out that Chézy coefficients may vary in time for one estuary, and in between different estuaries (from 30-80, see Winterwerp (2012)). Under mean tidal conditions, a phase lag difference of 50 minutes is representative for estuaries with semi-diurnal tides (Savenije, 2001)

For the calculation of $1/\beta$, some of the parameters are variable along the length axis of the estuary, others or constant. An overview is given in Table 4.

Table 4 – Overview of the parameters used to calculate $1/\beta$

Parameter	Scheldt	Elbe	Weser	Humber
1/b [m⁻¹]	2.42*E-5 (TIDE km 0-52) 3.74*E-5 (TIDE km 52-157) 3.39*E-5 (mean)	1.16*E-5 (TIDE km 0-24) 3.17*E-5 (TIDE km 24-149) 2.75*E-5 (mean)	2.79*E-5	2.17*E-5 (TIDE km 0-44) 5.4*E-5 (TIDE km 44-114) 4.18*E-5 (mean)
v [m/s]	Calculated for each “cubage” cross-section (based on cubage)			
ε [minutes]	50	50	50	50
c [m/s]	Calculated for each “cubage” cross-section			
h [m]	Calculated for each “cubage” cross-section			
η [m]	Calculated for each “cubage” cross-section (based on measured data)			
C [m^{1/2}/s]	50	50	50	50

3.2.3 Sediment fluxes

Introduction

Based on the derived tidal discharges calculated by applying the cubage technique (§3.2.1, see output parameters (b)) and the observed SPM values (see §3.1.4), sediment fluxes can be calculated according to the following equation:

$$SF = -C_s \frac{Q}{A} \quad (3)$$

With: SF = sediment flux per unit cross section (kg/m²/s)

C_s = concentration suspended particle matter (kg/m³)

Q = tidal discharge over one tidal cycle at mean tidal conditions, positive from up-estuary to down-estuary (ebb = + | flood = -) (m³/s)

A = wet section at mean tidal conditions during half tide (= mean of wet section at low water and high water) (m²)

Implementation

Tidal discharges over a tidal cycle, representative for mean tidal conditions, were calculated at every water level station (§3.1.2). For the Scheldt these tidal discharges were calculated under conditions of mean riverine discharges (see Plancke et al., 2011). For the Elbe, Weser and Humber tidal discharges were calculated under conditions of high and low riverine discharges (see Plancke et al., 2012a,b,c). If the netto discharge over a tidal cycle is positive than the water is transported in the ebb direction, if the netto discharge over a tidal cycle is negative than the water is transported in the flood direction. SPM values at

the water level stations were derived by use of linear interpolation (SPM stations not at the same locations as the water level stations, see Figure 9 till Figure 12). Based on the available SPM data and calculated tidal discharges (see Table 5), sediment fluxes were calculated according to equation (3). The sediment fluxes in the flood direction are hereby positive and the sediment fluxes in the ebb direction are negative (see equation (3)). Sediment fluxes under mean riverine discharges for the Elbe, Weser and Humber were determined by averaging the calculated sediment fluxes under high and low riverine discharge.

For each water level stations a netto sediment flux was calculated, as the sum of the different sediment fluxes per time step over a full tidal cycle.

Table 5 – Overview of the input parameters used to calculate sediment fluxes. (R = riverine discharge)

	SPM	Tidal discharges
Scheldt	surface and watercolumn	mean R
Elbe	surface	low and high R
Weser	surface	low and high R
Humber	surface	low and high R

It should be mentioned that this methodology is only a simple approximation of the real sediment fluxes. The methodology uses a constant SPM over the tidal cycle (due to limited data availability), while in reality the SPM will vary strongly over a tidal cycle (Figure 6). Therefore the calculated fluxes should be seen as a first approximation that will be used in the evaluation of topic 3.

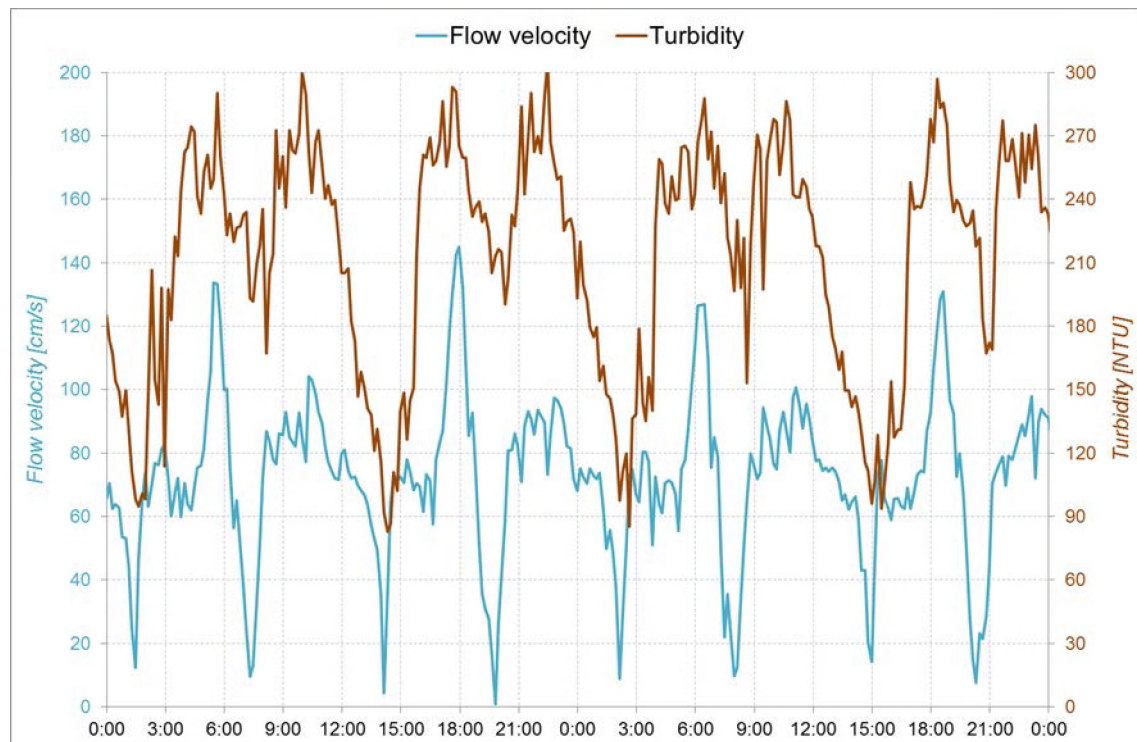


Figure 6 – Variation of flow velocity and SPM (turbidity) over tidal cycle for station Oosterweel (Scheldt estuary)

3.2.4 Tidal and fluvial energy (Dalrymple concept)

Introduction

The dalrymple energy-concept (Dalrymple et al., 1992) is used to calculate the total energy (E_{tot}) at a given cross-section in an estuary (i.e. the energy flux). The total energy is the sum of the total tidal energy (E_{tot}^{tide}) and the total fluvial energy (E_{tot}^q). The total tidal and fluvial energy are the sum of a kinematic and a potential energy component at a given cross-section, calculated according to the equations presented in Figure 7.

	Kinematic energy	Potential energy
	$\frac{m.v^2}{2}$	$m.g.h$
Tidal	$\frac{(\rho.V_{flood})(v_{flood})^2}{2}$	$(\rho.V_{flood})g.(MHW - MLW)$
Fluvial	$\frac{(\rho.(Q)T)\left(\frac{(Q)}{(A_{ebb})}\right)^2}{2}$	$(\rho.(Q)T)g.h_{topo}$

Figure 7 – Dalrymple energy-concept – equations used to calculate tidal and fluvial energy

With: ρ = density of water = 1000 kg/m³

V_{flood} = flood volume at mean tidal conditions (m³)

v_{flood} = mean flow velocity during flood at mean tidal conditions (m/s)

g = gravitation constant (9.81 m²/s)

MHW = mean high water level (m)

MLW = mean low water level (m)

Q = freshwater discharge (m³/s)

T = duration of a tidal cycle (s)

A_{ebb} = wet section at low water (m²)

h_{topo} = thalweg elevation relative to MLW at the most downstream cubage cross-section (m)

Implementation

Energy fluxes were calculated for every defined “cubage” cross-section. At these cross-sections, the necessary input parameters for the energy calculations, are the output parameters of the cubage calculation (see (§3.2.1)). As for the cubage calculations of the Elbe, Weser and Humber, energy fluxes were calculated for a winter and summer condition (using respectively P(95%) and P(5%) values for the freshwater discharge). Within this study, an earlier cubage calculation was used for the Scheldt using mean freshwater discharge (Plancke et al., 2011). Consequently, calculated energy fluxes are only representative for mean freshwater discharges. To make energy fluxes comparable within the interestuarine comparison (§5.3), mean fluxes were calculated for the Elbe, Weser and Humber by averaging the winter and summer energy fluxes.

3.2.5 Residence time

Introduction

Different simplified methods can be used to calculate residence times. A comparison between the different methodologies was made by Ides (2011b). It was found that for estuaries with a strong salinity gradient, the most appropriate method to calculate residence times is the fractional fresh water method (Dyer, 1973). As all estuaries within the TIDE project have a strong salinity gradient, the fractional fresh water method was applied, in which the residence time is defined as:

$$T = f \frac{V}{R}$$

With: T = residence time (days)

f = the fractional fresh water concentration = $(S_s - S_n)/S_s$

S_s = salinity at the most downstream cubage cross-section (PSU)

S_n = salinity in a given segment of the estuary (PSU)

V = volume of the estuary segment (m^3)

R = river discharge (m^3/s)

Implementation

The defined estuary segments were based on the cubage cross-sections (see Figure 3). For each estuary segment a fractional fresh water concentration was attributed based on the corresponding salinity profile. The segment volumes were calculated based on the mean cross-sectional area multiplied by the segment length. The mean cross-sectional area is hereby calculated as the average of the cross-sectional areas at MHWL and MLWL at both ends of the segment. River discharges for the Elbe and Weser are equal to the freshwater discharge of the main channel. Since the discharges of the tributaries are approximately 100 times smaller than the main channel discharge (see also §3.1.5), the river discharges along the estuary segments are constant. For the Scheldt and Humber this is not the case. There, each tributary has an important contribution to the river discharge (§3.1.5). As a consequence, the river discharge for the different estuary segments increases to the mouth by adding the discharges of the different tributaries. Residence times along the estuaries are eventually found by summing up the calculated residence times of the individual estuary segments.

3.3 Habitats

3.3.1 Classification

As described in §2, habitat quantification became an important parameter in research topic 2. As a first step in the quantification of habitats, a classification with 6 different classes was introduced:

- Subtidal deep (Sd): > 5 m below MLWL
- Subtidal moderately deep (Sm): 5 – 2 m below MLWL
- Subtidal shallow (Ss): 2 m below MLWL – MLWL
- Intertidal flat (If): MLWL – MHWL; slope < 2.5%
- Intertidal steep (Is): MLWL – MHWL; slope > 2.5%
- Marsh (M): > MHWL

This habitat classification was based on the work conducted by Bioconsult Schuchardt & Scholle for the TIDE project and by previous work by Brys et al. (2005).

3.3.2 Habitat mapping and quantification

A GIS algorithm was developed to map the different habitats based on above described classes. As a first step, MLWL and MHWL surfaces were created by interpolating (kriging) the water level values (see Figure

17) of the different water level stations (locations, see Figure 9, Figure 10, Figure 11 and Figure 12). By subtracting the MLWL surface with the topo-bathymetry grid², a subtidal grid file was created in which the 3 subtidal classes were defined. All pixel values below MLWL are thus defined as subtidal classes dependent on the depth, all values above MLWL were classified as 'NoData'. By subtracting the MHWL surface with the topo-bathymetry grid, a marsh grid was created in which the marsh class was defined. All pixel values above MHWL were defined as marsh, all values below MHWL were classified as 'NoData'. In a next step, a slope grid (intertidal grid) was created based on the topo-bathymetry grid. Pixels values below 2.5% were hereby classified as intertidal flat, pixel values above 2.5% were classified as intertidal steep. By merging the marsh grid, the subtidal grid and the intertidal grid (in this order), and executing a clip with the dyke lines, a habitat grid was created for each estuary. Finally, a habitat map was created by converting the habitat grid to a polygon shapefile.

The habitats were quantified in GIS in two ways: (1) by their surface area, and (2) by their relative width compared to the local estuary width. Surface areas were calculated using the polygon shapefile. Quantification by surface areas is not only important for the hydro-geomorphology study, but also for the ecology and ecosystem service studies within work package 3. The relative width of each habitat was quantified by intersecting the habitat map with the cubage cross-sections (§3.2.1). In this way the cross-section lines were split into separate lines in which each segment represents the width of a habitat. By summing the lengths of the distinct habitat segments, the total habitat length along a cross-section was calculated. Dividing these values by the total cross-section length (*100) returns the habitat percentages along each cross-section. These percentages were then related to the tidal range gradient (§5.2).

3.4 Mouth definition

Within the TIDE project it was agreed to plot estuary characteristics along the length profile of the estuaries against the so called TIDE kilometers (i.e. the distance to an up-estuary boundary, for example a weir). This agreement was made to easily compare the results of the different TIDE work packages (hydro-geomorphology, ecology, measures,...). However, within the interestuarine comparison of this hydro-geomorphological study, it was found that the TIDE kilometers approach was not suitable and that the definition of "a mouth" was necessary to make a proper comparison between the different estuaries.

Different criteria (shape, tidal influence, river influence, geology, salinity) can be used to define the mouth of an estuary (e.g., Savenije, 2005). Within this study it was decided to define the mouth dependent on the research topics (for an overview of the research topics see §2). Two definitions for the mouth will be used in this study:

- Mouth based on the width change ($\text{mouth}_{\text{geo}}$): once the width change at MHWL is below a certain threshold value, at that location the mouth area stops and the estuary starts (see Figure 8)
- Mouth based on salinity ($\text{mouth}_{\text{sal}}$): once the salinity of the summer salinity profile drops below 30 PSU, at that location the mouth area stops and the estuary starts

The definition based on the width change is for example necessary for research topic 1. There the effect of estuary funneling on the tidal amplification is studied. For research topic 3, saline intrusion plays an important role and there the mouth based on salinity is a more useful approach.

The relationship between the TIDE km's, the distance to the $\text{mouth}_{\text{geo}}$, and the distance to the $\text{mouth}_{\text{sal}}$ is given in Table 6.

² The topo-bathymetry grids described in §3.1.1 were used for the Elbe, Weser and Humber. For the Scheldt, a more recent topo-bathymetry grid was used (2007-2009), however with a coarser resolution (20 x 20).

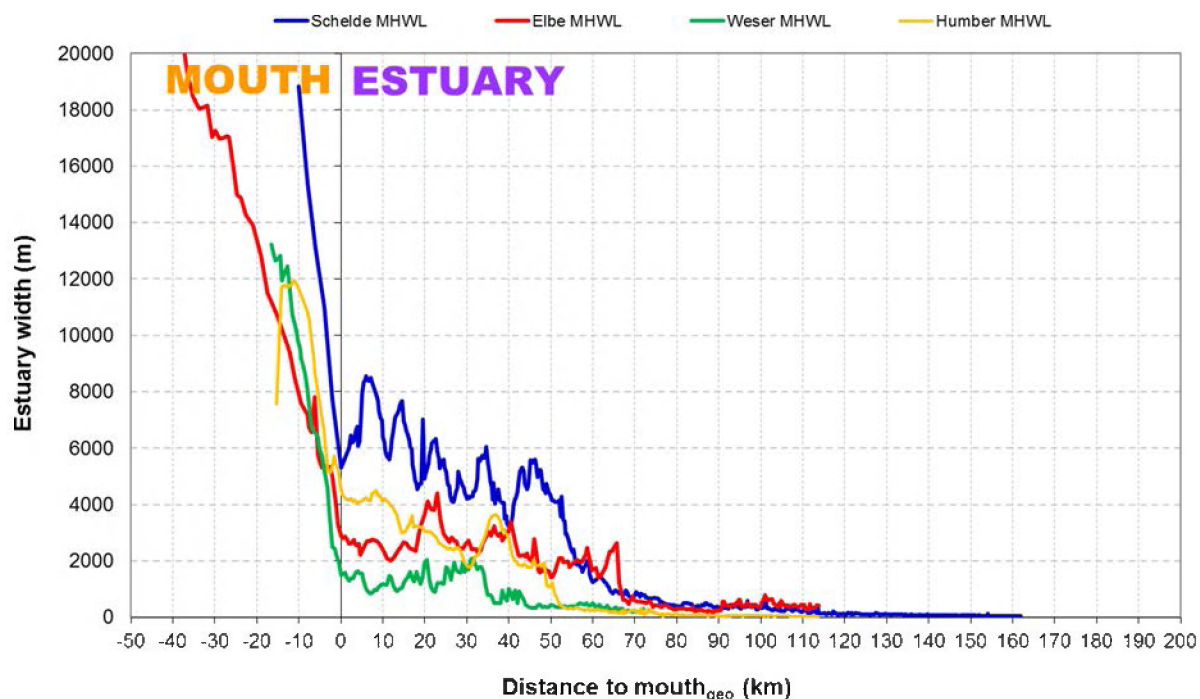


Figure 8 – Definition of the mouth_{geo} based on changes in estuary width

Table 6 – Relationship between the tide kilometers and kilometers to mouth_{geo} and mouth_{sal}. For the Scheldt, the distance to Vlissingen is also provided

TIDE km	Scheldt			Elbe		Weser		Humber	
	Mouth _{geo}	Mouth _{sal}	Vlissingen	Mouth _{geo}	Mouth _{sal}	Mouth _{geo}	Mouth _{sal}	Mouth _{geo}	Mouth _{sal}
160	2	-7	0	-46	-11	-88	-58	-46	-51
150	12	3	10	-36	-1	-78	-48	-36	-41
140	22	13	20	-26	9	-68	-38	-26	-31
130	32	23	30	-16	19	-58	-28	-16	-21
120	42	33	40	-6	29	-48	-18	-6	-11
110	52	43	50	4	39	-38	-8	4	-1
100	62	53	60	14	49	-28	2	14	9
90	72	63	70	24	59	-18	12	24	19
80	82	73	80	34	69	-8	22	34	29
70	92	83	90	44	79	3	32	44	39
60	102	93	100	54	89	13	42	54	49
50	112	103	110	64	99	23	52	64	59
40	122	113	120	74	109	33	62	74	69
30	132	123	130	84	119	43	72	84	79
20	142	133	140	94	129	53	82	94	89
10	152	143	150	104	139	63	92	104	99
0	162	153	160	114	149	73	102	114	109

4 TIDE estuaries

In this chapter an overview is given of estuary parameters along the longitudinal length axis (distances in this chapter in TIDE kilometers = the distance to the up-estuary boundary) of the four TIDE estuaries (Scheldt, Elbe, Weser and Humber). First, the estuary parameters are described per estuary (§4.1 - §4.4), followed by the figures where each parameter is presented for all 4 estuaries (§4.5). More general information on the four estuaries can be found in the TIDE fact sheets (http://www.tide-project.eu/index.php5?node_id=Downloads:83&lang_id=1).

4.1 Scheldt

The Scheldt (Figure 9) is a converging estuary characterized by a typical decrease in estuary width (from mouth to upstream boundary) (Figure 13). Towards the upstream boundary there is a general decrease in thalweg depth (Figure 14), whereas the decrease in cross-sectional averaged depth is more variable (Figure 15). From the mouth to TIDE kilometer 110, the cross-section averaged depth decreases, but at TIDE km 110 starts to increase again. At this point, the Scheldt estuary converts from a multiple channel system (i.e. several subtidal channels divided by intertidal areas) into a single channel system (i.e. one subtidal channel) (Figure 9). The general decrease in estuary width and estuary depth consequently leads to a decrease in the estuary's wet section (Figure 16).

The tidal range of the Scheldt is macrotidal with at mean tidal conditions a tidal range of 3.8 m near the mouth, a maximum tidal range of nearly 5.5 m at TIDE km 75, and a minimum tidal range of 2.7 m at the up-estuary boundary (Figure 18). As the tidal wave enters the estuary, the increase in tidal range (1-3 cm/km, see Figure 19) is caused by an increase in MHWL and a decrease in MLWL (Figure 17 and Figure 19). The maximum increase in tidal range is observed around TIDE km 120 (Figure 19). Once the maximum tidal range is reached, the strong decrease in tidal range in the upstream direction is mainly caused by an increase in MLWL (Figure 17 and Figure 19). In these upstream parts the tidal asymmetry (i.e. the ratio between mean tidal fall and mean tidal rise) is the highest with values up to 1.7 (Figure 20).

The mean freshwater discharge into the Scheldt estuary at Schelle (see Figure 9) is 107 m³/s. For a typical dry event (low discharge) the discharge is 34 m³/s (i.e. P(5%) value, see §3.1.5), for a typical flushing event this is 253 m³/s (i.e. P(95%) value, see §3.1.5). Low discharges are common during summer, whereas flushing events are more typical during winter (see Figure 21). For the Scheldt all tributaries have a significant contribution to the total river discharge at Schelle.

The mean and maximum cross sectional averaged flood and ebb flow velocities along the estuary respectively range from 0.1 to 1 m/s and from 0.25 to 1.5 m/s (Figure 22 and Figure 23). The maxima in v_{mean} and v_{max} are observed around TIDE km 70, which coincides with the maximum in tidal range (cf. Figure 22 and Figure 23 with Figure 18). The lowest flow velocities in the estuary are observed near the up-estuary boundary.

The tidal damping scale, which describes the tidal amplification and tidal damping in an estuary (see §3.2.2), is positive (amplification more important) from TIDE km 160 to 65 (Figure 24). This coincides with an increase in tidal range (see Figure 18 and Figure 19). From TIDE km 65, the tidal damping scale becomes negative (damping more important) and the tidal range decreases (see Figure 24 and Figure 19).

Under conditions of mean freshwater discharge, the fluvial energy in the estuary is more important from TIDE km 0-47, whereas the tidal energy is more important in the rest of the estuary (Figure 25). The tidal energy increases from the mouth to its maximum value at TIDE km 70. At this point the maximum tidal range occurs (cf. Figure 18 and Figure 25). The fluvial energy decreases from the up-estuary boundary towards the mouth, and reaches a value zero at TIDE km 110 where it no longer contributes to the total energy.

The Scheldt is a well-mixed estuary where it takes about 73 km for the mean salinity profile to decrease from 30 PSU to 1 PSU (i.e. a mean salinity gradient of 0.4 PSU/km) (Figure 26). During periods with low discharges (typical during summer) the salinity in the estuary increases, where during periods with high discharges (typical during winter) it significantly decreases (see Figure 26, respectively P(95%) and P(5%)

profiles). It takes about 83 km for the P(95%) profile to decrease from 30 to 1 PSU (i.e. a mean salinity gradient of 0.35 PSU/km), for the P(5%) profile this is 85 km (mean salinity gradient of 0.34 PSU/km). The maximum difference between the low and high discharge salinity profiles is about 13 PSU, whereas the maximum variation between low water and high water is about 6 PSU (Figure 27).

The suspended particle matter (representative for the mean over a tidal cycle, see §3.1.4) ranges from 30 mg/l near the mouth up to a maximum value of 300 mg/l (Figure 28). In the multi-channel part of the estuary (WesterScheldt) SPM values are low (30-50 mg/l) and no difference between the surface SPM and the depth-averaged SPM is observed. At about 100-110 km from the upstream weir there is clear increase in depth-averaged SPM which reaches a first peak at TIDE km 95 and a second one at TIDE km 57. Both turbidity maxima reach SPM values up to nearly 300 mg/l. For the surface SPM, the increase at TIDE km 110 is small and values further upstream do not exceed SPM values of 120 mg/l (Figure 28). At half tide conditions, the increase in depth-averaged SPM occurs further into the estuary (compared to the SPM values averaged over a tidal cycle), and SPM values reach maxima up to 400 mg/l (Figure 28).

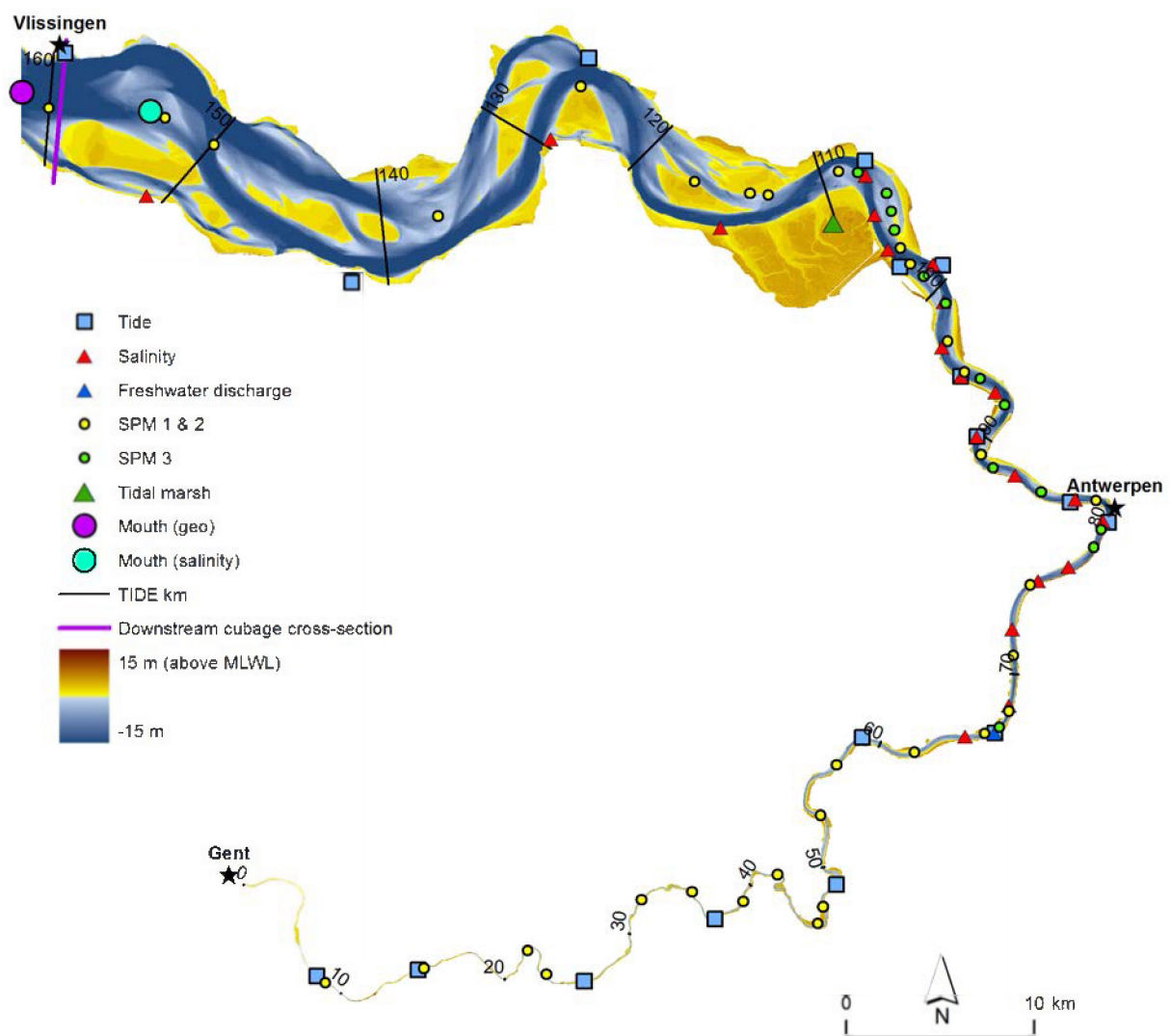


Figure 9 – Topo-bathymetry of the Scheldt estuary (2001) with indication of the different parameter locations, TIDE kilometers (i.e. distance to up-estuary boundary), and the most downstream cubage cross-section

4.2 Elbe

Whereas the Scheldt estuary can be considered as a typical converging estuary with a constant decrease in estuary width (Figure 13), the Elbe (Figure 10) is featured by 3 more or less prismatic channels (from TIDE km 113-68, from TIDE km 68-48, and from TIDE km 48-0, see Figure 13) which step-wise decrease in width. Remarkably, the thalweg depth is constant (due to dredging activities) up to the harbor of Hamburg (Figure 14). The Elbe is a multi-channel system from the mouth up to TIDE km 48, and a single channel in the most upstream part (TIDE km 48 – 0). At TIDE km 40 the Elbe splits into 2 single channels (the Northern and Southern Elbe) and merges again to one single channel at TIDE km 25 (Figure 10). The change in wet section is presented in Figure 16.

The Elbe is a mesotidal estuary with at mean tidal conditions a tidal range of 2.9 m near the mouth, a maximum tidal range of 3.6 m at Hamburg (Saint-Pauli), and a minimum tidal range of 2.15 m at the up-estuary boundary (Figure 18). As the tidal wave enters the estuary (from mouth_{geo}), the increase in tidal range (up to 2 cm/km, see Figure 19) is only important in the most upstream part of estuary (from TIDE km 75 towards up-estuary boundary, see Figure 18), whereas the tidal range in the downstream part of the estuary can be considered as more or less constant (from TIDE km 75 to mouth area, Figure 18). Once the maximum tidal range is reached, the strong decrease in tidal range in the upstream direction is caused by a decrease in MLWL (Figure 17 and Figure 19). The tidal asymmetry along the Elbe ranges between 1.1 and 1.6 with an increase in the upstream direction (Figure 20).

The mean freshwater discharge at Neu Darchau (see Figure 10) is 722 m³/s, calculated over the time period 2001-2010 (Figure 21). For a typical dry event (low discharge, P5) the discharge is 247 m³/s, for a typical flushing event (P95) this is 1709 m³/s. Low discharges are common during summer, whereas flushing events are more typical during winter (see Figure 21). For the Elbe, the main channel discharge (i.e. discharge at Neu Darchau) is about 100 times larger than the tributary discharges, and hence tributary discharges are negligible.

From the mouth to TIDE km 40, the mean and maximum ebb and flood flow velocities respectively range between 0.2 and 0.9 m/s (Figure 22), and between 0.4 and 1.3 m/s (Figure 23). High discharge conditions result in higher ebb flow velocities and lower flood flow velocities compared to low discharge conditions (summer) (Figure 22 and Figure 23). At the most upstream part of the estuary, this effect is even more pronounced (TIDE km 40-0): close to the up-estuary boundary, the high freshwater discharge results in the absence of a flood flow velocity (value zero, only vertical tide), but clearly reaches higher values for the ebb flow velocity (up to 1.5-2 m/s for v_{max} , see Figure 23).

The tidal damping scale which describes the tidal amplification and tidal damping in an estuary (see §3.2.2) is positive (amplification more important) from TIDE km 125 to 30 (Figure 24). This coincides with an increase in tidal range (see Figure 18 and Figure 24). From TIDE km 30, the tidal damping scale becomes negative (damping more important) and the tidal range decreases (see Figure 18 and Figure 24).

Under conditions with a high freshwater discharge, the fluvial energy in the Elbe estuary is higher and the tidal energy is lower compared to conditions with a low freshwater discharge (Figure 25). The point where fluvial energy becomes more important than tidal energy is for the winter (at TIDE km 40) and summer (at TIDE km 35) located close to each other.

The Elbe is a well-mixed estuary where it takes about 76 km for the mean salinity profile to decrease from 30 PSU to 1 PSU (i.e. a mean salinity gradient of 0.38 PSU/km) (Figure 26). During periods with low (typical during summer) and high discharges (typical during winter), the salinity in the estuary is respectively higher and lower compared to the mean salinity profile (see Figure 26, respectively P(95%) and P(5%) profiles). The maximum difference between the summer and winter salinity profiles is about 16 PSU, whereas the maximum variation between low water and high water is about 12 PSU for the winter, and 7 PSU for the summer (Figure 27).

The surface suspended particle matter (Elbe dataset representative for low water conditions, see §3.1.4) ranges between 25 mg/l and 250 mg/l and reaches a clear turbidity maxima at TIDE km 95 (Figure 28).

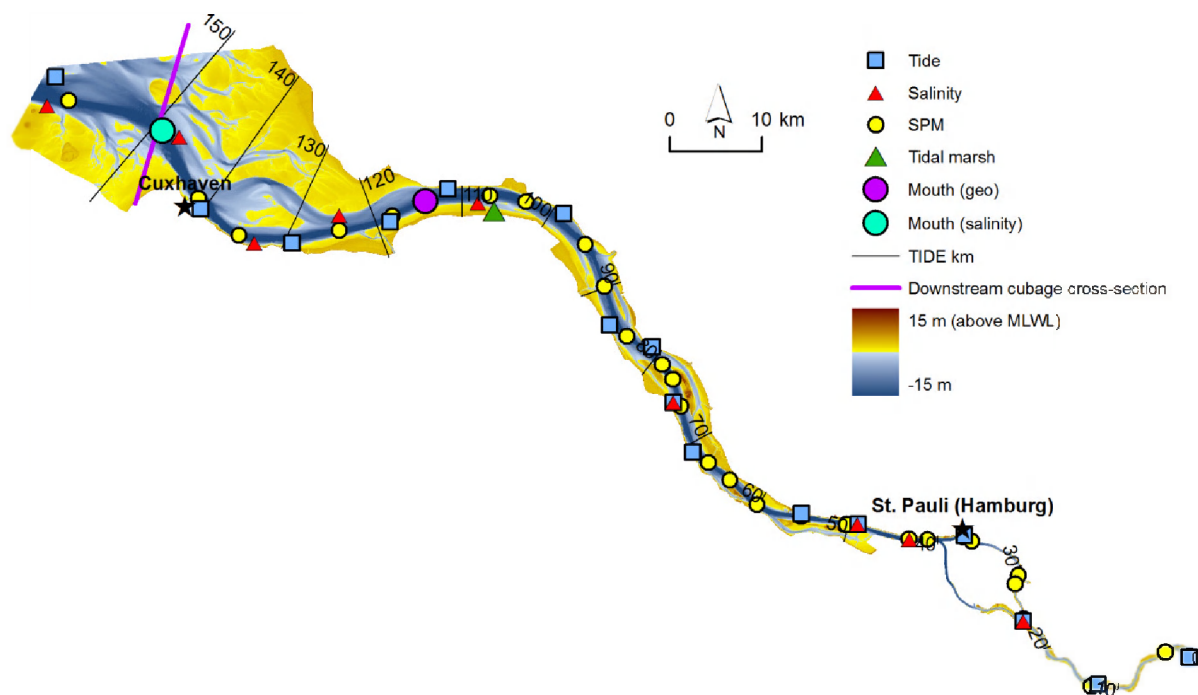


Figure 10 – Topo-bathymetry of the Elbe estuary (2006) with indication of the different parameter locations, TIDE kilometers (i.e. distance to up-estuary boundary), and the most downstream cubage cross-section

4.3 Weser

As for the Elbe, the Weser estuary (Figure 11) is featured by 3 more or less prismatic channels, one from TIDE km 72 to 38, one from TIDE km 38 to 28, and one at the most upstream part of the estuary (Figure 13). The thalweg depth gradually decreases from mouth to up-estuary boundary, with at TIDE km 10 a sudden shallowing of the thalweg depth (Figure 14). The Weser estuary is a multi-channel system from the mouth up to TIDE km 30, and a single channel in the most upstream part (TIDE km 30 – 0) (Figure 11). The wet section of the Weser has a typical decrease from mouth to up-estuary boundary (Figure 16).

The Weser is a predominant mesotidal estuary with only at the most upstream part (from TIDE km 20 to 0) a macrotidal regime (Figure 17). At mean tidal conditions, the tidal range at the mouth_{geo} is 3.8 m and reaches a maximum value in the most upper part of 4.1 m (Figure 17). Within the estuary there is a more or less constant increase of about 1 cm/km in MHWL. The constant tidal range between TIDE km 30 and 60 is caused by an increase in MLWL. For the rest of the estuary the tidal range increases, where from TIDE km 65-120 the increase in tidal range is caused by a small decrease in MLWL and an increase in MHWL. From TIDE km 0-30 the increase in tidal range is caused by only an increase in MHWL (see Figure 17, Figure 18 and Figure 19). The tidal asymmetry at mouth_{geo} has a value of 1 (duration of mean tidal fall and tidal rise is the same), but then increases in the upstream direction to a maximum value of 1.4 at the upstream boundary (Figure 20).

The mean freshwater discharge at Intschede (Figure 11) is 331 m³/s, calculated over a time period from 2001 to 2010 (Figure 21). For a typical dry event (low discharge, P5) the discharge is 122 m³/s, and for a typical flushing event (P95) this is 798 m³/s. Low discharges are common during summer, whereas flushing events are more typical during winter. For the Weser, the main channel discharge (i.e. discharge at Intschede) is significantly higher than the tributary discharges, and hence tributary discharges are negligible.

From the mouth to TIDE km 10, the mean and maximum ebb and flood flow velocities respectively range between 0.1 and 0.6 m/s (Figure 22), and between 0.2 and 1.3 m/s (Figure 23). High discharge conditions (winter) result in higher ebb flow velocities and lower flood flow velocities, compared to low discharge conditions (summer) (Figure 22 and Figure 23). At the most upstream part of the estuary, this effect is even more pronounced (TIDE km 10-0): close to the up-estuary boundary, the high freshwater discharge results

in the absence of a flood flow velocity (value zero, only vertical tide), but clearly reaches higher values for the ebb flow velocity (up to 1.5-2 m/s for v_{max} , see Figure 23).

The tidal damping scale which describes the tidal amplification and tidal damping in an estuary (see §3.2.2) is positive (amplification more important) for most of the estuary (Figure 24). Only between TIDE km 45 and 38 the tidal damping scale is negative and there no increase in tidal range is observed (see Figure 19 and Figure 24).

Under conditions of high freshwater discharge, the fluvial and tidal energy in the Weser estuary are respectively higher and lower compared to conditions with low freshwater discharge (Figure 25). The point where the fluvial energy becomes more important than the tidal energy is for the winter located near the mouth (at TIDE km 82), and for summer near the up-estuary boundary (at TIDE km 15). This is in contrast with the Elbe, where both points are located close to each other (Figure 25)

The Weser is a well-mixed estuary where it takes about 68 km for the mean salinity profile to decrease from 30 PSU to 1 PSU (i.e. a mean salinity gradient of 0.43 PSU/km) (Figure 26). During periods with low (typical during summer) and high discharges (typical during winter), the salinity in the estuary is respectively higher and lower compared to the mean salinity profile (see Figure 26, respectively P(95%) and P(5%) profiles). The maximum difference between the summer and winter salinity profile is about 16 PSU, whereas the maximum variation between low water and high water is about 11 PSU for winter and summer (Figure 27).

The surface suspended particle matter (Weser dataset representative for low water conditions, see §3.1.4) varies between 20 and 100 mg/l, and reaches a maximum at TIDE km 35 (Figure 28).

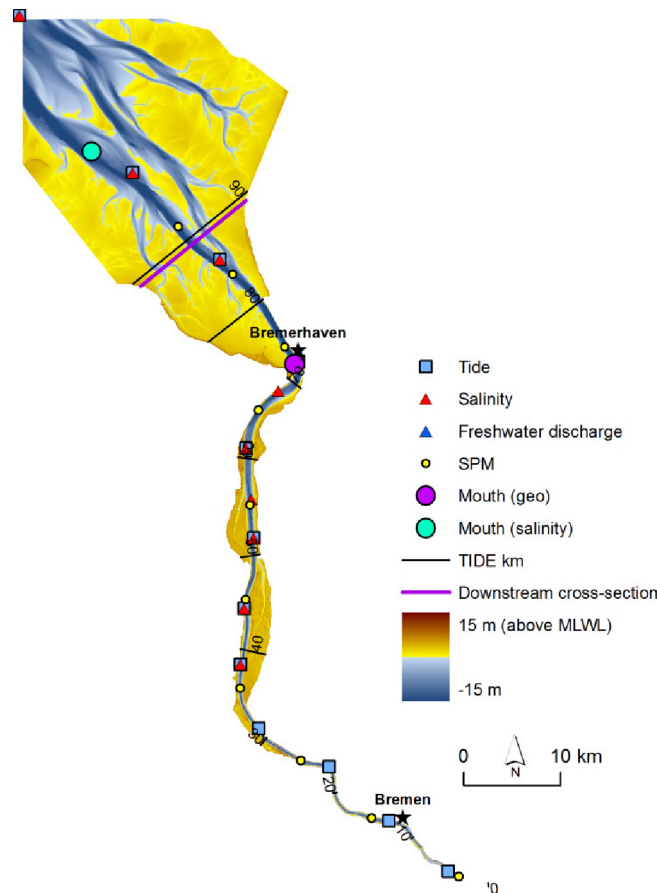


Figure 11 – Topo-bathymetry of the Weser estuary (2009) with indication of the different parameter locations, TIDE kilometers (i.e. distance to up-estuary boundary), and the most downstream cubage cross-section

4.4 Humber

As for the Scheldt, the Humber estuary (Figure 12) is a typical converging estuary, mainly from TIDE km 112 to TIDE km 82 (Figure 13). The thalweg depth clearly decreases from the mouth up to TIDE km 90, whereas the decrease from TIDE km 90 up to the up-estuary boundary is more gentle (Figure 14). The Humber-Ouse estuary can be considered as a multi-channel system from TIDE km 95 up to the junction with the Trent. The Ouse, Trent, and the most downstream part of the Humber (downstream TIDE km 95) can be considered as single channel systems (i.e. only one subtidal channel) (Figure 12). The decrease from mouth to up-estuary boundary in estuary width and/or estuary depth results in a decrease of the wet section (Figure 16).

The Humber is a macrotidal estuary with at mean tidal conditions a tidal range of 4.3 m at the mouth_{geo}, a maximum tidal range of 5 m at TIDE km 90, and a tidal range of 1.3 m at the Ouse up-estuary boundary (Figure 18). The increase in tidal range from mouth_{geo} to TIDE km 90 is caused by an increase in MHWL and a decrease in MLWL (Figure 17 and Figure 19). From then on a decrease in tidal range occurs, caused by a stronger decrease in MLWL than the increase in MHWL (Figure 18 and Figure 19).

The mean freshwater discharge at Skelton (Ouse up-estuary boundary) and North Muskam (Trent up-estuary boundary) is respectively 44 and 72 m³/s for the year 2010 (Figure 21). Including the Trent, the Ouse and all tributaries of the Ouse (Wharfe, Derwent, Aire and Don), this results in a mean discharge into the Humber of 209 m³/s. During flushing events (P95, typical during winter) and dry events (P5, typical during summer) the discharge at Skelton is respectively 143 and 9 m³/s, and at North Muskam respectively 177 and 29 m³/s.

The mean and maximum ebb and flood flow velocities respectively range between 0.1 and 1.5 m/s and between 0.1 and 2 m/s (Figure 22 and Figure 23). In Elbe and Weser high discharge conditions (winter) lead to higher ebb flow velocities and lower flood flow velocities in the entire estuary. For the Humber, this is only the case for the most upstream part (from TIDE km 40-0) due to the lower discharges (cf. estuaries in Figure 22). As for the Elbe and Weser, high discharges lead to the disappearance of the flood

The tidal damping scale which describes the tidal amplification and tidal damping in an estuary (see §3.2.2) is positive (amplification more important) in the most downstream part of the estuary (up to TIDE km 95, Figure 24). In the rest of the estuary the tidal damping scale is negative and there no increase in tidal range is observed (see Figure 19 and Figure 24).

Under conditions of high freshwater discharge, the fluvial and tidal energy in the Humber estuary are respectively higher and lower compared to conditions with low freshwater discharge (Figure 25). Only for the most downstream part of the estuary (TIDE km 71 to mouth) the tidal energy is also higher (i.e. the selection of a slightly higher tide in the estuary for the winter condition (Figure 25). The point where the fluvial energy becomes more important than the tidal energy is for the winter located at TIDE km 80, and for the summer near the up-estuary boundary (at TIDE km 10).

The Humber is a well-mixed estuary where it takes about 60 km for the mean salinity profile to decrease from 30 PSU to 1 PSU (i.e. a mean salinity gradient of 0.48 PSU/km) (Figure 26). During periods with low (typical during summer) and high discharges (typical during winter), the salinity in the estuary is respectively higher and lower compared to the mean salinity profile (see Figure 26, respectively P(95%) and P(5%) profiles). The maximum difference between the summer and winter salinity profile is nearly 16 PSU, whereas the maximum variation between low water and high water is about 6 PSU for winter and summer (Figure 27).

The surface suspended particle matter (representative for the mean over a tidal cycle, see §3.1.4) varies between 20 and 720 mg/l, and reaches a maximum at TIDE km 88 (Figure 28). Surface SPM values are for the Humber estuary clearly higher than for the other estuaries (cf. estuaries in Figure 28).

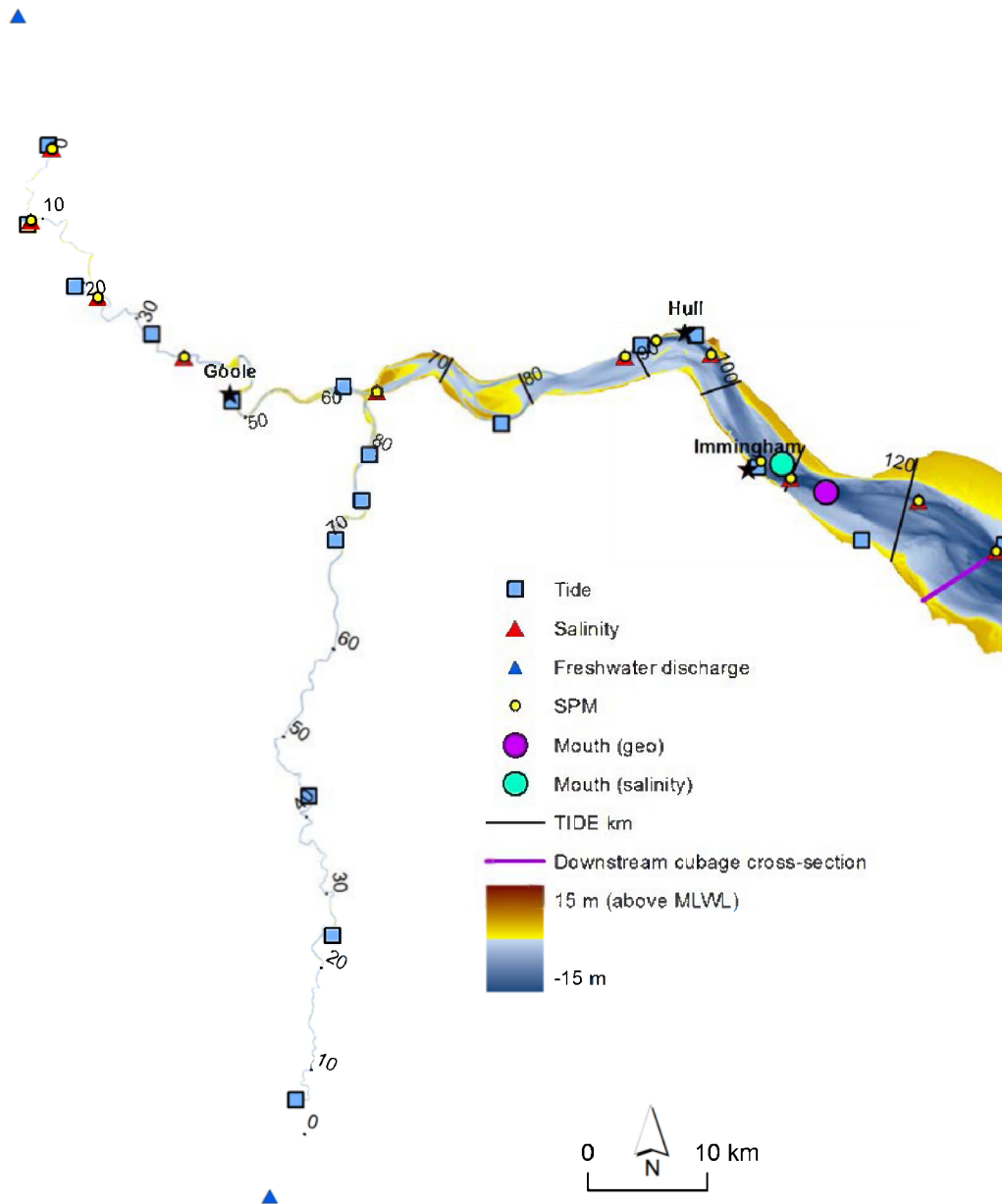


Figure 12 – Topo-bathymetry of the Humber estuary (2005) with indication of the different parameter locations, TIDE kilometers (i.e. distance to up-estuary boundary), and the most downstream cubage cross-section

4.5 Parameters of the 4 estuaries (TIDE km)

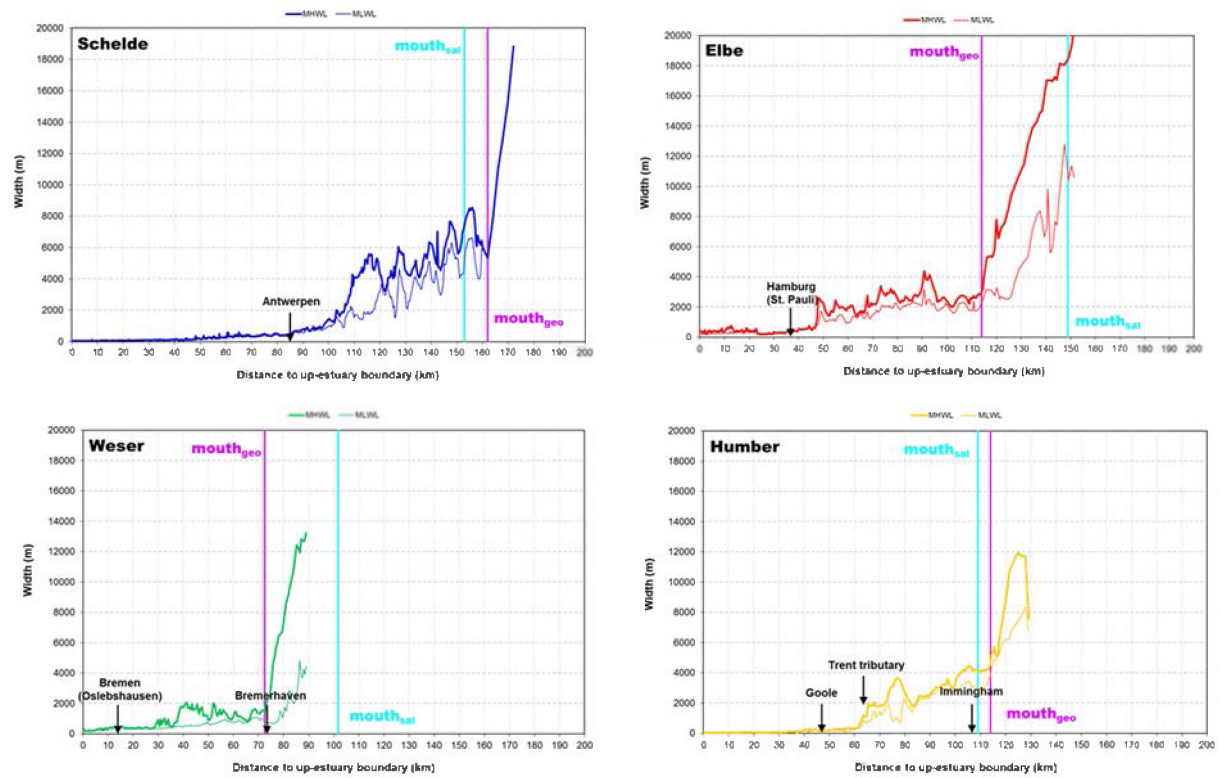


Figure 13 – Width at MHWL and MLWL for the Scheldt, Elbe, Weser and Humber-Ouse

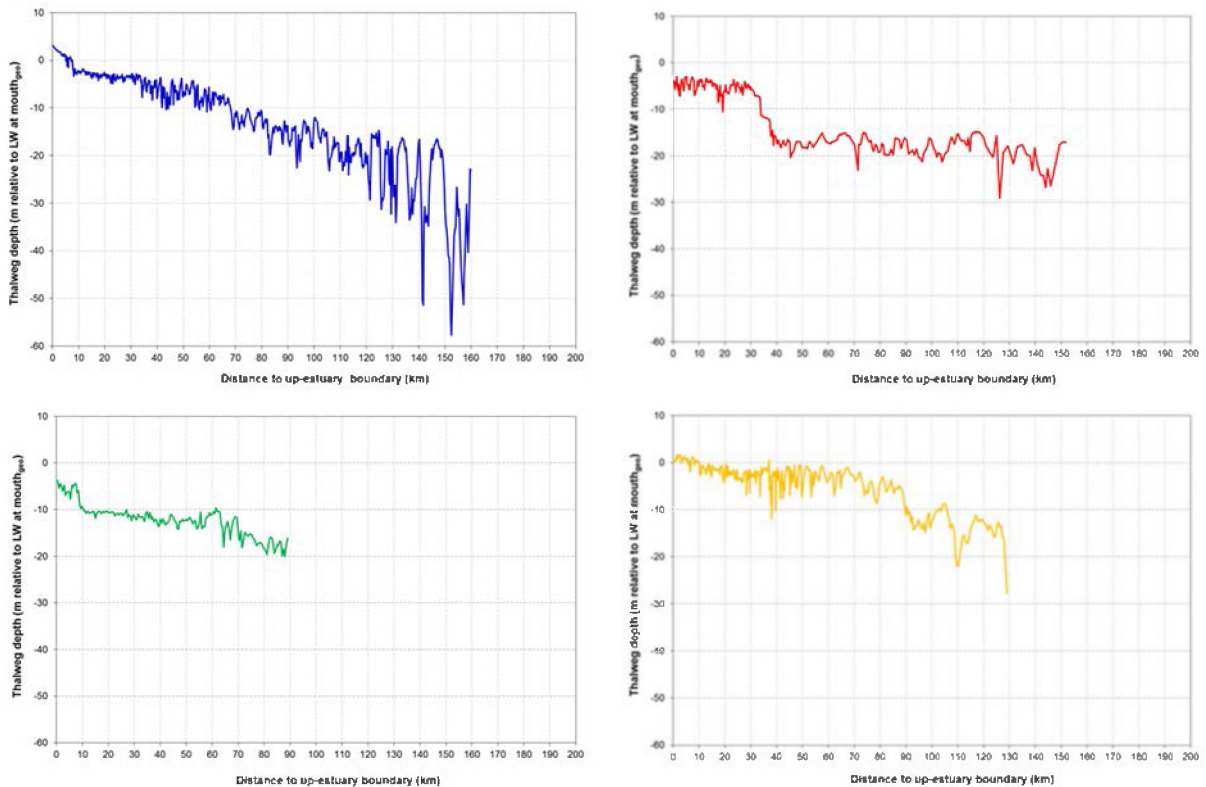


Figure 14 – Thalweg depth for the Scheldt (blue), Elbe (red), Weser (green) and Humber-Ouse (yellow), relative to low water level at mouth_{geo}

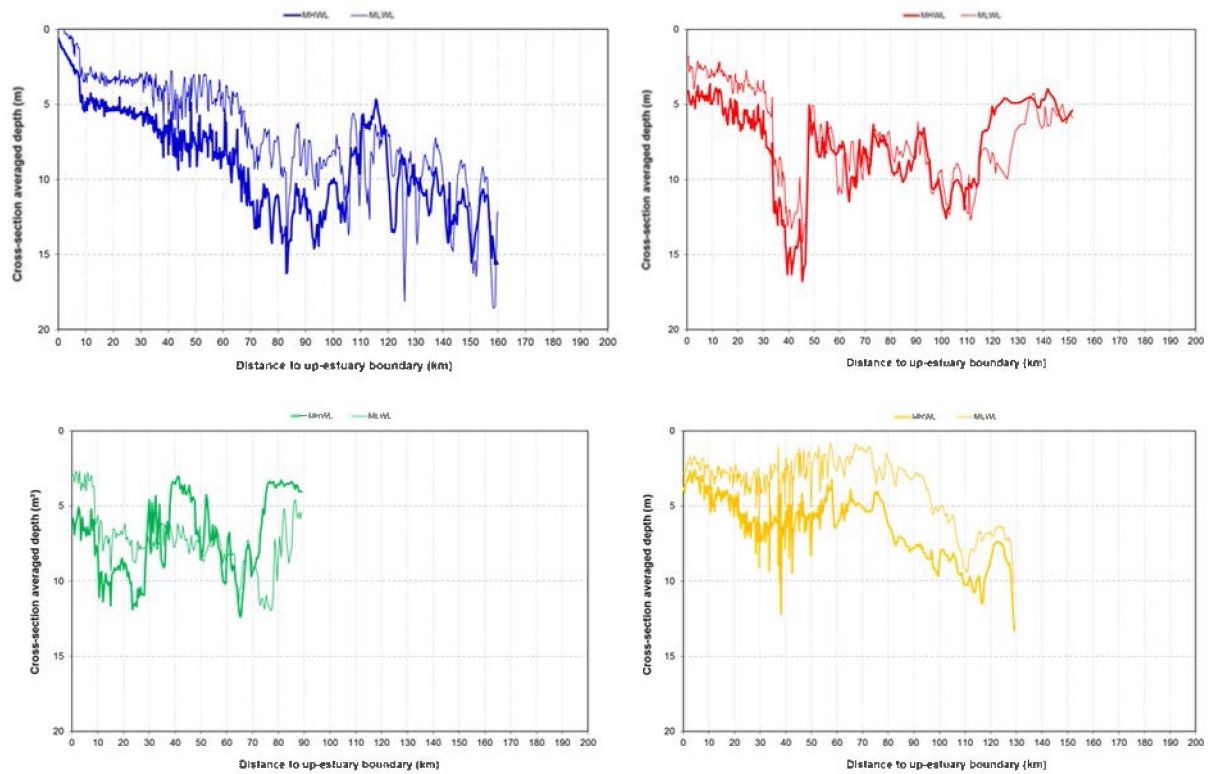


Figure 15 – Cross-section averaged depth at MHWL and MLWL for the Scheldt (blue), Elbe (red), Weser (green) and Humber-Ouse (yellow)

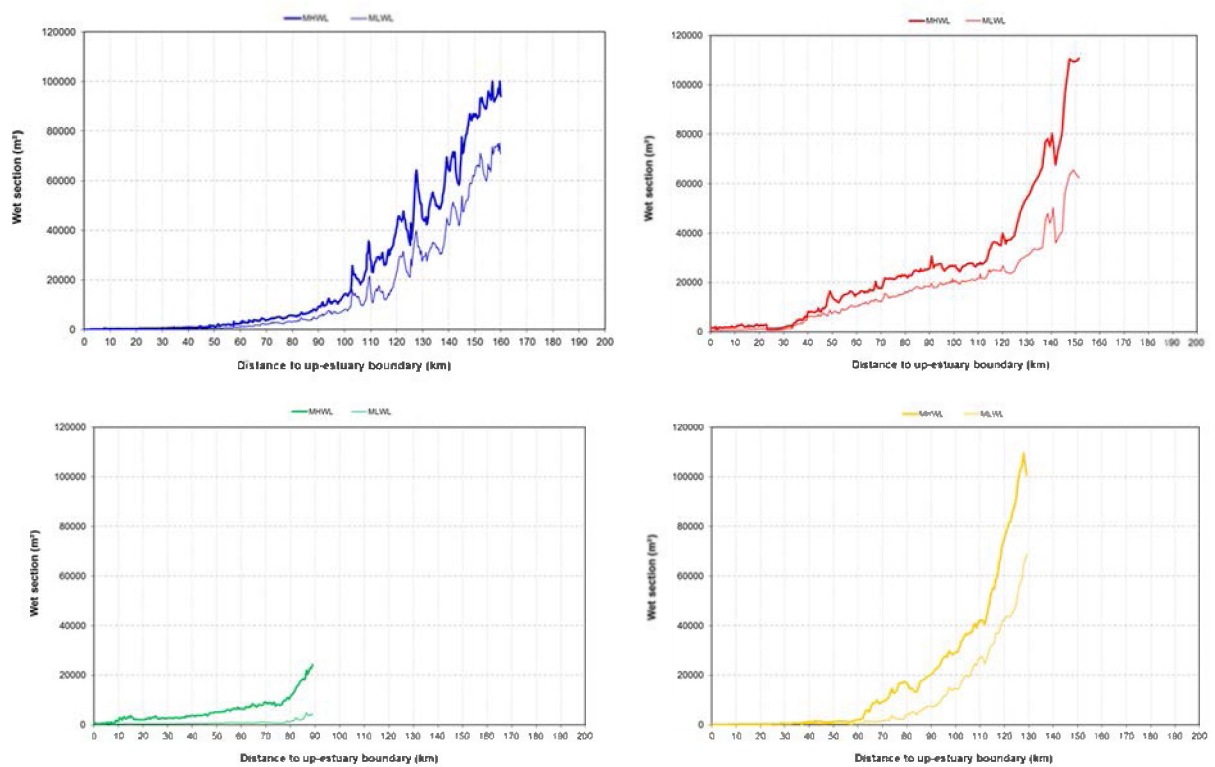


Figure 16 – Wet section at MHWL and MLWL for the Scheldt (blue), Elbe (red), Weser (green) and Humber-Ouse (yellow)

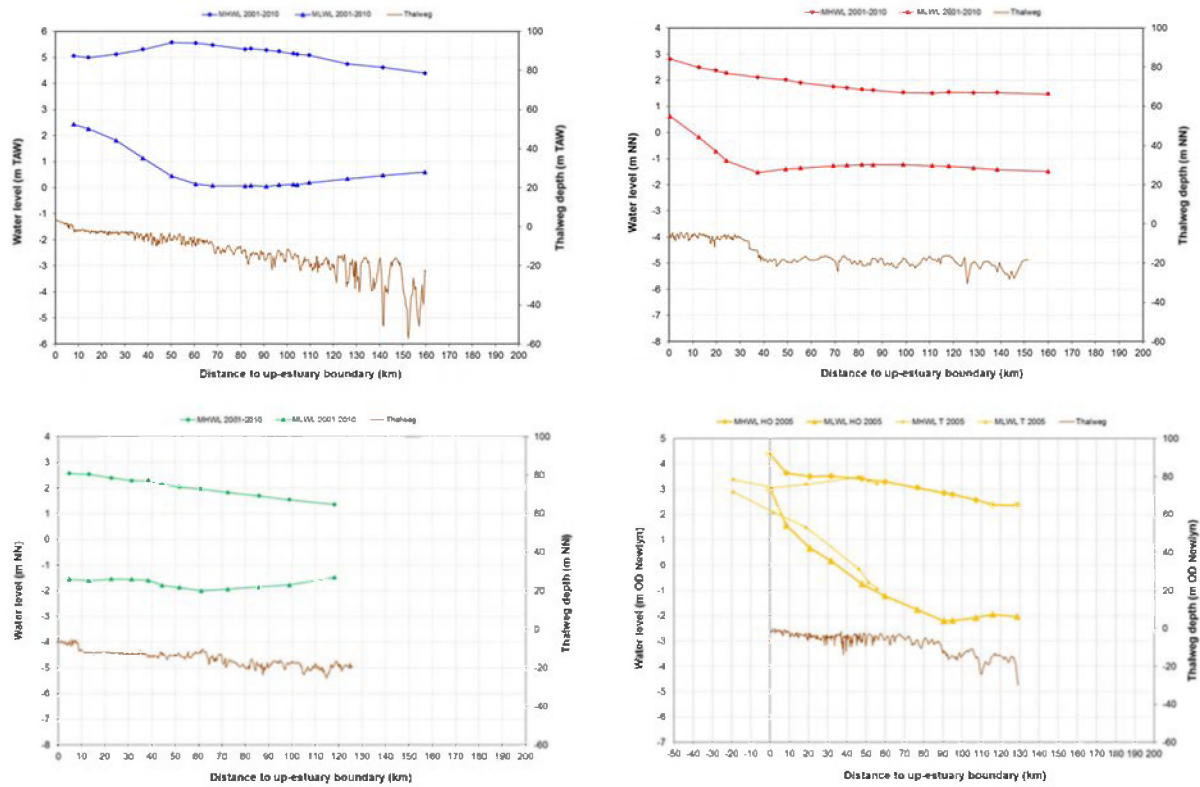


Figure 17 – Mean high water level (MHWL), mean low water level (MLWL) and thalweg depth along the Scheldt (blue), Elbe (red), Weser (green), Humber-Ouse and Trent (yellow); (m TAW = Belgian ordnance level; m NN = German ordnance level; OD Newlyn = British ordnance level)

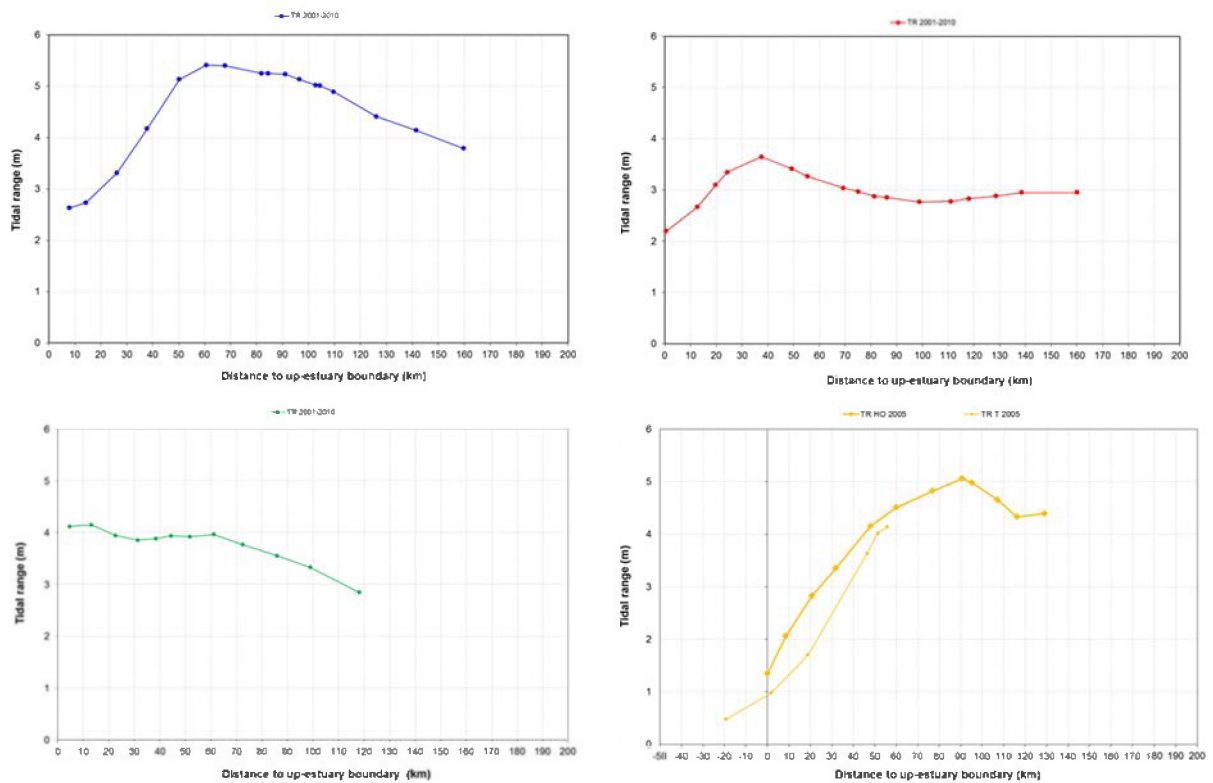


Figure 18 – Mean tidal range along the Scheldt (blue), Elbe (red), Weser (green), Humber-Ouse and Trent (yellow)

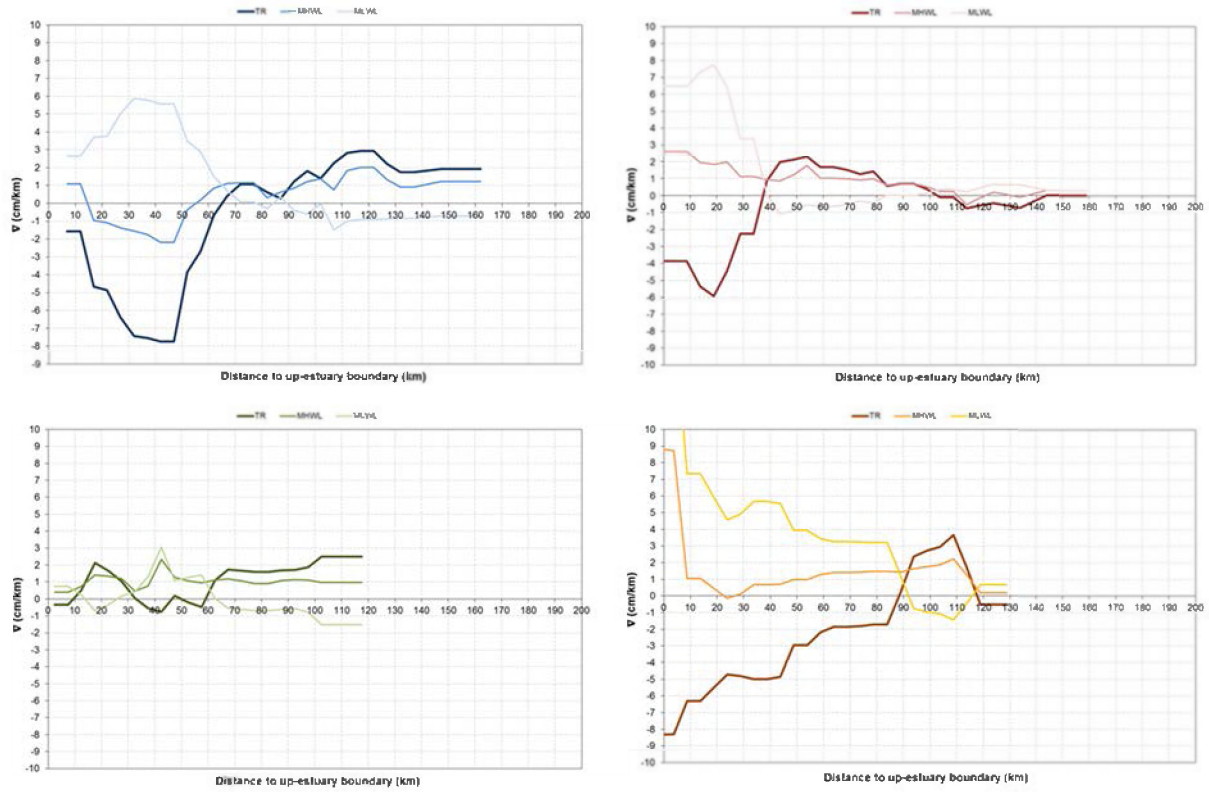


Figure 19 – Gradient (averaged over 5 km blocks) for the tidal range, MHWL and MLWL, for the Scheldt (blue), Elbe (red), Weser (green) and Humber-Ouse (yellow)

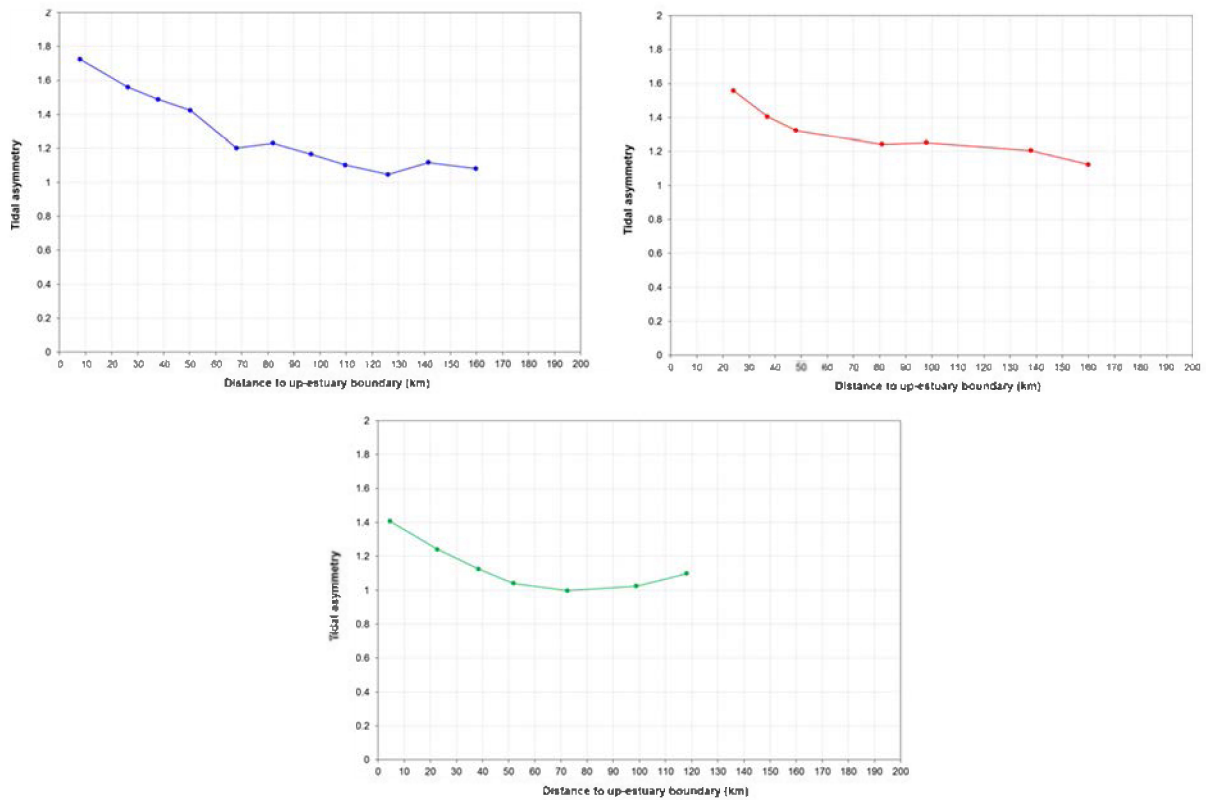


Figure 20 – Tidal asymmetry for the present situation along the Scheldt (blue), Elbe (red) and Weser (green). Tidal asymmetry presented by the ratio between mean tidal fall and mean tidal rise

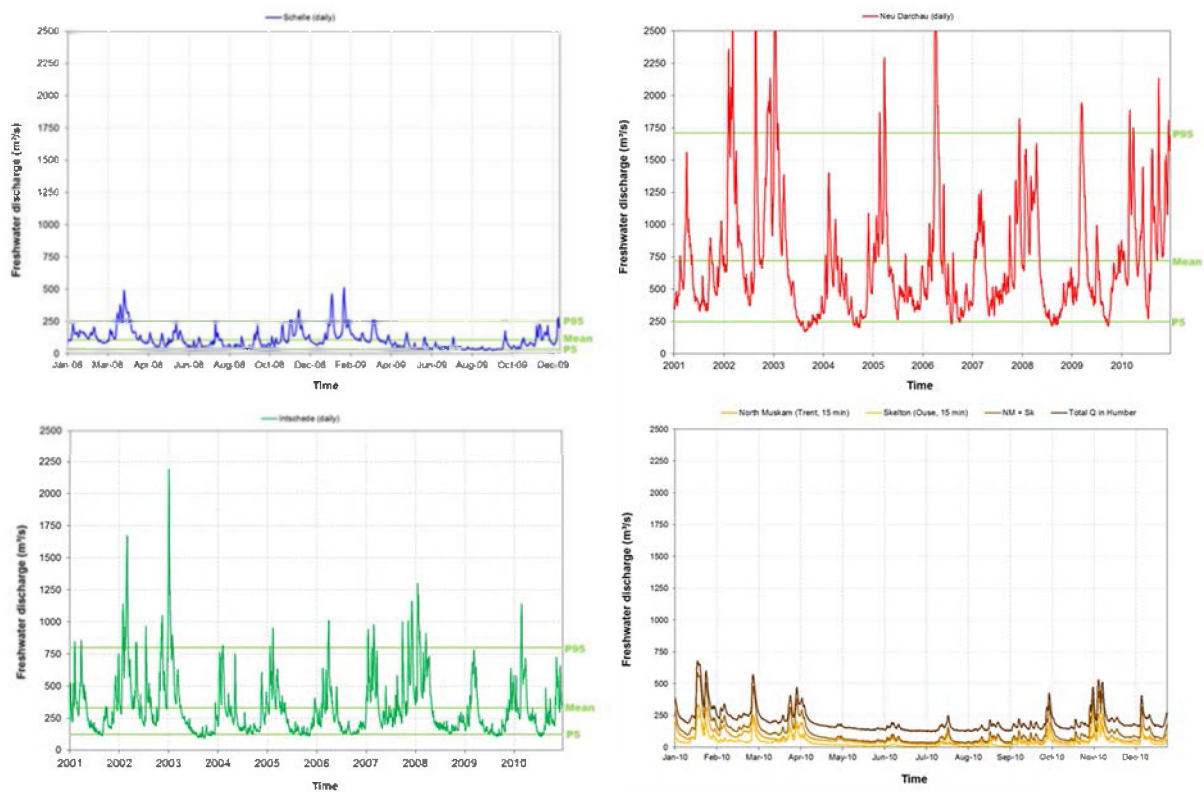


Figure 21 – Freshwater discharge at Schelle (Scheldt), Neu Darchau (Elbe), and Intschede (Weser). For the Humber, the freshwater discharge is presented at North Muskam (Trent up-estuary boundary) and Skelton (Ouse up-estuary boundary). Total Q in the Humber is sum of the discharges at North Muskam and Skelton, and the mean discharges of the other tributaries (Wharfe, Derwent, Aire and Don)

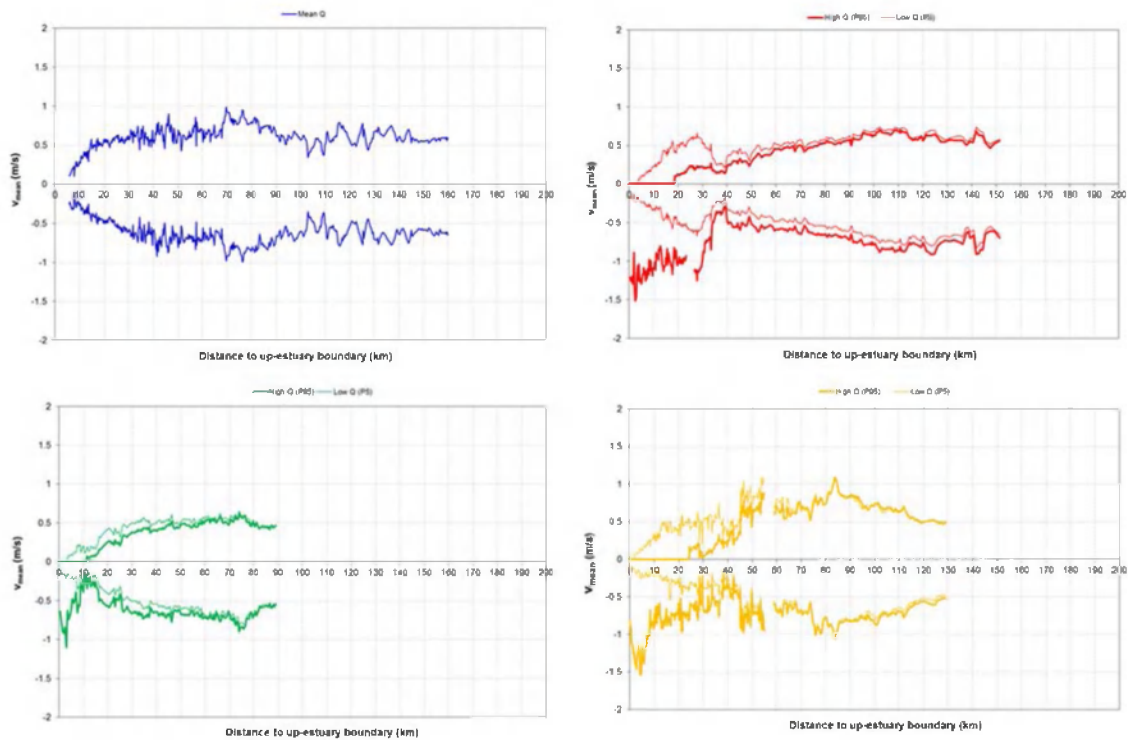


Figure 22 – Mean flood (+) and ebb (-) flow velocities (cross-section averaged) (v_{mean}) along the Scheldt (blue), Elbe (red), Weser (green) and Humber-Ouse (yellow), under high (winter) and low (summer) freshwater discharge conditions. For the Scheldt, flow velocities are only calculated under mean freshwater discharge conditions

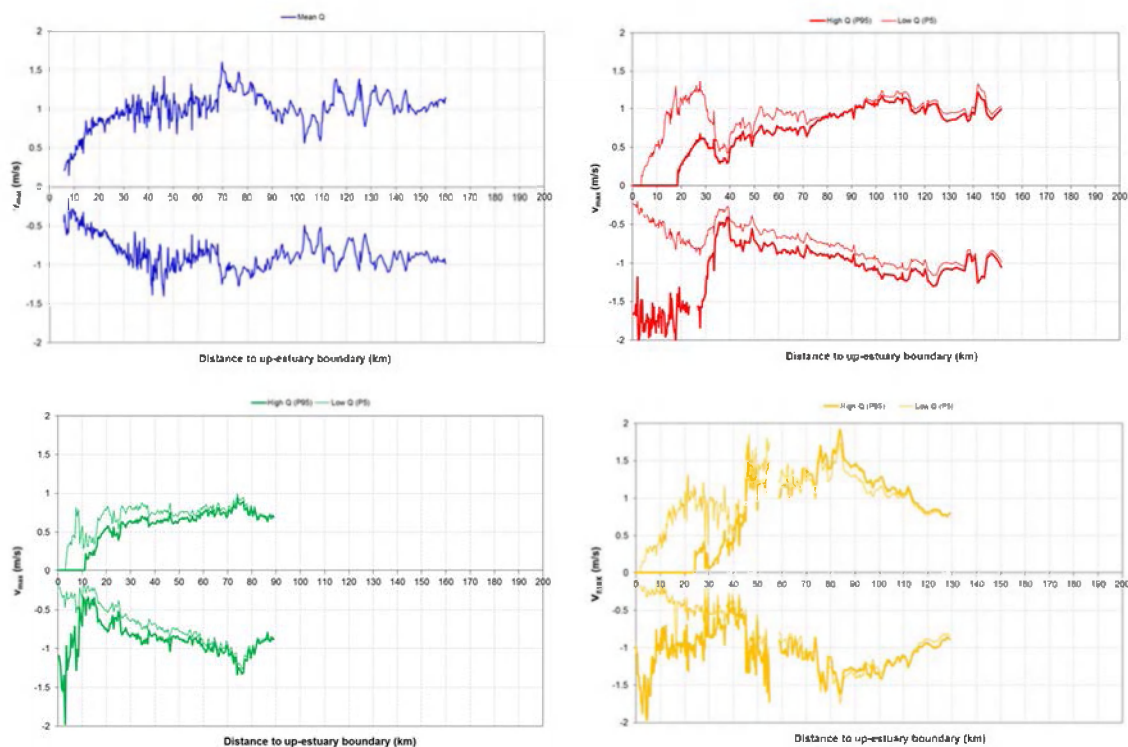


Figure 23 – Maximum flood (+) and ebb (-) flow velocities (cross-section averaged) (v_{max}) along the Scheldt (blue), Elbe (red), Weser (green) and Humber-Ouse (yellow), under high (winter) and low (summer) freshwater discharge conditions. For the Scheldt, flow velocities are only calculated under mean freshwater discharge conditions

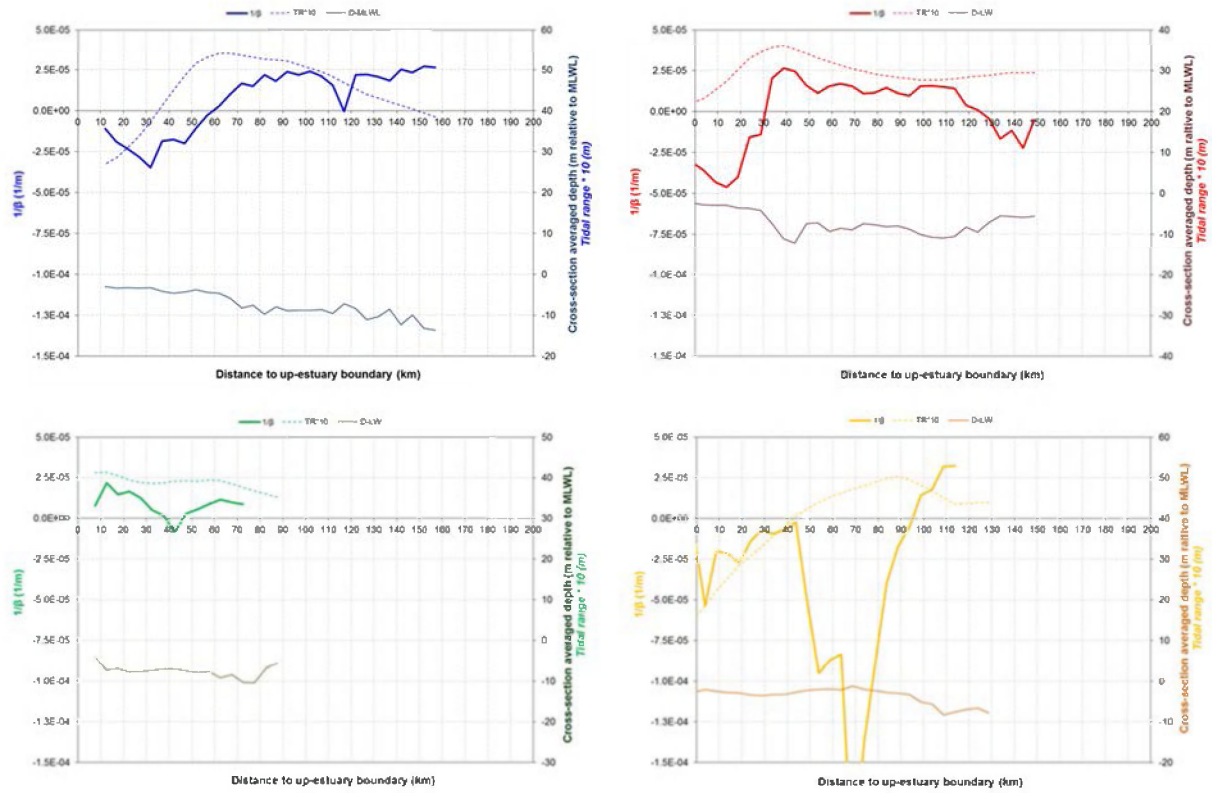


Figure 24 – Tidal damping ($1/\beta$) (averaged over 5 km blocks) for the Scheldt (blue), Elbe (red), Weser (green) and Humber-Ouse (yellow)

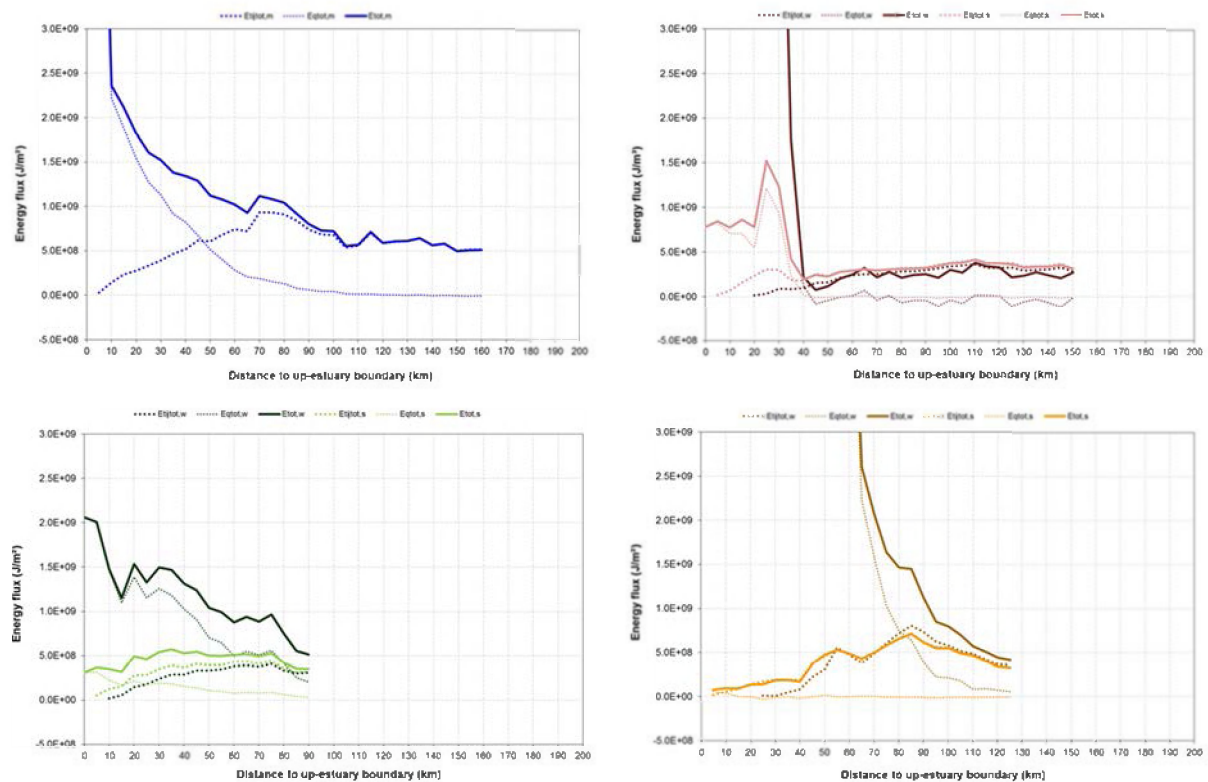


Figure 25 – Energy fluxes (tidal = $E_{tj,tot}$, fluvial = $E_{q,tot}$ and total = E_{tot} , averaged over 5 km blocks) along the Scheldt (blue), Elbe (red), Weser (green) and Humber-Ouse (yellow), under high (winter) and low (summer) freshwater discharge conditions. For the Scheldt, energy fluxes are only calculated under mean freshwater discharge conditions

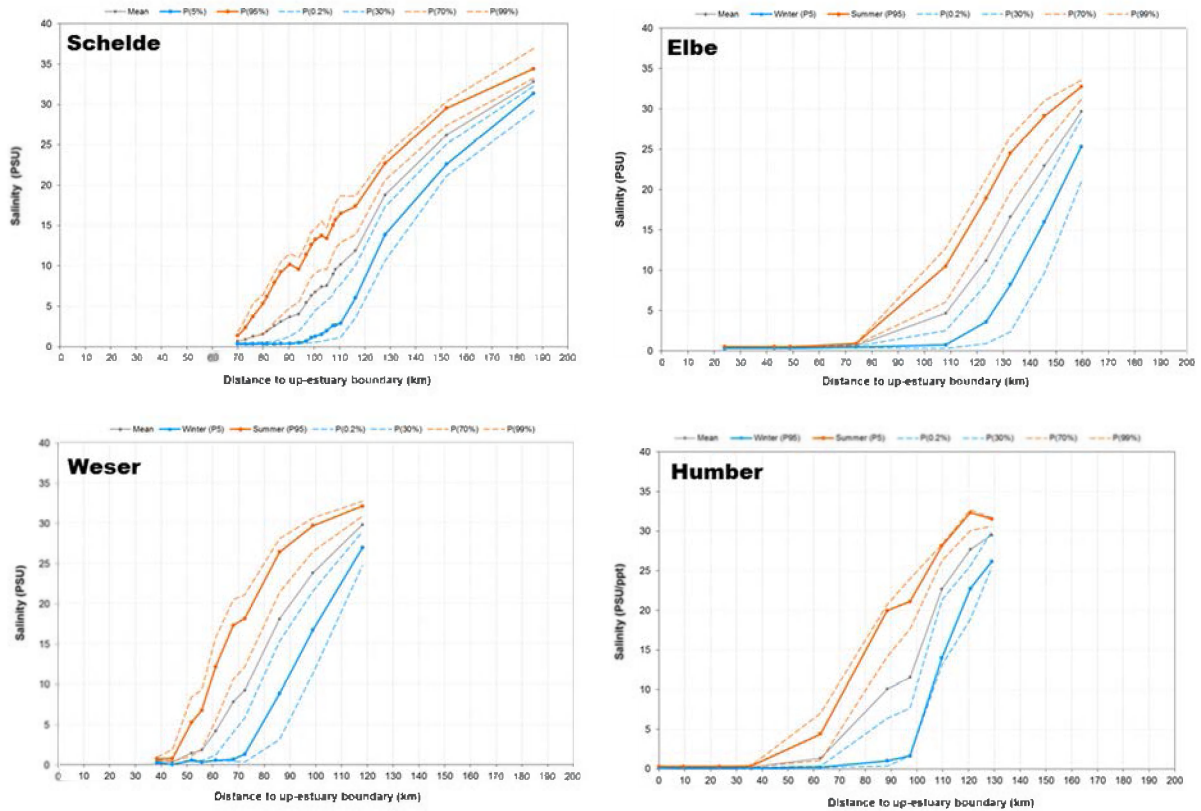


Figure 26 – Longitudinal mean (grey), winter (blue) and summer (orange) salinity profiles along the 4 TIDE estuaries, with indication of the low and high water envelopes for winter (P0.2 and P30) and summer (P70 and P99). Humber = Humber-Ouse

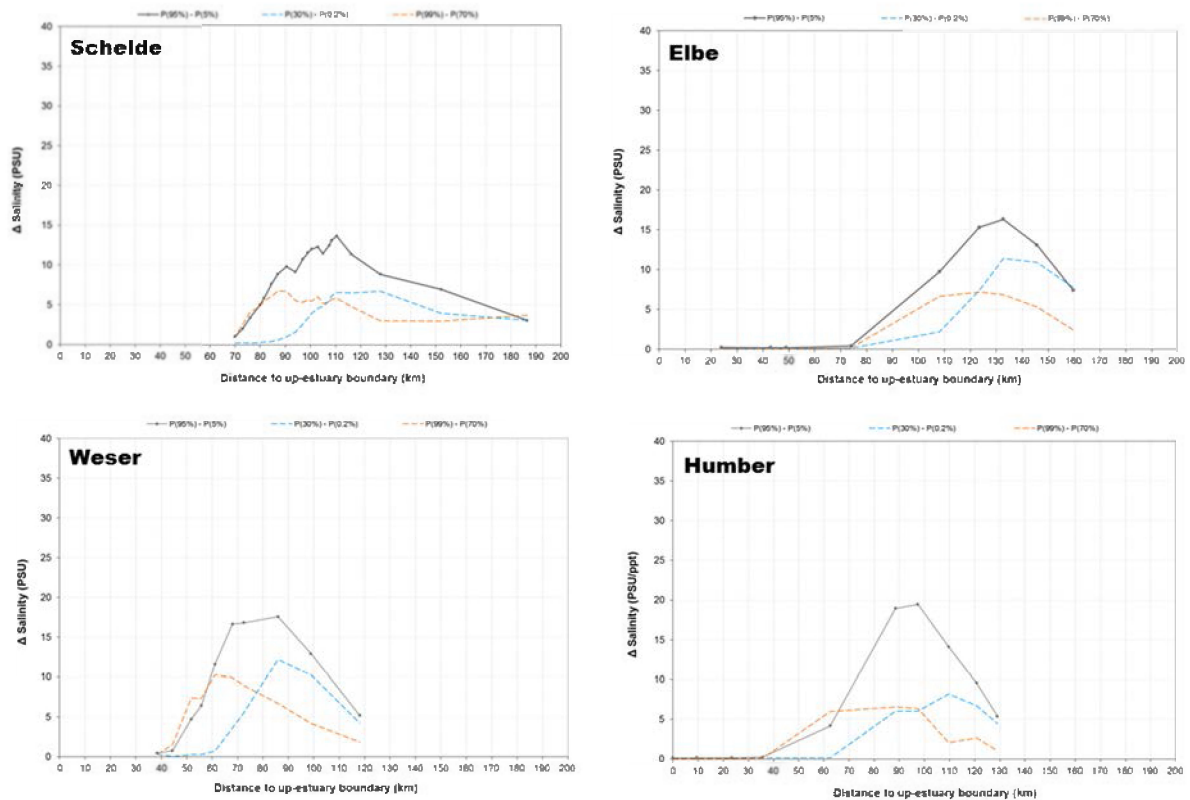


Figure 27 – Difference in salinity between the summer and winter profiles (grey), and between the high and low water envelopes (blue for winter, orange for summer) of Figure 26. Humber = Humber-Ouse

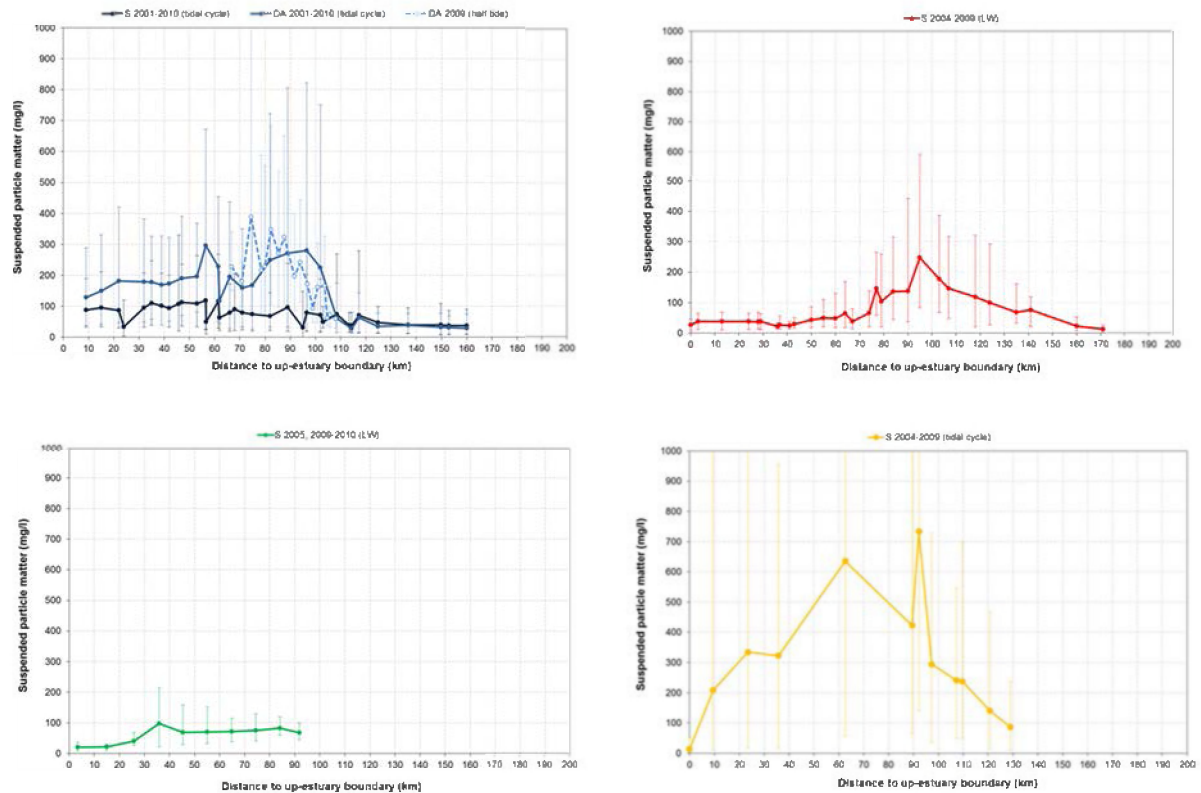


Figure 28 – SPM data for the 4 TIDE estuaries. For the Scheldt (blue): 3 different datasets are presented: (1) surface SPM for the period 2001-2010 (mean values over a tidal cycle), (2) depth-averaged SPM for the period 2001-2010 (mean values over a tidal cycle), and (3) depth-averaged SPM for the year 2009 at half tide conditions. For the Elbe (red): surface SPM at low water conditions. For the Weser (green): surface SPM at low water conditions. For the Humber-Ouse (yellow): surface SPM averaged over a tidal cycle. Error bars represent the P5 and P95 values.

5 Interestuarine comparison

5.1 TOPIC 1 – Tidal amplification

In this topic we study the factors that influence tidal amplification/tidal damping in an estuary. Moreover, we look at how tidal amplification in an estuary can be stopped or even be reduced. To study this topic, we used tidal data and topo-bathymetry data (see §3.1.2 and §3.1.1). Secondly, we calculated the tidal damping scale (§3.2.2), a parameter which describes tidal amplification/damping in an estuary.

5.1.1 Tidal range

The tidal range characteristics are unique for each estuary (Figure 29). The most important differences between the four estuaries are:

- The tidal range at the mouth
- The maximum tidal range
- The position of the maximum in tidal range
- The number of kilometers with increase/decrease in tidal range
- The strength of the increase/decrease in tidal range (i.e. the tidal range gradient)

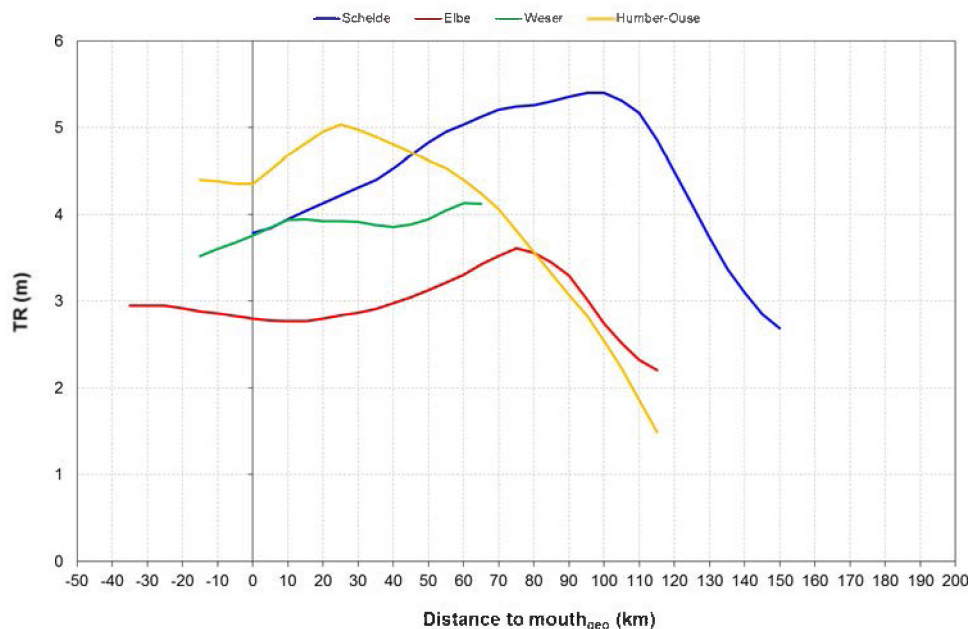


Figure 29 – 10-yearly averages for the tidal range (2001-2010) along the different estuaries. For the Humber, data are averaged over a time period of 1 year (2005)

The smallest and highest tidal ranges at the mouth are respectively observed for the Elbe and Humber. Scheldt and Weser have intermediate tidal ranges and are comparable (Figure 29). The tidal range in the Scheldt, Elbe and Weser estuaries is almost everywhere higher than the tidal range at the mouth (Figure 30, Figure 31: >80% estuary length). For the Humber, this is only the case for about 50% of the estuary length (Figure 31). Although the tidal range in the Weser estuary is for the entire estuary higher than the tidal range at the mouth, it is featured by the lowest TR_x/TR_0 values (Figure 30 and Figure 31). Two factors are important in determining TR_x/TR_0 values : (1) the value of the tidal range gradient, and (2) the distance over which increase/decrease in tidal range occurs (see Figure 32 and Figure 33). As a consequence, the rather low maximum in tidal range increase (2 cm/km), and the limited distance over which increase in tidal range occurs results in rather low TR_x/TR_0 values for the Weser. This is in contrast to the Scheldt estuary, where larger maximum values occur (up to 3 cm/km), and where the increase in tidal range occurs over a large distance (Figure 32 and Figure 33). In general we may conclude that tidal amplification is the highest

in the Scheldt ($TR_x/TR_0 \sim 1.4$), followed by the Elbe ($TR_x/TR_0 \sim 1.3$) and Humber ($TR_x/TR_0 \sim 1.15$), and that tidal amplification in the Weser is the smallest ($TR_x/TR_0 \sim 1.1$). Similar values are observed by van Rijn (2011)



Figure 30 – Dimensionless presentation of the tidal range defined by TR_x/TR_0 (with TR_x = tidal range at distance x in the estuary; TR_0 = tidal range at $mouth_{geo}$, $mouth_{geo}$ see Figure 9, Figure 10, Figure 11 and Figure 12).

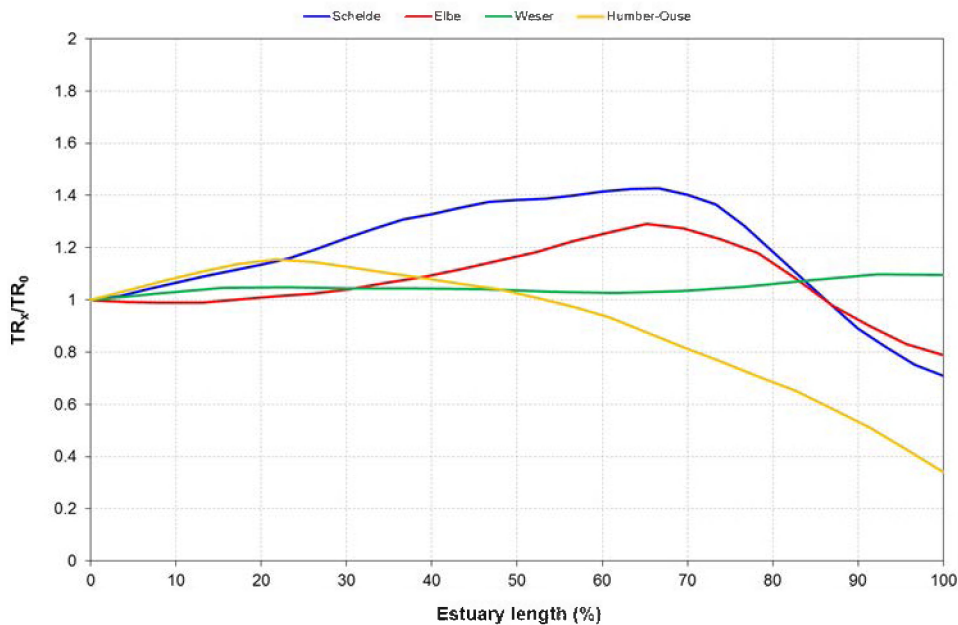


Figure 31 – Dimensionless presentation of the tidal range and distance along the estuary

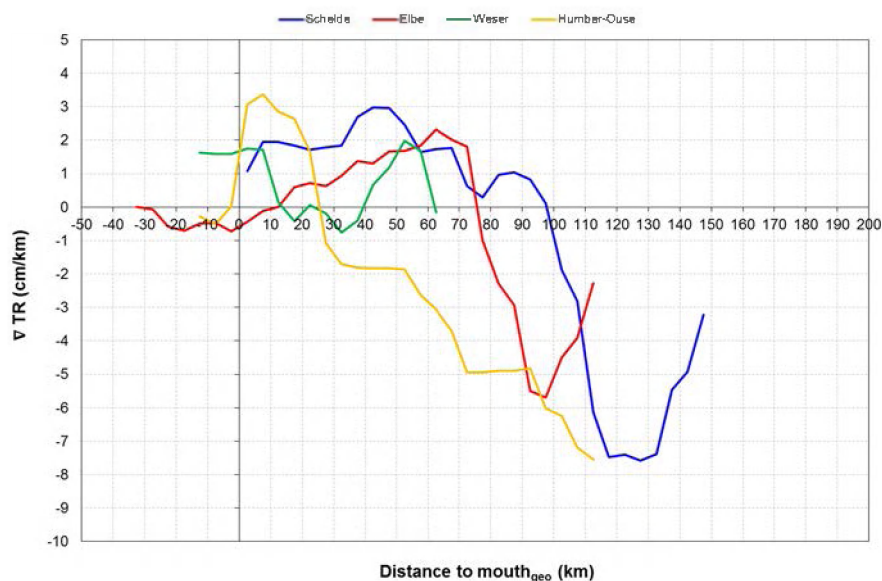


Figure 32 – Tidal range gradient along the 4 estuaries calculated over 5 km blocks

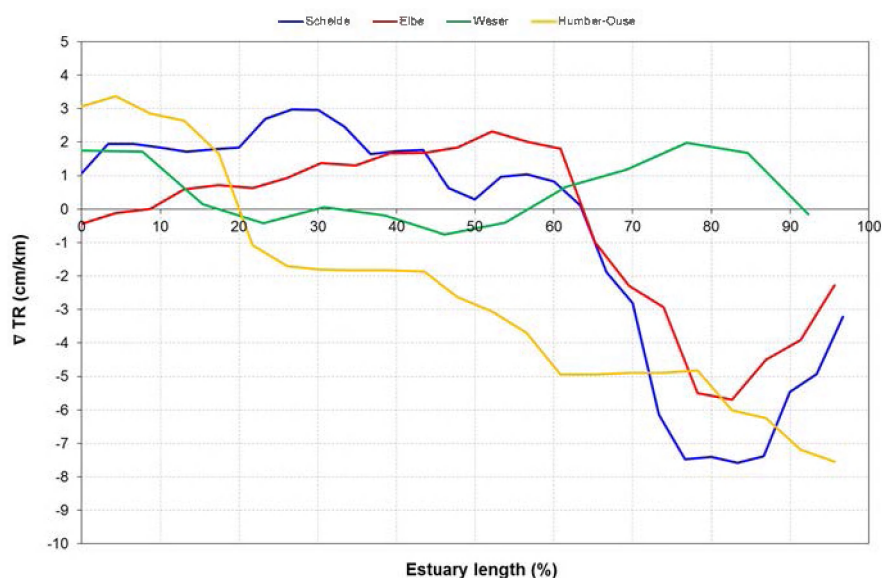


Figure 33 – Tidal range gradient along the 4 estuaries (dimensionless)

5.1.2 Damping or amplification?

Tidal damping and tidal amplification was in this study evaluated in two ways:

- By the theoretical derived tidal damping scale parameter (Savenije, 2001) (see §3.2.2): if $1/\beta > 0$ amplification prevails, if $1/\beta < 0$ damping prevails
- By the observed tidal range gradient: if $\nabla TR > 0$ amplification prevails, if $\nabla TR < 0$ damping prevails

We observe that there is a good agreement between the theoretical tidal damping ($1/\beta$) and the observed changes in tidal range gradient. Data points with $1/\beta > 0$ (amplification) correspond with an increase in tidal range ($\nabla TR > 0$), data points with $1/\beta < 0$ (damping) correspond with a decrease in tidal range ($\nabla TR < 0$) (Figure 34). These observations are valid for all estuaries. Note that for the Weser, the tidal damping is very limited (see also Figure 32 and Figure 33).

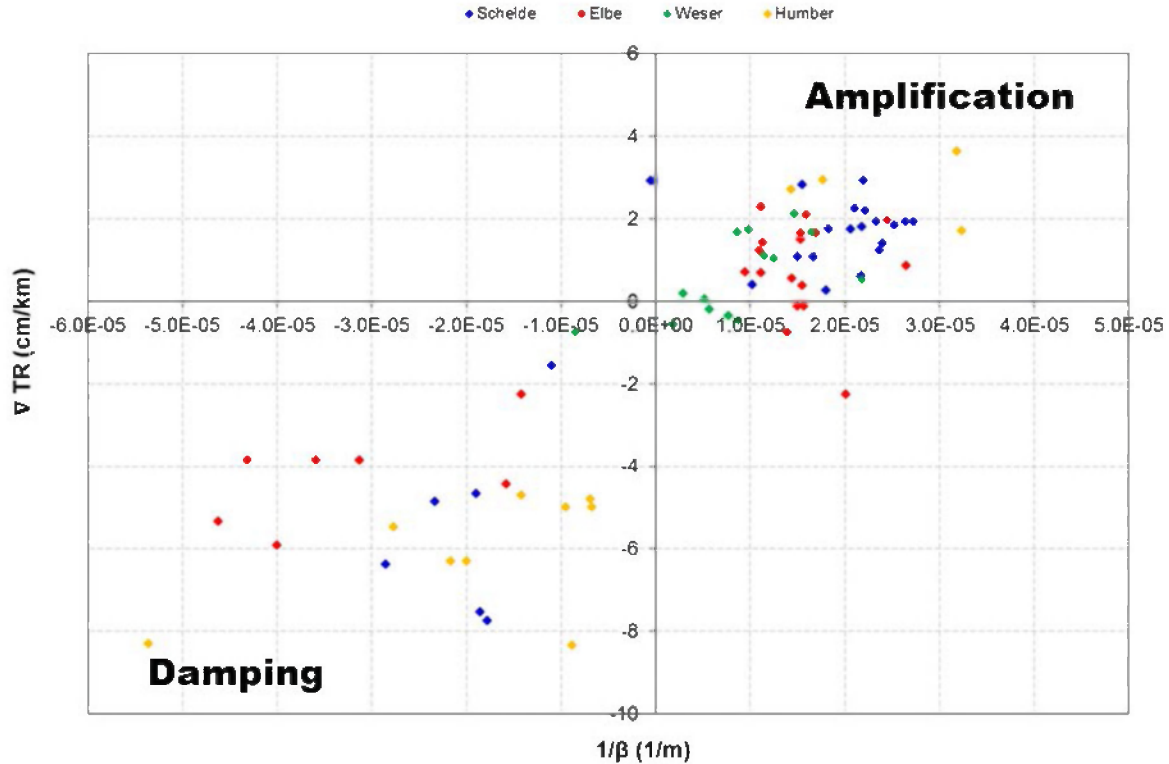


Figure 34 – Theoretical tidal damping ($1/\beta$) versus the observed tidal range gradient (∇TR). Humber = Humber-Ouse

5.1.3 Critical threshold values for depth and estuary convergence

It is assumed that the convergence of the estuary is an important driver for the tidal amplification, while limited water depth will cause friction and lead to a damping of the tidal range. In the next paragraphs we present threshold values in estuary depth, for which we can expect tidal amplification/damping, taking into account the estuary convergence.

Based on the theoretical tidal damping ($1/\beta$)

The relationship between the cross section averaged depth at LW (measure for the friction) and the theoretical tidal damping ($1/\beta$) shows that for the most convergent estuary (Humber, $1/b = 4.18 \cdot 10^{-5}$, see Table 4 and Figure A 4) tidal amplification ($1/\beta > 0$) occurs at D-LW > 4.2 m and that tidal damping ($1/\beta < 0$) occurs at D-LW < 4.2 m (i.e. based on a logarithmic trendline) (Figure 35 and Table 7). For the least convergent estuary (Elbe, $1/b = 2.75 \cdot 10^{-5}$, see Table 4 and Figure A 2) the critical threshold value for D-LW occurs at 6.4 m, and for the intermediate converging estuary (Scheldt, $1/b = 3.39 \cdot 10^{-5}$, see Table 4 and Figure A 1) at 5.6 m (Figure 35). For the Weser it was not possible to establish a proper trendline due to the lack of data points representing tidal damping (Figure 35).

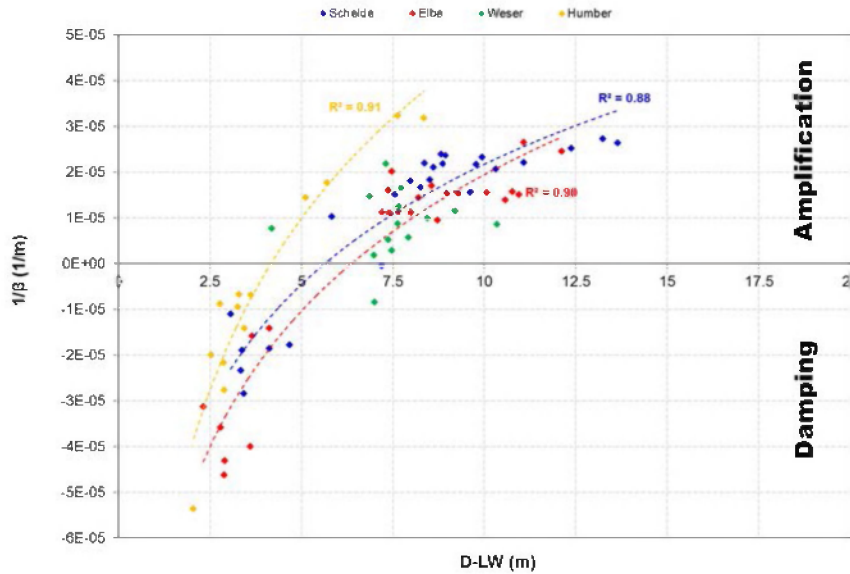


Figure 35 – The cross-section averaged depth at MLWL versus tidal damping ($1/\beta$). For $1/\beta < 0$ tidal damping, for $1/\beta > 0$ amplification.

Based on the found threshold values for D-LW (Figure 35) and the estuary convergence, tidal amplification and tidal damping in an estuary can be described as a function of the estuary convergence and the estuary depth (Figure 36). We observe that for more convergent estuaries, amplification occurs at more shallow conditions compared to less convergent estuaries. The found threshold values for tidal amplification/damping range between 4.2 m (for the most convergent estuary, i.e. the Humber) and 6.4 m for the least convergent estuary (i.e. the Elbe).

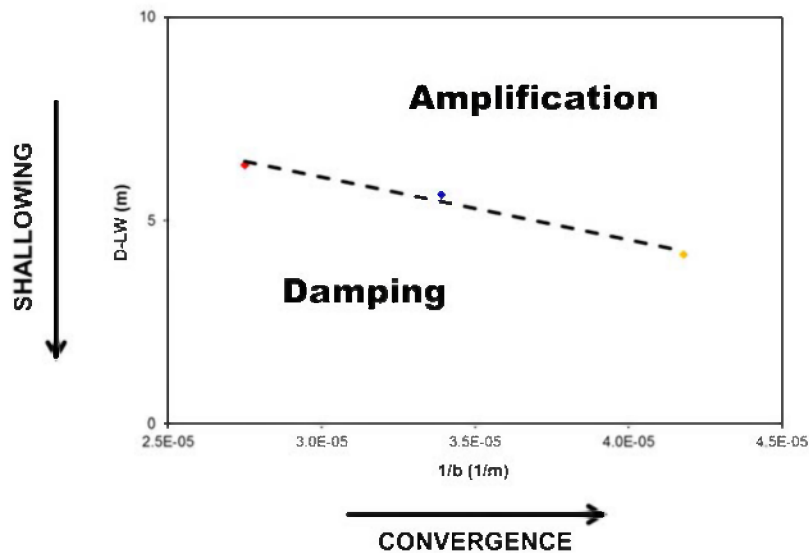


Figure 36 – Relationship between the estuary convergence and the cross-section averaged depth, based on the calculated tidal damping scale. The threshold between amplification/damping is based on the intersections of the regression lines at $1/\beta = 0$ (see Figure 35)

Based on the observed tidal range gradient (∇TR)

The relationship between the cross section averaged depth at LW (measure for the friction) and the observed tidal range gradient (∇TR) shows that for the most convergent estuary (Humber, $1/b = 4.18 \cdot 10^{-5}$ -

5, see Table 4 and Figure A 4) tidal amplification ($\nabla TR > 0$) occurs at $D-LW > 5.3$ m and that tidal damping ($\nabla TR < 0$) occurs at $D-LW < 5.3$ m (i.e. based on a logarithmic trendline) (Figure 37 and Table 7). For the least convergent estuary (Elbe, $1/b = 2.75 \cdot 10^{-5}$, see Table 4 and Figure A 1) the critical threshold value for $D-LW$ occurs at 7.7 m, and for the intermediate converging estuary (Scheldt, $1/b = 3.39 \cdot 10^{-5}$) at 7.4 m (Figure 37).

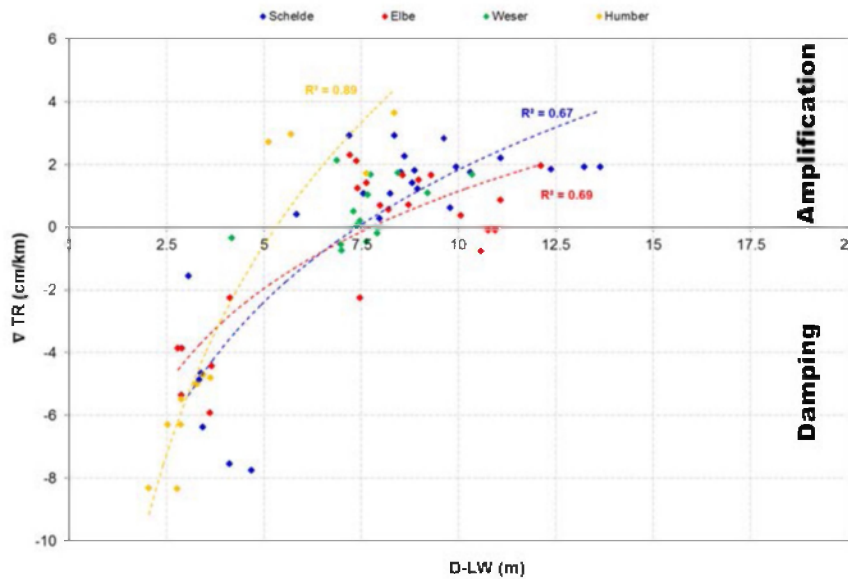


Figure 37 – The cross-section averaged depth at MLWL versus the observed gradient in tidal range (∇TR). For $\nabla TR < 0$ tidal damping, for $\nabla TR > 0$ amplification.

Based on the found threshold values for $D-LW$ (Figure 37) and the estuary convergence, tidal amplification and tidal damping in an estuary can be described in function of the estuary convergence and the estuary depth (Figure 38), similarly as for the theoretical tidal damping parameter $1/\beta$ (Figure 36). Again, we observe that for more convergent estuaries, amplification occurs at more shallow conditions compared to less convergent estuaries. The found threshold values for tidal amplification/damping range between 5.3 (for the most convergent estuary, i.e. the Humber) and 7.7 for the least convergent estuary (i.e. the Elbe).

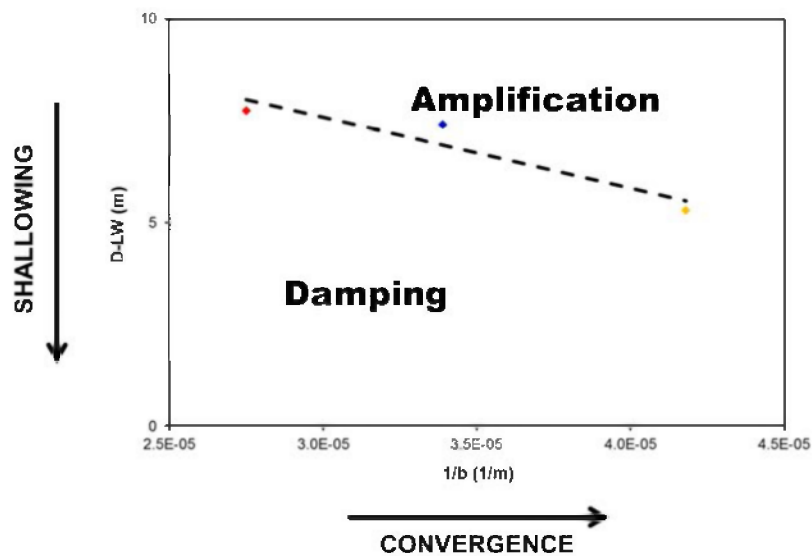


Figure 38 – Relationship between the estuary convergence and the cross-section averaged depth, based on the observed gradient in tidal range. The threshold between amplification/damping is based on the intersections of the regression lines at $\nabla TR = 0$ (see Figure 37)

Table 7 – R^2 and $D-LW_{cr}$ for the logarithmic regression lines in Figure 35 and Figure 37. All found trendlines are significant. $D-LW_{cr}$ is the critical D-LW value for tidal damping/amplification. Below this value tidal damping occurs, above this value tidal amplification occurs

	Humber		Scheldt		Elbe	
	R^2	$D-LW_{cr}$	R^2	$D-LW_{cr}$	R^2	$D-LW_{cr}$
D-LW ~ $1/\beta$	0.91	4.2	0.88	5.6	0.9	6.4
D-LW ~ ∇TR	0.89	5.3	0.67	7.4	0.69	7.7

5.1.4 Conclusions

The two most important factors that influence tidal amplification and tidal damping in an estuary are: (1) the funneling of the estuary (i.e. estuary convergence) leading to tidal amplification, and (2) the friction in the estuary (controlled by the estuary depth) which leads to tidal damping. Based on the theoretical tidal damping parameter $1/\beta$, we found that tidal amplification for several converging estuaries occurs at an estuary depth larger than 4.2 - 6.4 m (cross-section averaged at LW) and that tidal damping occurs at an estuary depth smaller than 4.2 - 6.4 m. Based on the observed tidal range gradients (∇TR) this critical threshold value is somewhat higher, ranging from 5.3 - 7.7 m. The range in these threshold values (both for $1/\beta$ and ∇TR) is influenced by the estuary convergence: the more convergent an estuary, the lower the critical threshold depth.

We recommend for the observed estuaries an estuary depth smaller than 4.2 - 7.7 m (i.e. cross-section averaged depth at LW) to have important tidal damping. As analysis were performed over 5 km blocks, this critical estuary depth should be present for at least 5 km along the estuary. The range in critical estuary depth (4.2 – 7.7 m) is a consequence of the estuary convergence: the more convergent the estuary, the smaller the critical estuary depth. However, we are convinced that it is necessary to include more estuaries in the analysis to improve the accuracy of the found threshold values in estuary depth.

Shallowing of the subtidal channels is thus a possible measure to lower the cross-section averaged depth at LW, and in this way increase the tidal damping. However, also other measures could be taken to introduce more friction in an estuary, for example by creating more intertidal area. This is further elaborated in the next topic (§5.2) where we relate tidal damping/amplification to habitat occurrence.

5.2 TOPIC 2 – Habitats

In this topic we looked at the effect of different habitats (subtidal, intertidal and marsh habitats) on the horizontal tide (flow velocities) and the vertical tide (tidal range). To study this topic we used tidal data (§3.1.2) and topo-bathymetry data (§3.1.1) to delineate habitat maps according to 6 defined habitat classes (§3.3) (see Appendix B, Figure B 1 - Figure B 10). These habitats were also used for the ecosystem services report within TIDE. Flow velocities were calculated based on the cubage technique (§3.2.1).

5.2.1 Quantification

Areas

Large differences occur in the total estuary surface area. The Scheldt estuary is for example 3.5 times larger than the Weser estuary and about 2 times the size of the Humber (Figure 39). Consequently this will affect the available area of each habitat within the different estuaries.

In the Scheldt the deep subtidal habitat (Sd) has an area of 17000 ha which is about 2 times the Sd area of the Elbe, and 5-10 times the Sd area of the Weser and Humber (Figure 40). For the moderately deep and shallow subtidal habitat (Sm and Ss) surface areas are comparable for the 4 estuaries, only for the Weser surface areas are clearly smaller. The Scheldt estuary contains almost 8000 ha of intertidal flat habitat (If) which is significantly higher than the other estuaries. Concerning the intertidal steep habitat (Is) surface areas are very comparable. The Elbe and Weser have the highest marsh (M) area (for the Elbe about 5300 ha), whereas the Humber has the smallest area (about 700 ha). It should be pointed out that the used methodology for habitat mapping is based on physiotores, whereby the marsh habitat is defined as the area above MHWL (see §3.3.2). For the Elbe and Weser several of these marsh areas are used as pastures (with still a connection to the estuary), and hence do not have the typical tidal marsh vegetation. Due to these differences in marsh characteristics, the relative percentages in habitat area are also provided excluding the tidal marshes (Figure 42).

The large area of Sd habitat in the Scheldt covers about half of the total estuary's surface (Figure 41). This is clearly higher than the Elbe (37 %), whereas the Weser and Humber only have a quarter of deep subtidal. All estuaries have 50 - 75% subtidal habitat, except for the Weser where only 35% is subtidal. Remarkably is the dominance of the deep subtidal habitat compared to the other subtidal habitat classes for the Scheldt, Elbe and Weser, and the equal distribution of the subtidal habitats ($\pm 25\%$) for the Humber. For all estuaries, the total intertidal area (If + Is) varies between 20 - 30%, whereas the relative marsh area is clearly higher for Elbe and Weser than for the Scheldt and Humber, due to the difference in marsh characteristics (Elbe and Weser include pastures). The relative importance of the subtidal areas versus the intertidal areas is presented in Figure 42.

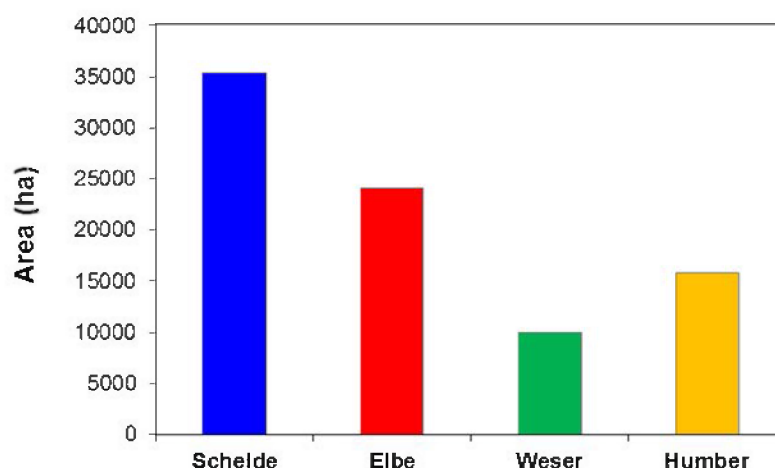


Figure 39 – Total estuary surface area (in hectares, calculated from mouth_{geo} to up-estuary boundary)

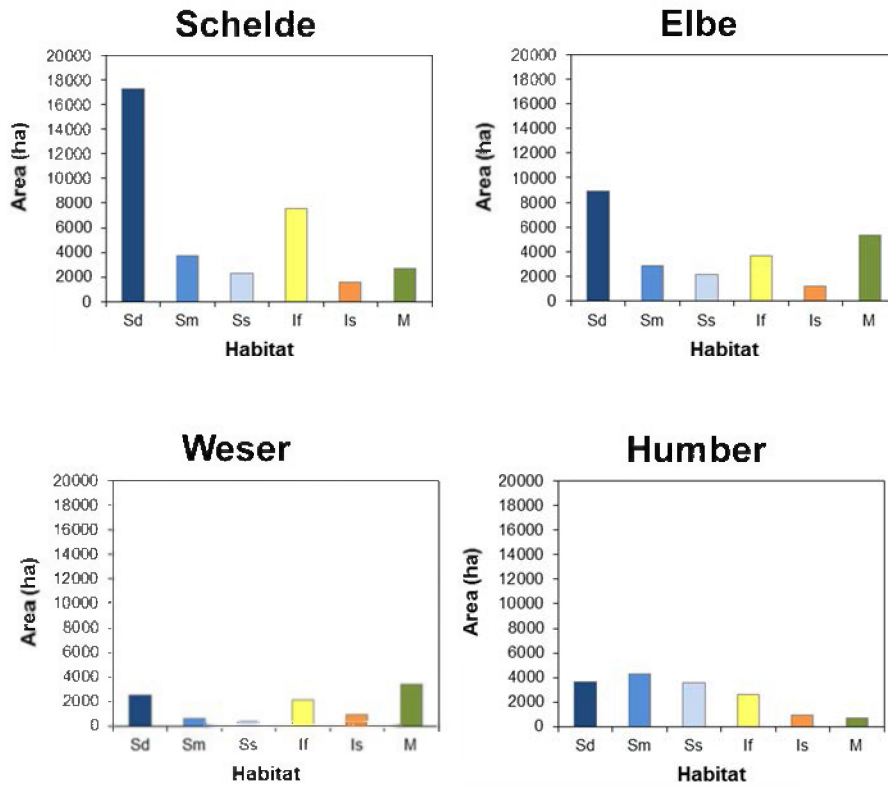


Figure 40 – Absolute habitat areas (in hectares) for the 4 estuaries (calculated from mouth_{geo} to up-estuary boundary, Sd = subtidal deep, Sm = subtidal moderately deep, Ss = subtidal shallow, If = intertidal flat, Is = intertidal steep, M = marsh)

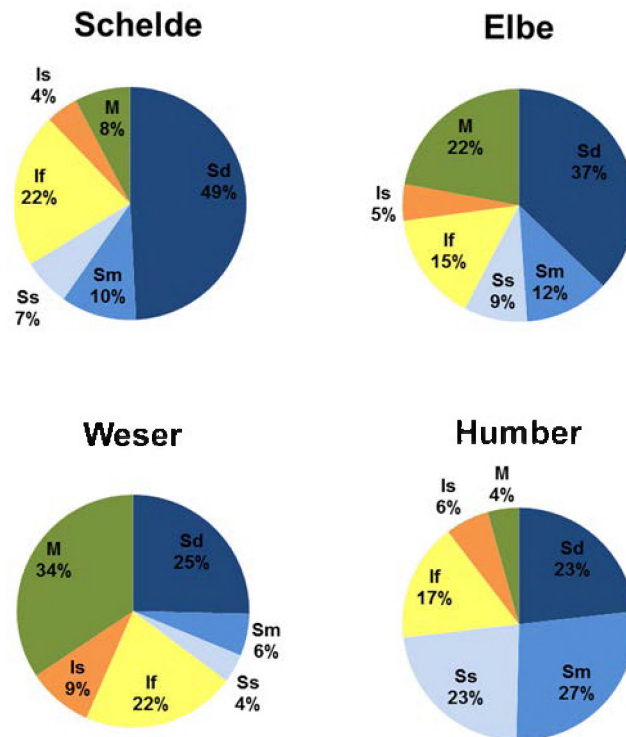


Figure 41 – Relative presentation of the habitat areas (percentages) for the 4 estuaries (from mouth_{geo} to up-estuary boundary)

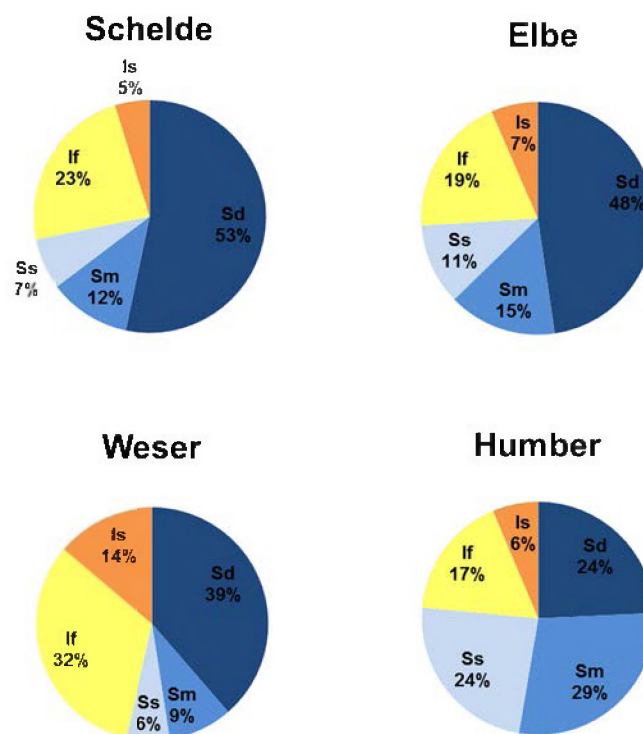


Figure 42 – Relative presentation of the subtidal and intertidal habitat areas (percentages) for the 4 estuaries (from mouth_{geo} to up-estuary boundary)

Widths

In general, the subtidal is the dominant habitat type along the different estuaries with a relative width of 50% or more (Figure 43). Only for the middle part of the Weser, the subtidal is clearly lower with values around 25%. For the Scheldt, Elbe and Weser, the deep subtidal habitat has the largest portion in the total subtidal, with exception of the upper parts, where the moderately deep and shallow subtidal habitats become more important. For the Humber, moderately deep and shallow subtidal are clearly dominant along the entire estuary, only close to the mouth the deep subtidal is important. Intertidal flat areas are important along the multi-channel systems of the estuaries. Moreover in the mouth areas of the Elbe and Weser they are by far the dominant habitat type. In the Scheldt and Humber, intertidal steep habitats are important in the more upstream parts of the estuaries. Finally, the marsh habitat is in particular abundant along the Weser estuary (15 – 50%) and is rather scarce along the Humber. A comparison between the four estuaries for the relative and absolute widths of each individual habitat can be found in Appendix C).

By plotting the tidal range on the habitat width distribution, we observe for each estuary an increase in tidal range where the deep subtidal habitat is important, and a decrease in tidal range where the deep subtidal habitat is rather scarce or absent. Relationships between the relative habitat width and the tidal range gradient are further elaborated in §5.2.3.

It should be pointed out that in the most upstream parts of the estuaries, the accuracy of the habitat width determination might be affected by the coarse grid resolution compared to the estuary width, especially for the Scheldt estuary where habitat mapping is based on a topo-bathymetry grid of 20 x 20 m (see §3.3.2).

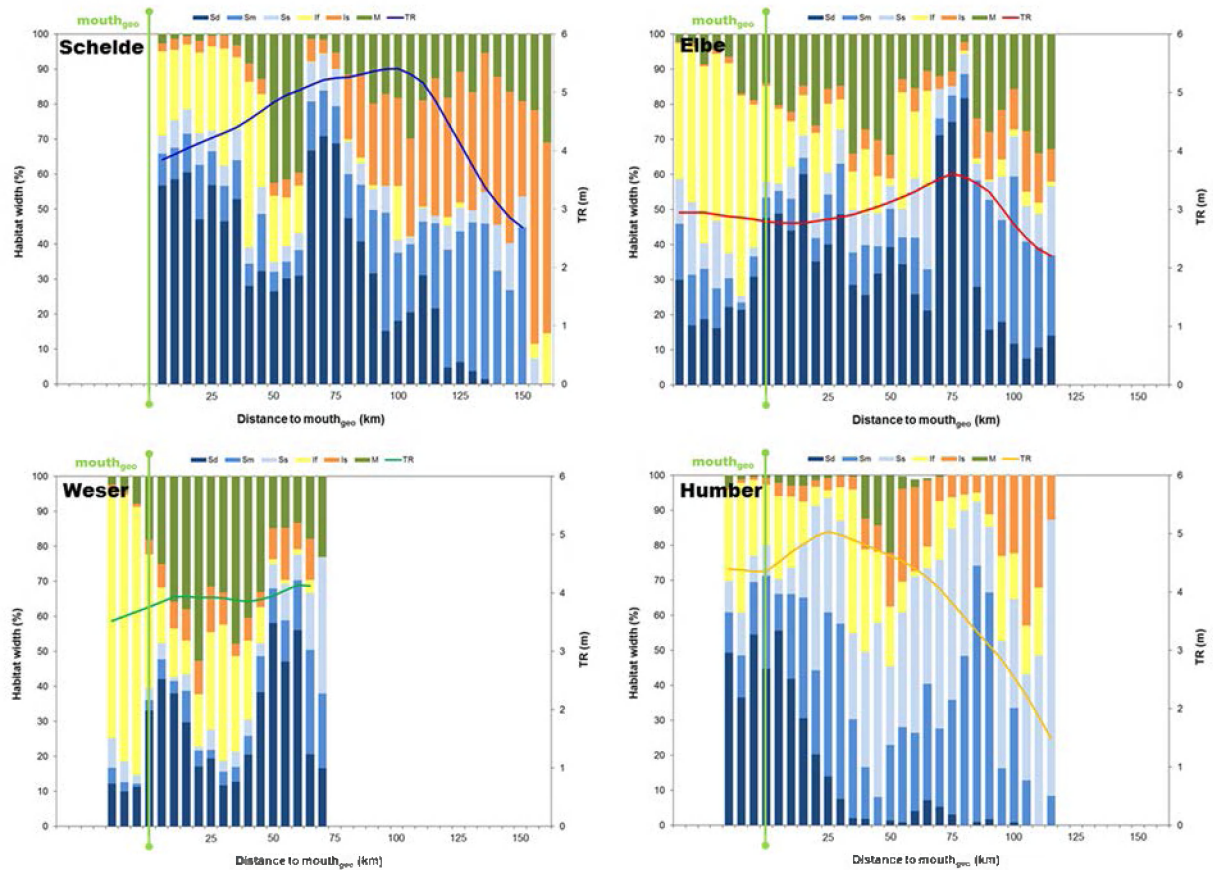


Figure 43 – Habitat width (%) and tidal range along the 4 estuaries (for the Humber along Humber-Ouse), averaged over 5 km blocks. Habitat legend: Sd = subtidal deep, Sm = subtidal moderately deep, Ss = subtidal shallow, If = intertidal flat, Is = intertidal steep, M = marsh.

5.2.2 Relation between flow velocity and habitats

To test the initially stated hypothesis in topic 2 (see §2), the maximum flood flow velocity is related to the amount of shallow and intertidal habitat. We observe for all four estuaries that flow velocity does not influence the relative width of these habitats (see Figure 44 and Figure 45).

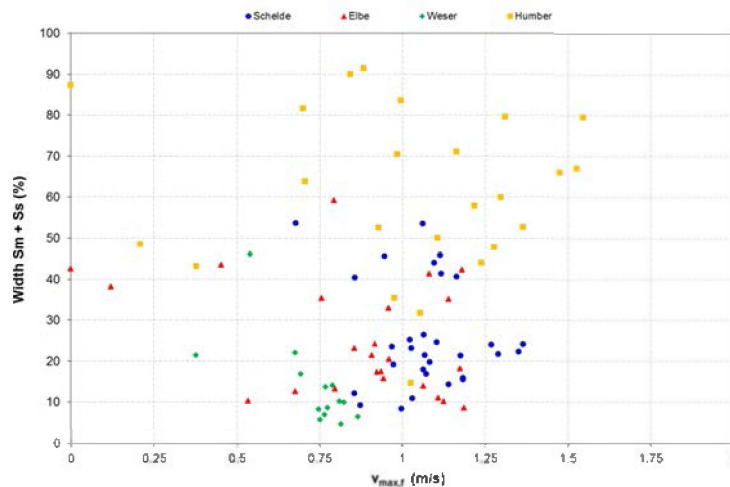


Figure 44 – Maximum flood flow velocity versus the width of the moderately deep and shallow subtidal habitat (%)

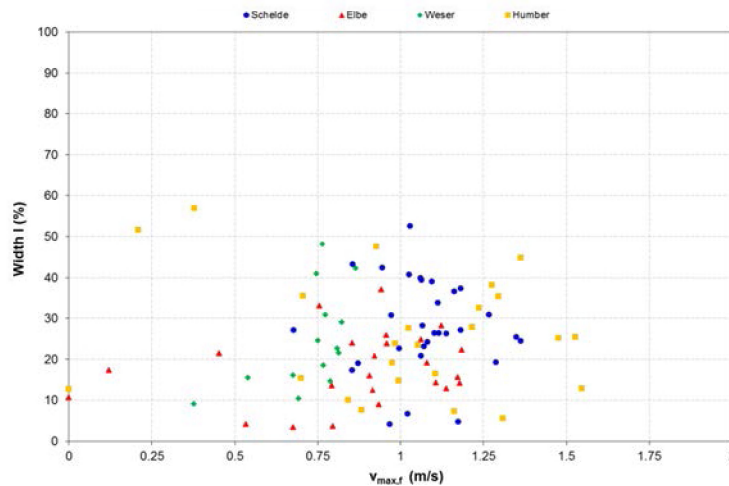


Figure 45 – Maximum flood flow velocity versus the width of the intertidal habitat (%)

5.2.3 Relation between habitats and tidal damping/amplification

A clear relationship exists between the percentage of deep subtidal habitat (Sd) and the tidal range gradient (∇ TR) (Figure 46). For a restricted width of Sd (< 20%) the tidal range gradient is lower than zero, meaning a damping of the tidal range. If Sd becomes more important (> 30%), only tidal amplification occurs (with exception of a few points) with ∇ TR varying between 0 and 4 cm/km, but without an increase in ∇ TR for increasing % Sd values.

For the moderately deep (Sm) and shallow subtidal (Ss) habitat, the relationship between % habitat and ∇ TR is opposite to the deep subtidal habitat (Figure 47, cf. Figure 46 and Figure 47). Here, low values (< 25%) for Sms (= Sm + Ss) result in mostly tidal amplification, whereas for higher values of Sms (> 35%) tidal damping prevails.

In contrast to the subtidal habitats, no relationships between % habitat and ∇ TR are observed for the intertidal and marsh habitats. Here, for an increase in % habitat, tidal damping and tidal amplification are equally important (Figure 48 and Figure 49).

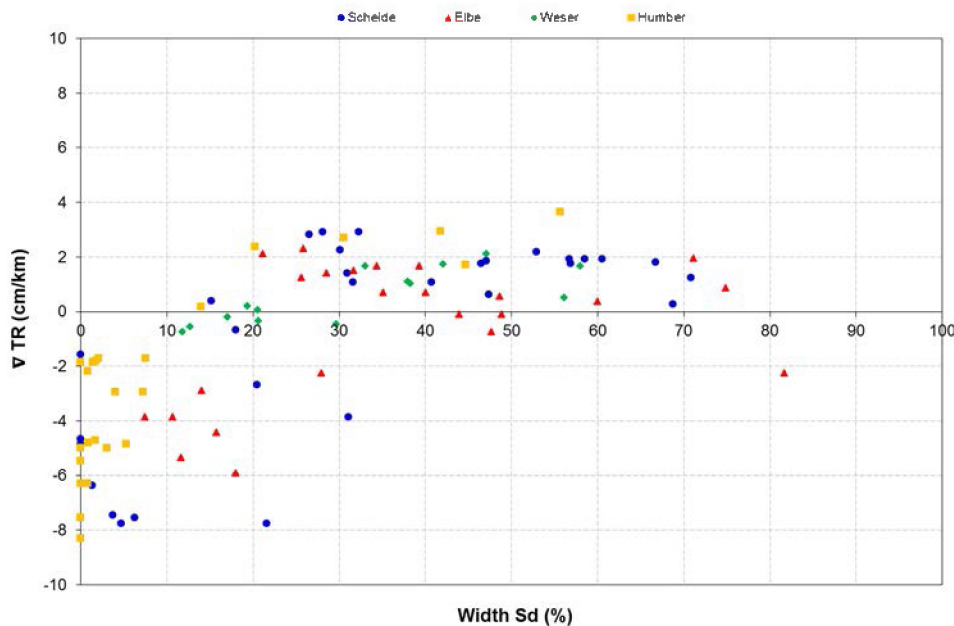


Figure 46 – Width of the deep subtidal habitat (%) versus the tidal range gradient

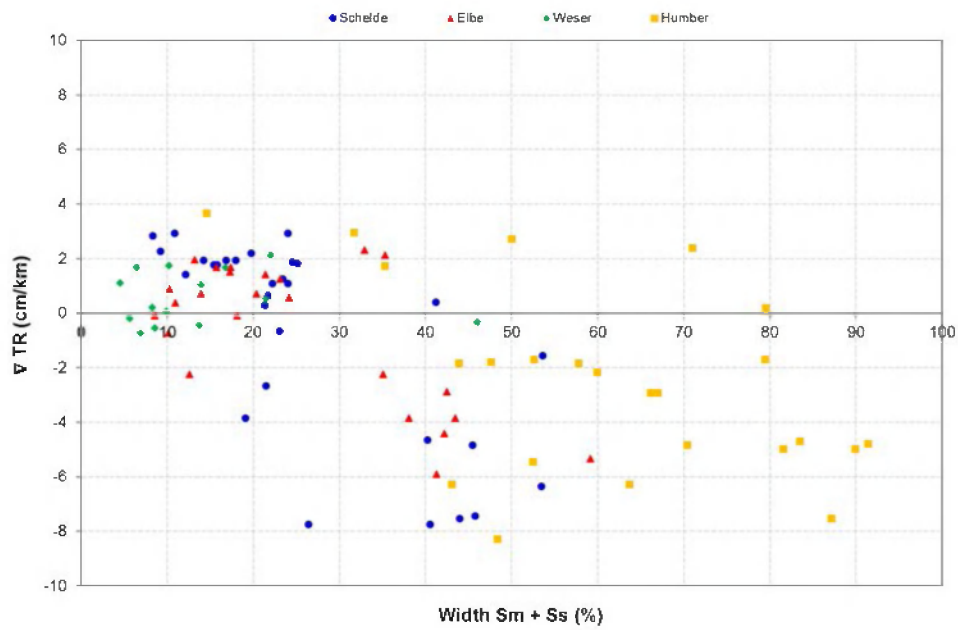


Figure 47 – Width of the moderately deep and shallow subtidal habitat (%) versus the tidal range gradient

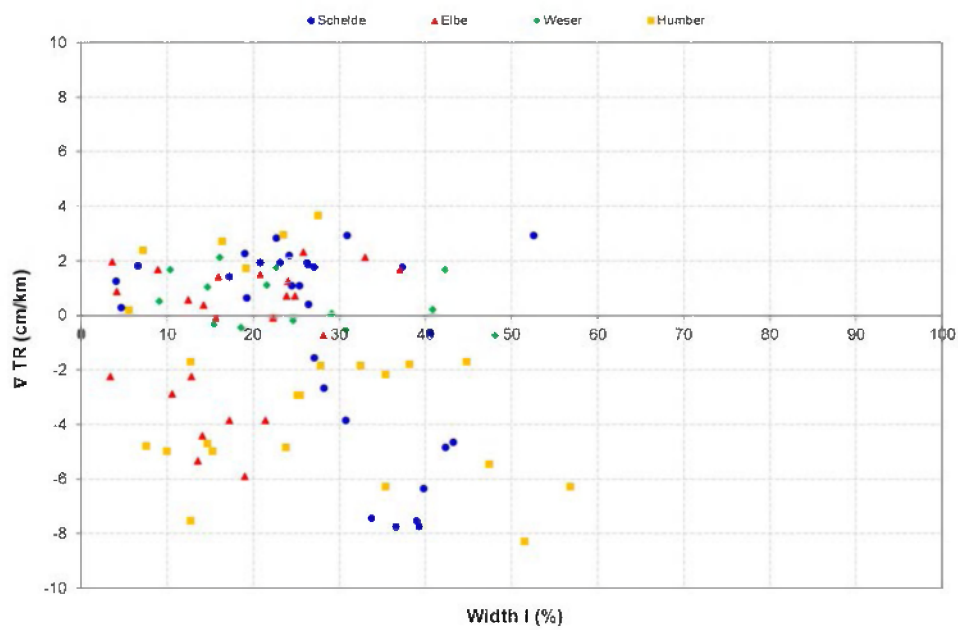


Figure 48 – Width of the intertidal habitat (%) versus the tidal range gradient

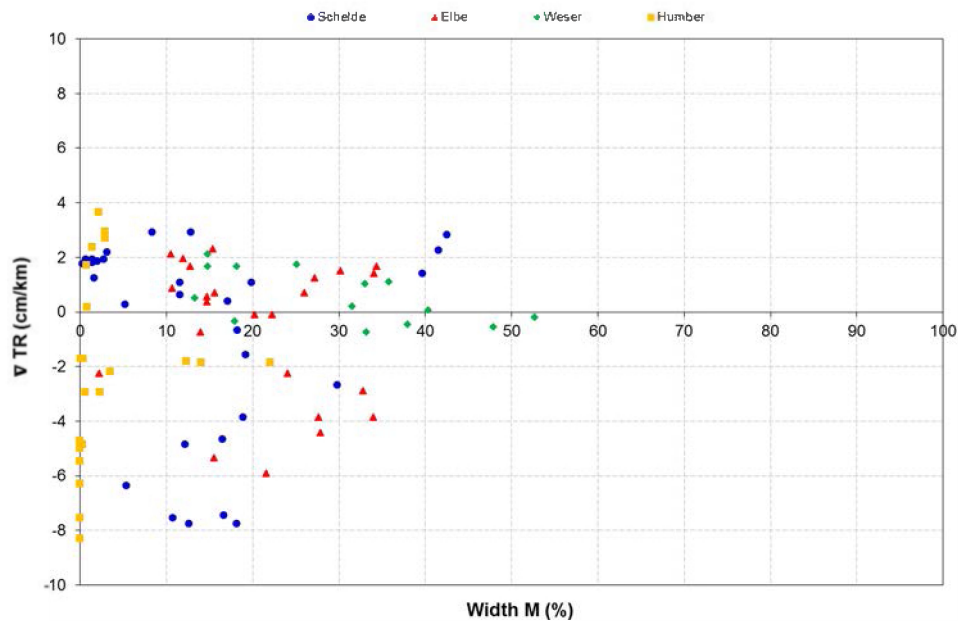


Figure 49 – Width of the marsh habitat (%) versus the tidal range gradient

5.2.4 Conclusions

Tidal amplification (vertical tide) in estuaries are to a large extent determined by the subtidal habitats, whereas intertidal and marsh habitats have no significant influence based on the observations (i.e. for mean tidal conditions). Tidal amplification occurs when the relative width in deep subtidal habitat (> 5 m below LW) is larger than 30% ($S_d > 30\%$) and the sum of the moderately deep and shallow subtidal habitats (5 - 0 m below LW) is smaller than 25%. Tidal damping occurs when $S_d < 20\%$ and $S_{ms} > 35\%$. To induce tidal damping in an estuary we thus recommend to have over a distance of 5 km (data were averaged over 5 km blocks), no excessive width in deep subtidal habitat ($< 20\%$) and sufficient width in moderately deep and shallow subtidal habitat ($> 35\%$), which corresponds with a rounded shallow channel shape rather than a deep and wide trapezoidal channel shape. The latter is often the shape of deepened (dredged) channels, representative for the main channels of the Scheldt, Elbe and Weser. The cross section of the subtidal Humber is a naturally formed channel (no artificial dredging), with exception of a small section in the mouth area (from TIDE km 117-122). The subtidal habitat distribution of the Humber (Figure 41) suggests a more round profile and generally shallower average depths, giving a much greater emphasis to tidal damping than the other estuaries.

We further recommend an extensive statistical analysis (regressions for the different estuaries, co-variance between the different % habitats, etc.) of this dataset to improve above stated threshold values (% habitat) for tidal damping/amplification. Before doing these analyses, the determination of the % habitat should be improved (mainly for the most upstream parts of the estuary) by: (1) working with a finer topo-bathymetry grid (especially for the Scheldt for which we worked in this study with a 20 x 20 m grid), and (2) improving the interpolation method for the LW and HW surfaces. Initially, the habitat mapping was aimed to calculate habitat areas for which this methodology was considered as sufficiently (methodology see §3.3.2).

Initially, topic 2 would study the relationship between flow velocities (horizontal tide) and the occurrence of intertidal and shallow subtidal habitats. The hypothesis hereby brought forward was: “higher average flow velocities in an estuary result in less intertidal and shallow water area”. However, we did not find any relationship between these parameters and therefore habitats were also related to tidal damping/amplification (vertical tide). It should be pointed out that the “cubage” technique (§3.2.1) calculates cross-section averaged flow velocities. This could explain why no relationship was found between the flow velocity and the habitats since habitat areas are more likely influenced by local variations in flow velocity.

5.3 TOPIC 3 – Relation between sediment load and tidal/riverine characteristics

In topic 3 we study the similarities and differences between the estuaries with regard to their suspended sediment loads in relation to their tidal and riverine characteristics. We further look at which factors influence the position of the turbidity maximum. For this topic we used SPM data (§3.1.4) and salinity data (§3.1.3), and we calculated the netto sediment flux for each water level station (§3.2.3) and tidal energy according to the Dalrymple energy concept (§3.2.4).

5.3.1 Suspended particle matter (SPM)

Surface SPM values are the lowest in the Scheldt and Weser estuary (< 150 mg/l), intermediate in the Elbe (up to 250 mg/l), and high in the Humber (up to 750 mg/l) (see Figure 50). In the Humber and Elbe one or more estuarine turbidity maximum(s) (ETM) (i.e. a zone in which the suspended particle matter concentrations are higher than those in the river or further downstream the estuary) are well developed. For the Humber two peaks are observed: one close to Hull and one at the junction with the Trent (see Figure 50 and Figure 55). For the Elbe one distinct ETM is observed just downstream Glückstadt (see Figure 50 and Figure 53). The Schelde and Weser have less pronounced ETM (Figure 50). For the Scheldt higher SPM values are mainly observed between Temse and Dendermonde, and to less extent downstream from Antwerp (see Figure 51). For the Weser higher SPM values occur at the town of Emsfleth and downstream from Bremerhaven (Figure 54). It should be pointed out that the presented surface SPM values are averaged over different seasonal and tidal conditions (more info, see §3.1.4).

Only for the Scheldt, sufficient depth-averaged SPM data were available to present the variation along the estuary. We observed earlier that some important differences exist between surface and depth-averaged SPM data (see Figure 28 upper left panel and §4.1). Firstly the depth-averaged SPM values in the single channel system of the Scheldt are clearly higher compared to the surface SPM values (Figure 28), and secondly the extent of the ETM zones differs between the depth-averaged and the surface SPM. Although the locations of ETM zones are similar for surface and depth-averaged SPM, we observe that the largest zones with increased SPM occurs upstream Temse for the surface SPM, and downstream Antwerpen for the depth-averaged SPM (cf. Figure 51 and Figure 52). Despite the higher observed depth-averaged SPM values, a positive correlation exists between depth-averaged and surface SPM values ($r = 0.76$, Figure 56). For low SPM values (< 50 mg/l), depth-averaged SPM values are more or less equal to surface SPM values (i.e. in the multiple-channel system of the Western Scheldt, Figure 28 and Figure 56), while for higher SPM values (> 50 mg/l) depth-averaged SPM values are clearly higher (i.e. in the single channel system of the Sea Scheldt, Figure 28 and Figure 56).

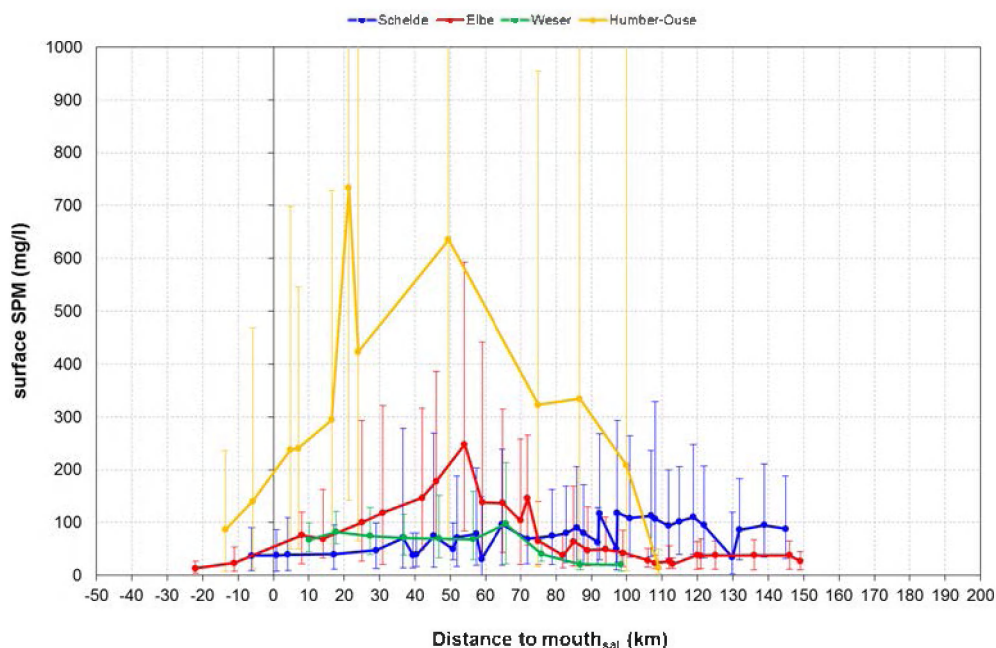


Figure 50 – Mean surface SPM values along the four TIDE estuaries. Error bars represent the P5 and P95 values

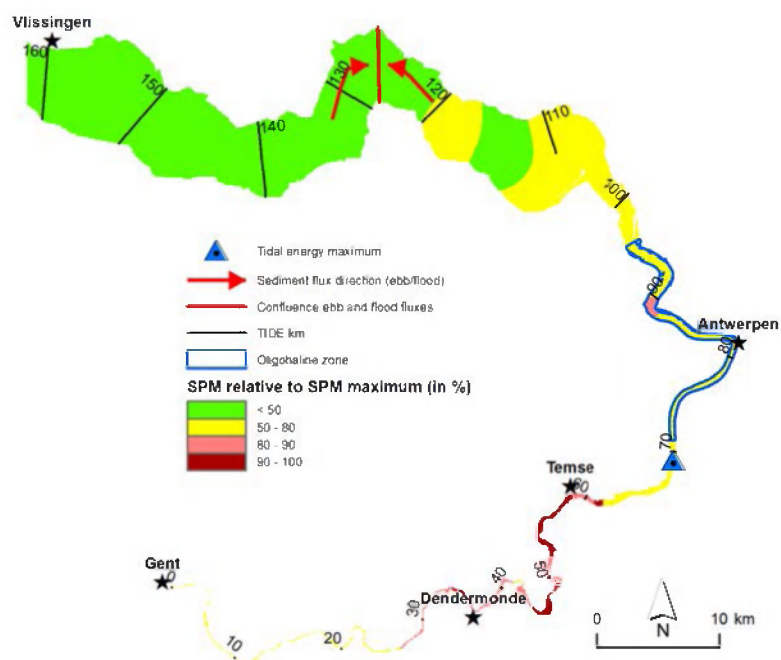


Figure 51 – Surface SPM (averaged over a tidal cycle) relative to the maximum observed surface SPM in the Scheldt estuary. Under mean tidal conditions, sediment fluxes are directed in the flood direction from TIDE km 125-160, and in the ebb direction from TIDE km 0 -125. The maximum tidal energy occurs around TIDE km 69.

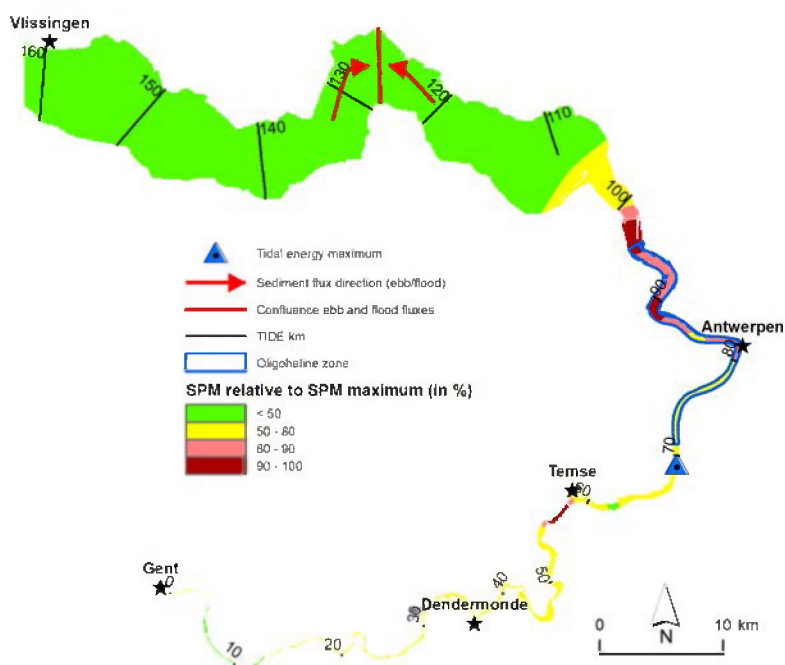


Figure 52 – Depth-averaged SPM (averaged over a tidal cycle) relative to the maximum observed depth-averaged SPM in the Scheldt estuary. Under mean tidal conditions, sediment fluxes are directed in the flood direction from TIDE km 125-160, and in the ebb direction from TIDE km 0 -125. The maximum tidal energy occurs around TIDE km 69.

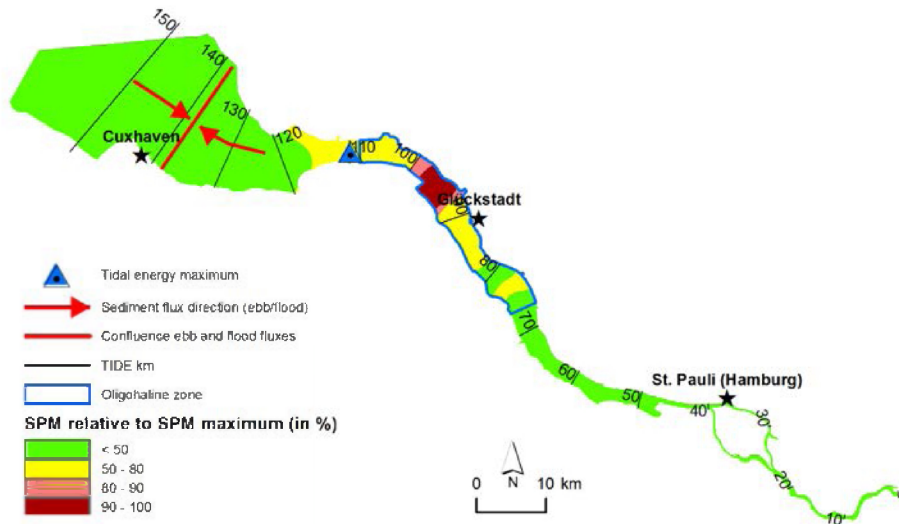


Figure 53 – Surface SPM (at low water conditions) relative to the maximum observed surface SPM in the Elbe estuary. Under mean tidal conditions, sediment fluxes are directed in the flood direction from TIDE km 138-150, and in the ebb direction from TIDE km 0-138. The maximum tidal energy occurs around TIDE km 110.

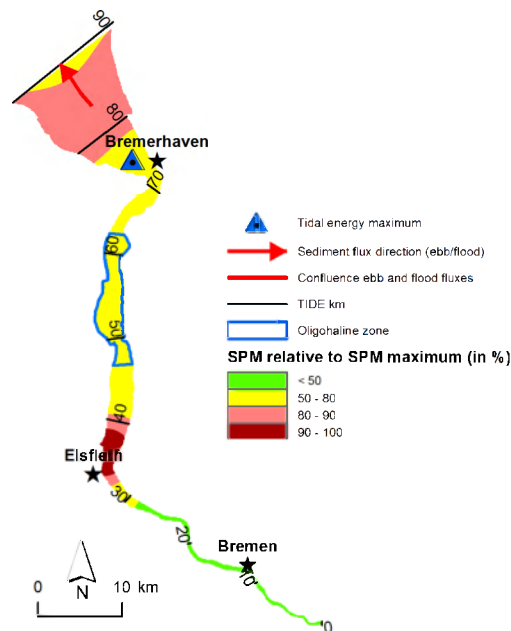


Figure 54 – Surface SPM (at low water conditions) relative to the maximum observed surface SPM in the Weser estuary. Under mean tidal conditions, sediment fluxes are directed in the ebb direction for the entire estuary. The maximum tidal energy occurs around TIDE km 74.

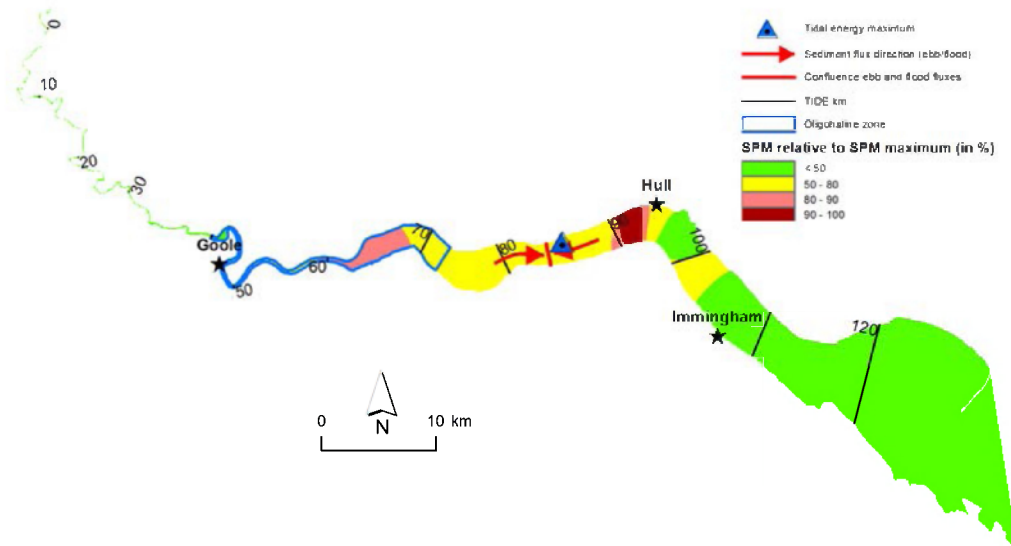


Figure 55 – Surface SPM (averaged over a tidal cycle) relative to the maximum observed surface SPM along the Humber-Ouse tributary. Under mean tidal conditions, sediment fluxes are directed in the flood direction from TIDE km 84-130, and in the ebb direction from TIDE km 0-84. The maximum tidal energy occurs around TIDE km 84.

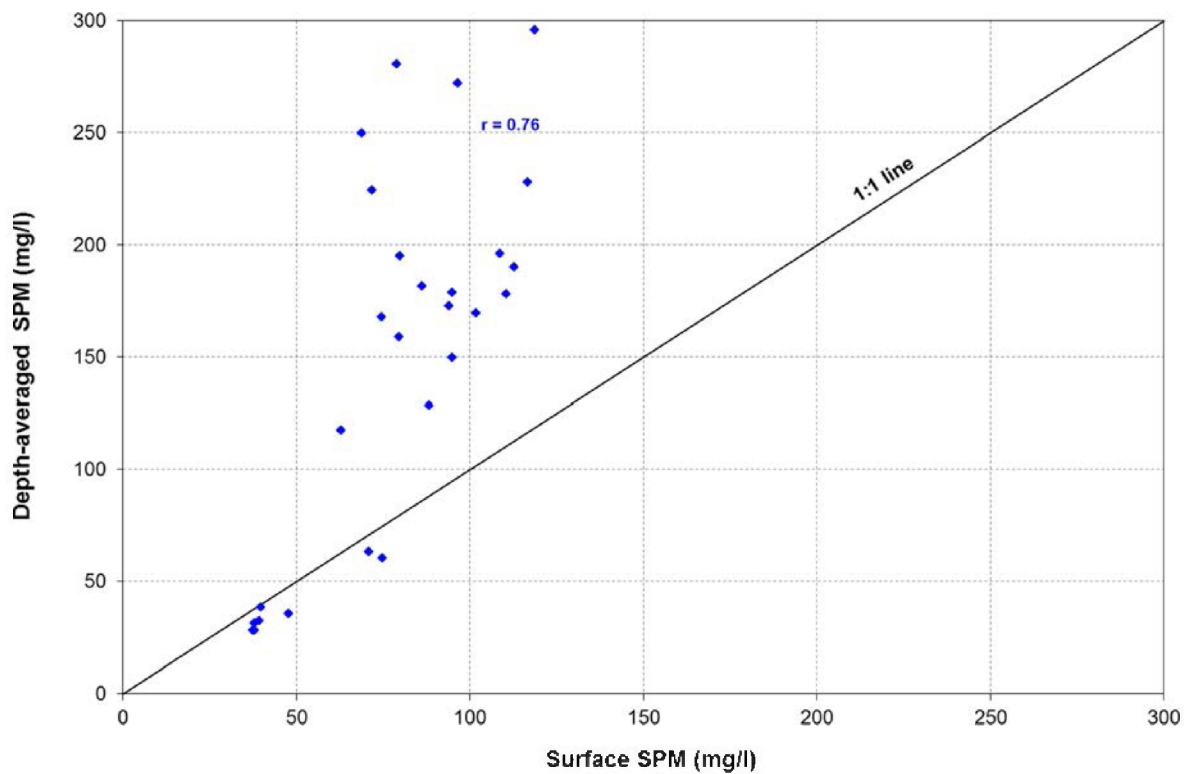


Figure 56 – Relation between surface SPM and depth-averaged SPM in the Scheldt estuary

5.3.2 Sediment fluxes

Mean riverine discharge

For the Scheldt, Elbe and Weser sediment fluxes for mean tidal range are dominantly in the ebb direction, with sediment flux values between 0 and $-1.5 \text{ kg/m}^2/\text{s}$ under conditions of mean riverine discharge (- sign refers to sediment transport in the ebb direction) (Figure 57). We observe for the Scheldt that sediment flux values based on depth-averaged SPM values result in higher sediment fluxes in the ebb direction (cf. blue and dark blue lines in Figure 57) due to the higher depth-averaged values compared to surface SPM values (see Figure 28 and Figure 56). Although sediment fluxes along the Scheldt and Elbe estuaries are dominantly in the ebb direction, values become positive (transport in the flood direction) in the most downstream part of the estuary. Nevertheless, these values are a factor 10-100 smaller (0 till $0.015 \text{ kg/m}^2/\text{s}$) compared to fluxes in the ebb direction (from 0 till $-1.5 \text{ kg/m}^2/\text{s}$). For the Scheldt, flood transport changes into ebb transport around 26 km from $\text{mouth}_{\text{sal}}$, for the Elbe this is at 15 km from $\text{mouth}_{\text{sal}}$ (see also Figure 51, Figure 52 and Figure 53). For the Weser sediment fluxes are only orientated in the ebb direction (see Figure 54 and Figure 57). Compared to the other estuaries the Humber has a significant transport in the flood direction (up to $1.2 \text{ kg/m}^2/\text{s}$). However, the sediment transport in the ebb direction is also much larger compared to the other estuaries (up to $-5.9 \text{ kg/m}^2/\text{s}$ around km 100 from $\text{mouth}_{\text{sal}}$). Sediment fluxes in the flood direction change into sediment fluxes into the ebb direction around 25 km from $\text{mouth}_{\text{sal}}$ (Figure 55 and Figure 57).

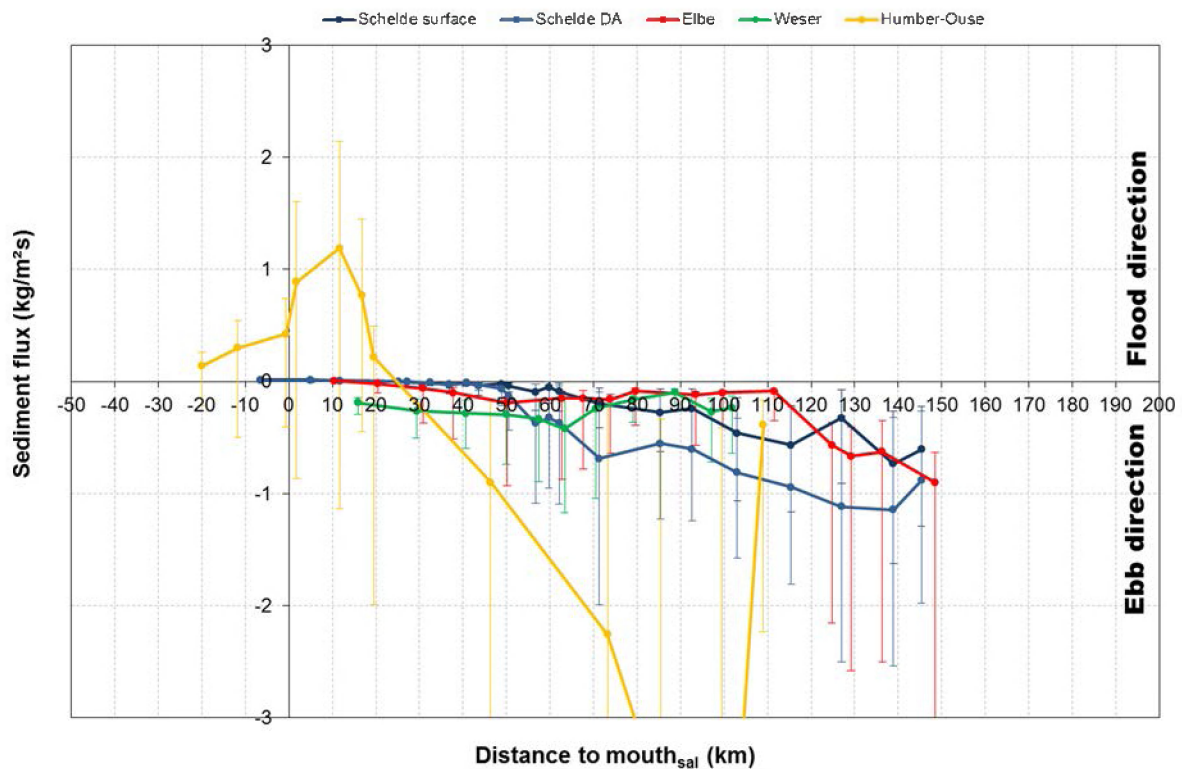


Figure 57 – Sediment fluxes for the four TIDE estuaries, under conditions of mean tidal range and mean riverine discharge. Positive values represent sediment transport in the flood direction, negative values represent transport in the ebb direction. Sediment fluxes are calculated based on the surface SPM values, for the Scheldt flux values are also calculated based on the depth-averaged SPM values (see §3.2.3). Error bars are calculated based on the P5 and P95 values of the SPM values (see Figure 28).

High and low riverine discharge

In general, high riverine discharges result in higher sediment fluxes (for mean tidal range) in the ebb direction and this over a longer distance along the estuary (towards the mouth) compared to low riverine discharges (see Figure 58). For the Elbe, flood transport changes into ebb transport under conditions of

high riverine discharge around 12 km from mouth_{sal}, while this is at km 105 from mouth_{sal} under conditions of low riverine discharge (see red arrows in Figure 58). It should be pointed out that the sediment fluxes during low riverine discharge are very low (values range between $-5.8 \cdot 10^{-4}$ and $6.75 \cdot 10^{-5}$ kg/m²/s) compared to conditions with high riverine discharge (Figure 58). For the Humber, flood transport changes into ebb transport under conditions of high riverine discharge around 18 km from mouth_{sal}, while this is at km 62 from mouth_{sal} under conditions of low riverine discharge (see yellow arrows in Figure 58). During low riverine discharge, the sediment fluxes in the ebb and flood direction are comparable in the Humber (between -0.8 and 0.8 kg/m²/s). This is not the case under conditions of high riverine discharge where ebb fluxes reach values up to -17 kg/m²/s, while sediment fluxes in the flood direction are limited to 1.9 kg/m²/s. In the Weser, sediment transport is exclusively orientated in the ebb direction, both under conditions of high and low riverine discharge. For low riverine discharge, sediment fluxes are about 1/3 of the sediment fluxes at high riverine discharge (see Figure 58).

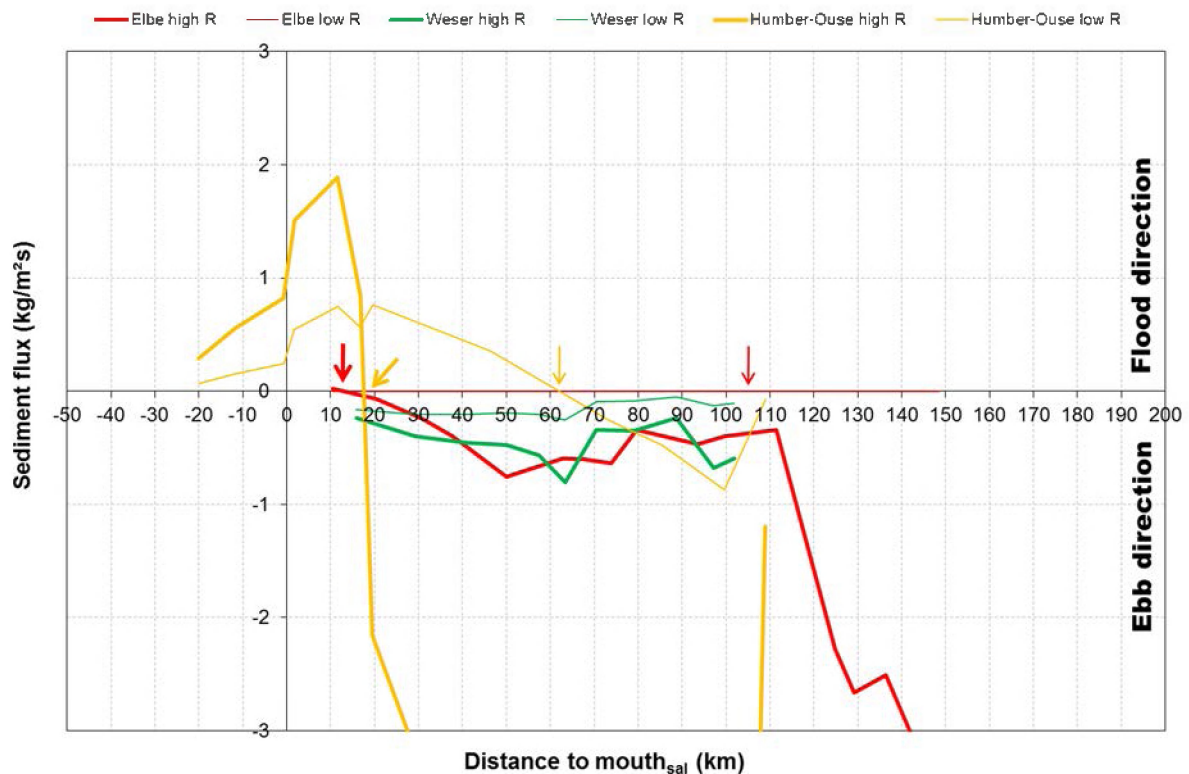


Figure 58 – Sediment fluxes for 3 TIDE estuaries, under conditions of mean tidal range and low and high riverine discharge. Positive values represent sediment transport in the flood direction, negative values represent transport in the ebb direction. Sediment fluxes under mean riverine discharge are presented in Figure 57

5.3.3 Relation between tidal energy and SPM

For all the SPM datasets executed during similar tidal conditions (half tide for the Scheldt, low water for the Elbe and Weser), an exponential relationship exists between the tidal energy and the SPM (Figure 59 and Figure 60). As the tidal energy becomes high, there is thus a strong increase in SPM, and consequently turbidity maxima occur at locations around (or close to) the maximum in tidal energy (Figure 59, and Figure 53 and Figure 54). For the SPM data averaged over a tidal cycle (available for Scheldt and Humber, see Figure 60), no exponential relationship exists and data are much more scattered. Nevertheless, we do observe that the highest SPM values occur at relatively high tidal energy values.

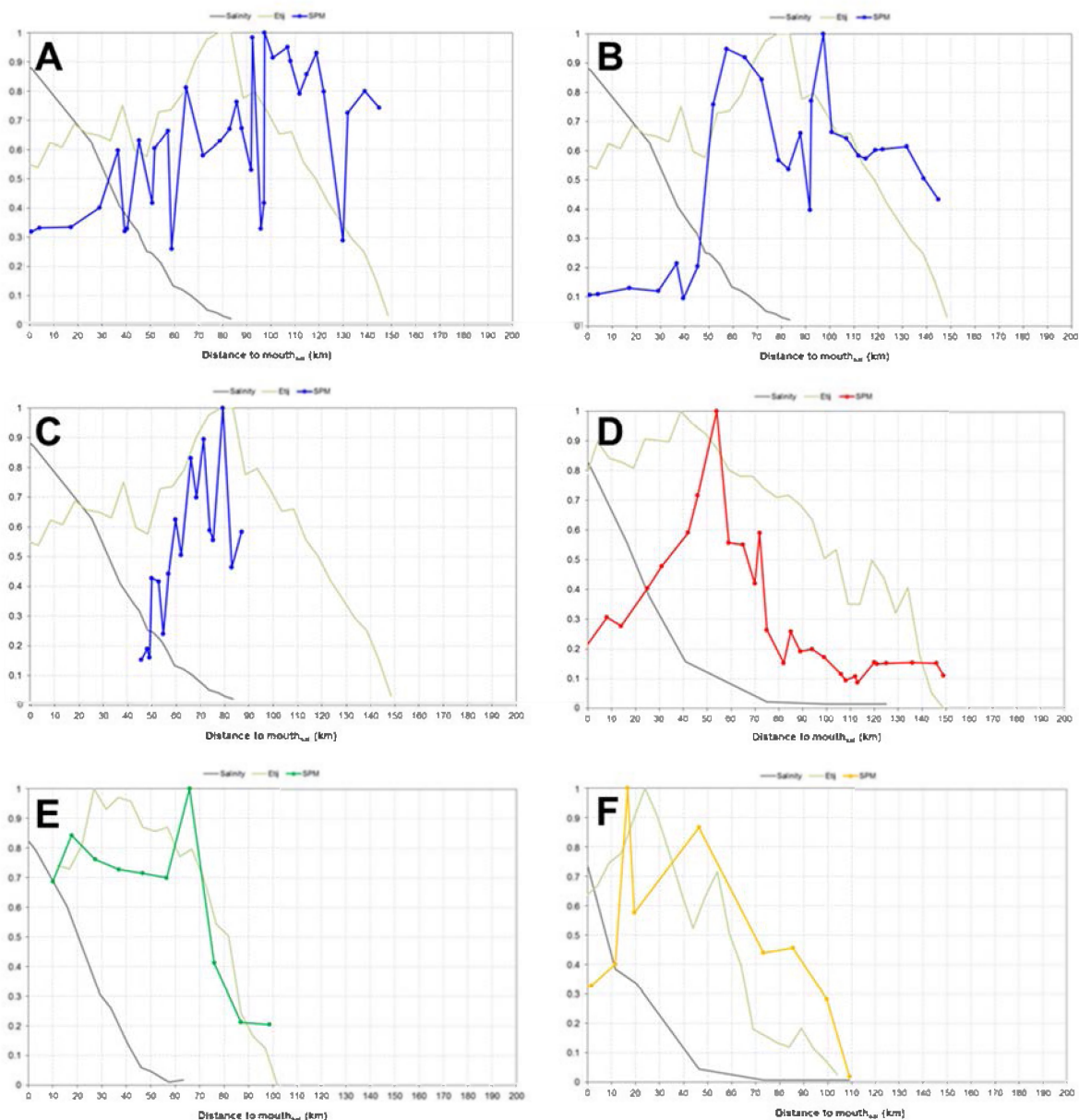


Figure 59 – Relative presentation of the mean salinity (grey line, compared to 30 PSU), mean tidal energy (light green line, compared to maximum tidal energy) and SPM data (compared to maximum SPM) for the different estuaries. Salinity zones (relatively to 30 PSU) – freshwater: < 0.017, oligohaline: 0.017-0.17, mesohaline: 0.17-0.6, polyhaline: 0.6-1. (a) surface SPM 2001-2010 for the Scheldt, (b) depth-averaged SPM 2001-2010 for the Scheldt, (c) surface SPM 2009 for the Scheldt, (d) surface SPM 2004-2009 for the Elbe, (e) surface SPM 2005, 2009-2010 for the Weser, (f) surface SPM 2004-2009 for the Humber

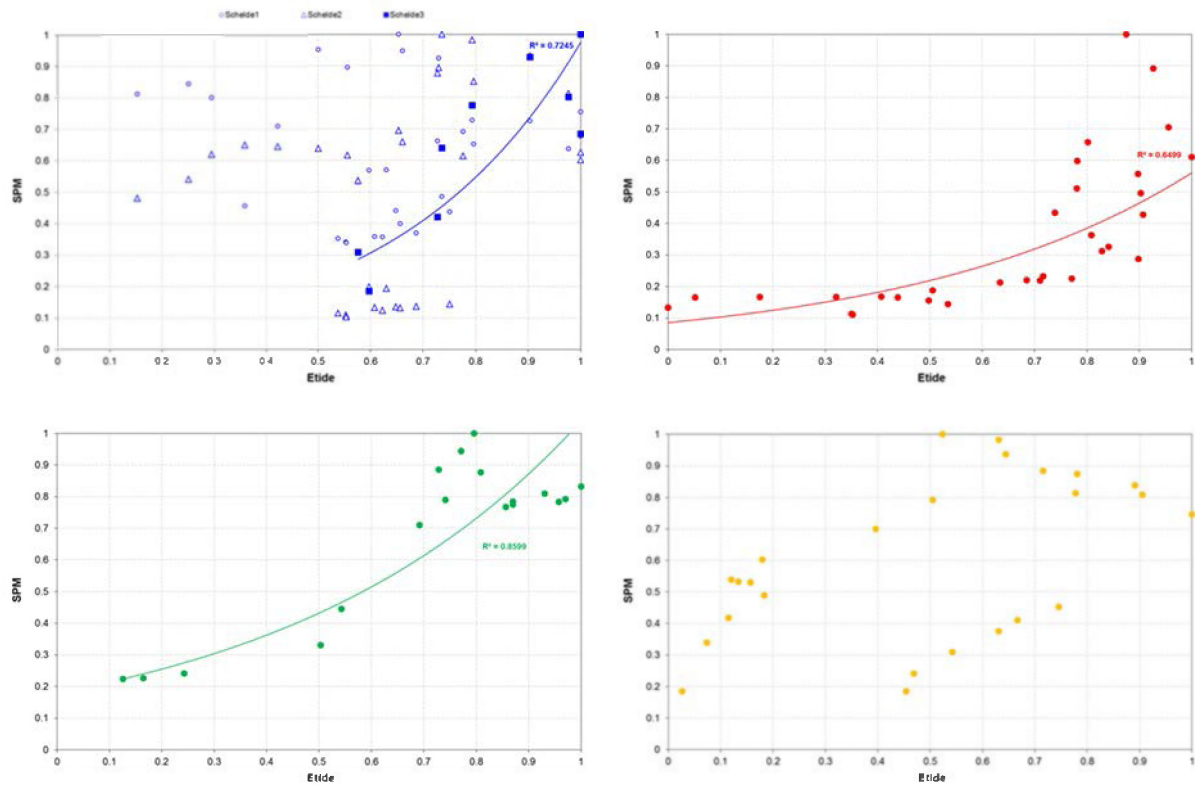


Figure 60 – Relationship between the tidal energy and the SPM for the Scheldt (blue), Elbe (red), Weser (green) and Humber (yellow). Data averaged over 5 km blocks and presented relatively by dividing with the maximum value

5.3.4 Relation between salinity and SPM

As the salinity decreases, we observe for the Scheldt, Elbe and Humber an increase in surface SPM (Figure 61). For the Weser however, SPM values are over the entire salinity range close to the turbidity maximum of 1 (turbidity maximum for the Weser not plotted here since located in the freshwater zone, see Figure 59e). For the Humber, SPM values remain high for the salinity range 0 till 0.4 (> 12 PSU) and then drop to much lower values once the salinity is larger than 0.4 (> 12 PSU). For the Scheldt and Elbe, SPM values already attain lower values once the salinity is larger than 0.1-0.2 (> 3-6 PSU).

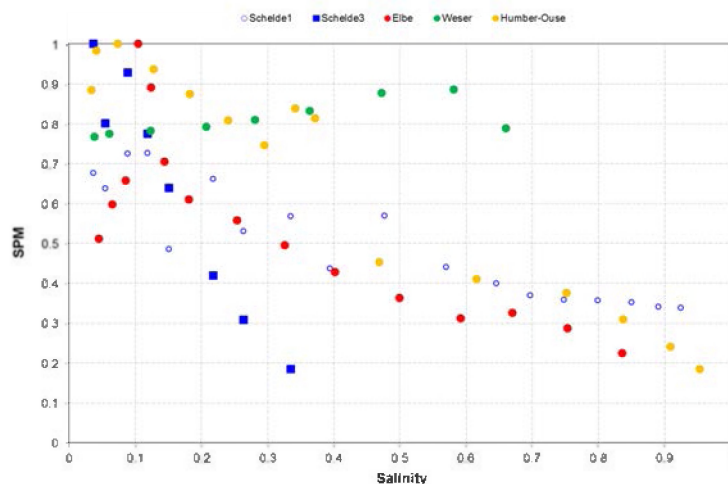


Figure 61 – Relationship between the salinity and the SPM for the four TIDE estuaries. Data averaged over 5 km blocks and presented relatively by dividing with the maximum value (for SPM) and by 30 (for salinity). Data for the freshwater zone are excluded

5.3.5 Conclusions

SPM data is rather sparse for the different estuaries. Therefore the available data differ for each estuary (samples taken at different stages of the tidal cycle), and an interestuarine comparison of SPM was not evident. It should be mentioned that all conclusions formulated below are done based on the available SPM-data, and that differences due to different sample strategies have been taken into account as much as possible. Where a lot of necessary additional data (e.g. type of sediment, up-estuarine fluxes of sediment coming into the system, spatial (over depth, cross section,...) and temporal variation (tidal cycle, spring-neap cycle,...) was lacking, these conclusions should be rather seen as an indication, than scientific well argumentated.

The Humber is a high turbid system compared to the Scheldt, Elbe and Weser (750 mg/l versus values < 250 mg/l, see Figure 50). The high turbidity of the Humber is explained by the high import of sediment, both at the sea boundary as at the river boundary (Figure 57). For the other estuaries, sediment fluxes are clearly lower compared to the Humber (Figure 57). The Weser for example has suspended sediment transport only in the ebb direction (see Figure 57 and Figure 58), which implies that sediment is flushed much more easily out of the estuary. The Scheldt and Elbe are still featured by sediment transport from the sea, however these sediment fluxes are very small (factor 10-100) compared to the sediment fluxes in the ebb direction (Figure 57). It should be pointed out that all sediment fluxes are calculated under mean tidal conditions, while important variations may occur with spring-neap tide variation. Moreover, the turbidity in the estuaries is not only affected by the tidal conditions but also by the flushing times (or residence times, see also §5.4) and sediment availability and riverine import. In long, more slowly flushed estuaries (e.g., the Scheldt) the turbidity in the estuary is higher during the fast currents of large spring tides, while in short, more rapidly flushed estuaries (e.g., the Weser), fine sediments are quickly lost to the coastal zone during the ebb currents of the spring tides (Uncles, 2002). The importance of riverine discharge variations (and thus variation in flushing/residence time) is also demonstrated by the confluence of ebb and flood dominated sediment fluxes, and by the absolute values of the sediment fluxes (see Figure 58).

For SPM data collected during similar tidal conditions (low water, half tide), we observe an exponential relationship between the tidal energy and the SPM (Figure 60), which means that an estuarine turbidity maximum (ETM) occur at locations with high tidal energy. This exponential relationship is not present for SPM data averaged over a tidal cycle, but nevertheless are high SPM values observed at locations with relatively high tidal energy. This is not surprising since higher flow velocities and higher turbulence keeps fine sediment more easily in suspension. We may conclude that for all estuaries, elevated SPM values occur at locations where the tidal energy is high, but this does not imply that ETM automatically coincide with the absolute maximum in tidal energy (see Figure 51 until Figure 55). Other mechanisms may also play their role. Firstly, in the Humber estuary, the ebb and flood directed sediment fluxes meet in between the two ETM's. One would expect that at the location where these fluxes meet, an ETM occurs. The fact that ETM's occur upstream and downstream from this location, may be a consequence of the shifting of the confluence of both sediment fluxes due to variations in riverine discharge (see yellow arrows, Figure 58). Secondly, for the Scheldt and Elbe, an ETM occurs in the oligohaline zone of the estuary which means that besides tidal energy also deflocculation/flocculation processes may lead to an increase in SPM values. Indeed, it has been demonstrated in the Scheldt that for PSU values < 5 deflocculation processes start to occur, and that deflocculation is complete for PSU values < 1 (Wollast, 1967, 1973). This means that in the oligohaline zone, flocculated sediment particles start to fall apart, stay longer in suspension, and hence lead to higher values in suspended sediments. For the Elbe, the turbidity maximum also occurs in the oligohaline zone, here at a PSU value around 3.

5.4 TOPIC 4 – Residence time

The residence time is an important input parameter for the ecology study within the TIDE project. In this topic we mainly focus on the differences in residence time between the estuaries. Residence times are calculated according to the fractal freshwater method (§3.2.5) which requires as input parameters: salinity (§3.1.3), riverine discharge (§3.1.5) and estuarine volume (based on the topo-bathymetry, see §3.1.1 and §3.2.1).

5.4.1 Parameters determining residence time

An overview of the parameters used to calculate residence times according to the fractal freshwater method (see §3.2.5) is given in Figure 62, Figure 63 and Figure 64. The Scheldt has clearly the largest estuarine volume, but in general has lower fractional freshwater concentration values f (for definition of f , see §3.2.5) along the length axis of the estuary (Figure 62). Lower f values along the length axis imply higher salinity values which means that for the Scheldt the tidal intrusion is relatively more important than the freshwater discharge, compared to other estuaries. The Elbe for example is characterized by high freshwater discharges (Figure 64) and a rather low tidal range at the mouth (limiting tidal intrusion, see Figure 29). As a consequence f values are high over the entire estuary ($f > 0.7$, excluding the mouth area, Figure 62).

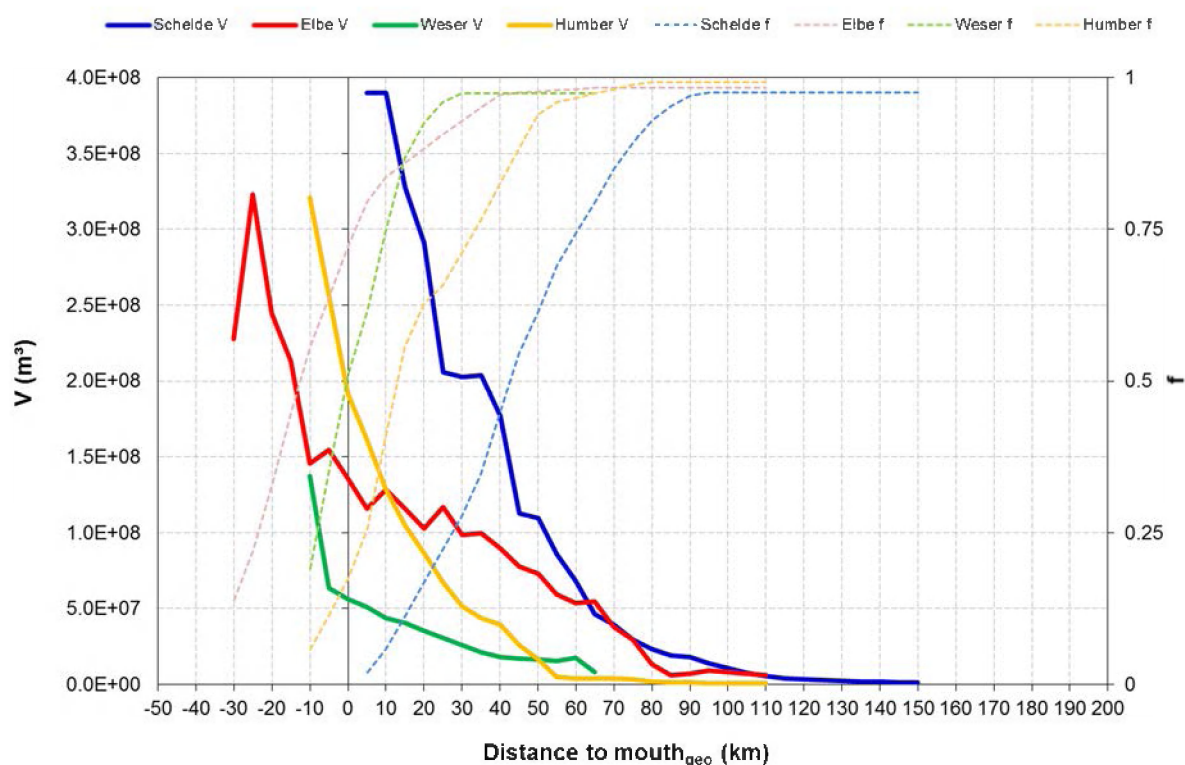


Figure 62 – Estuary volume V (over 5 km) and fractional freshwater concentration f for the four estuaries

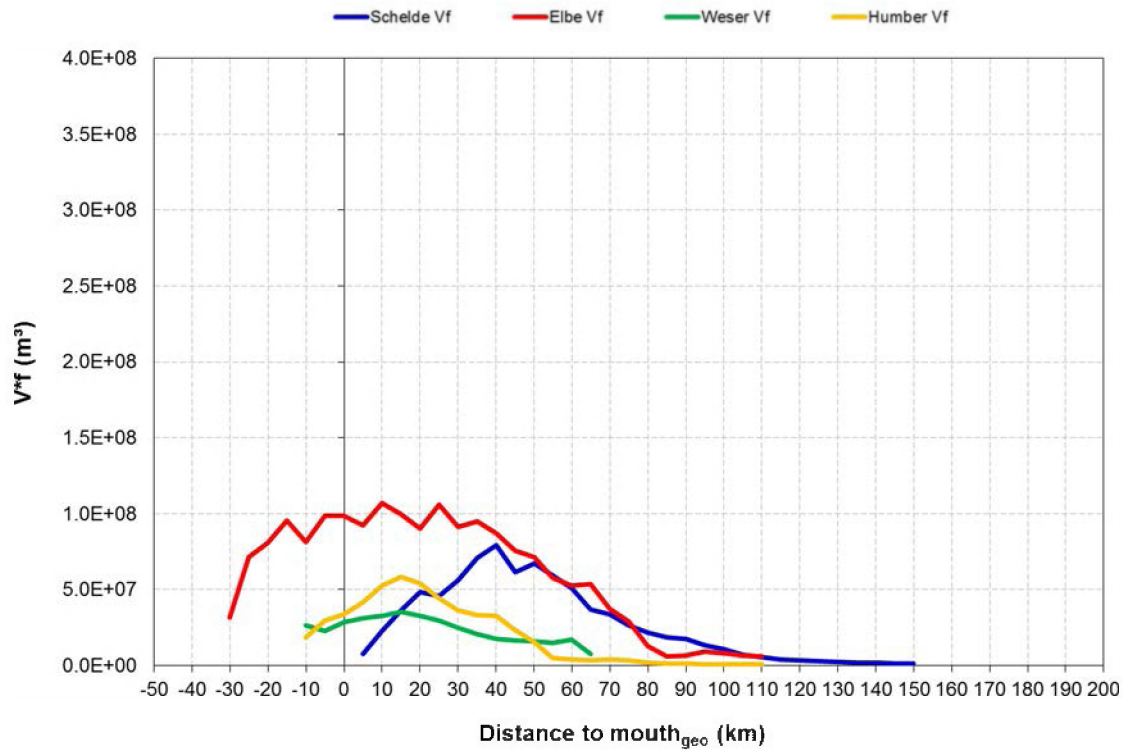


Figure 63 – The total volume of fresh water ($V_f = V \cdot f$) in each estuary segment (over 5 km), calculated according to the fractional freshwater method (Dyer, 1973)

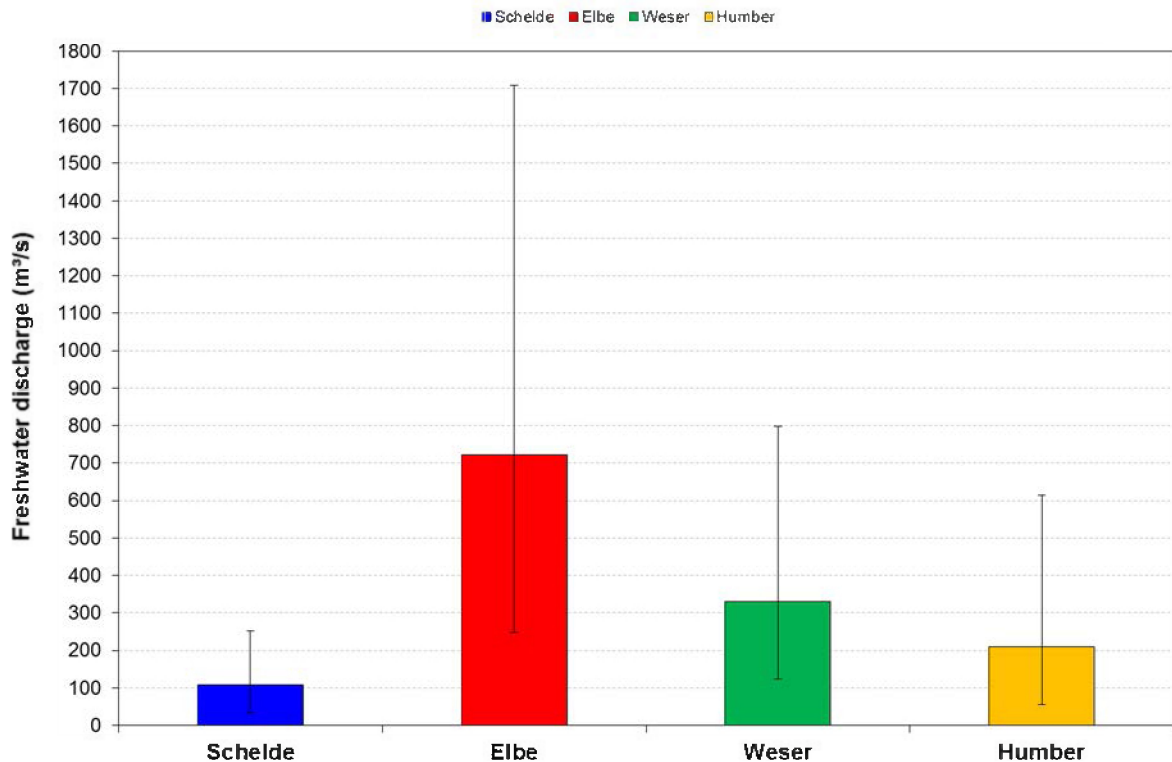


Figure 64 – Mean freshwater discharges for the 4 estuaries. Error bars are representative for typical high (P95) and low (P5) freshwater discharge values

5.4.2 Residence time for low, mean and high river discharges

The available freshwater volume is the highest for the Scheldt and Elbe (Figure 63), however calculated residence times for the Scheldt are clearly higher than for the Elbe (Figure 65) due to the much lower discharges in the Scheldt than for the Elbe (Figure 64). Or in other words, it takes in the Scheldt much more time to replace the available fresh water volume due to the low freshwater discharge. The Weser estuary is characterized by a low estuarine volume (Figure 62), low fresh water volumes (Figure 63), and an intermediate freshwater discharge (Figure 64), and consequently has lower residence times compared to the other estuaries.

Cumulating the calculated residence times for each estuary segment from the up-estuary boundary to the mouth_{geo} (Figure 66) returns the total residence time for each estuary (Figure 67). This is thus the time needed for a water molecule to flow from the up-estuary boundary the mouth_{geo}. The bars in Figure 67 represent the residence times under conditions of mean freshwater discharge, while the error bars represent the residence times for high (P95 value) and low (P5 value) freshwater discharges (respectively lower and upper error bar). During summer conditions freshwater discharges are generally lower than the mean freshwater discharge and residence times will range between the mean residence time and the upper error bar. During winter residence times will range between the mean residence time and the lower error bar (Figure 67). The residence times calculated over the different estuary segments (Figure 65) further allows the calculation of residence times over the different TIDE zones (Geerts et al., 2011) (see Table 9), which is important for the ecology study performed within the TIDE project.

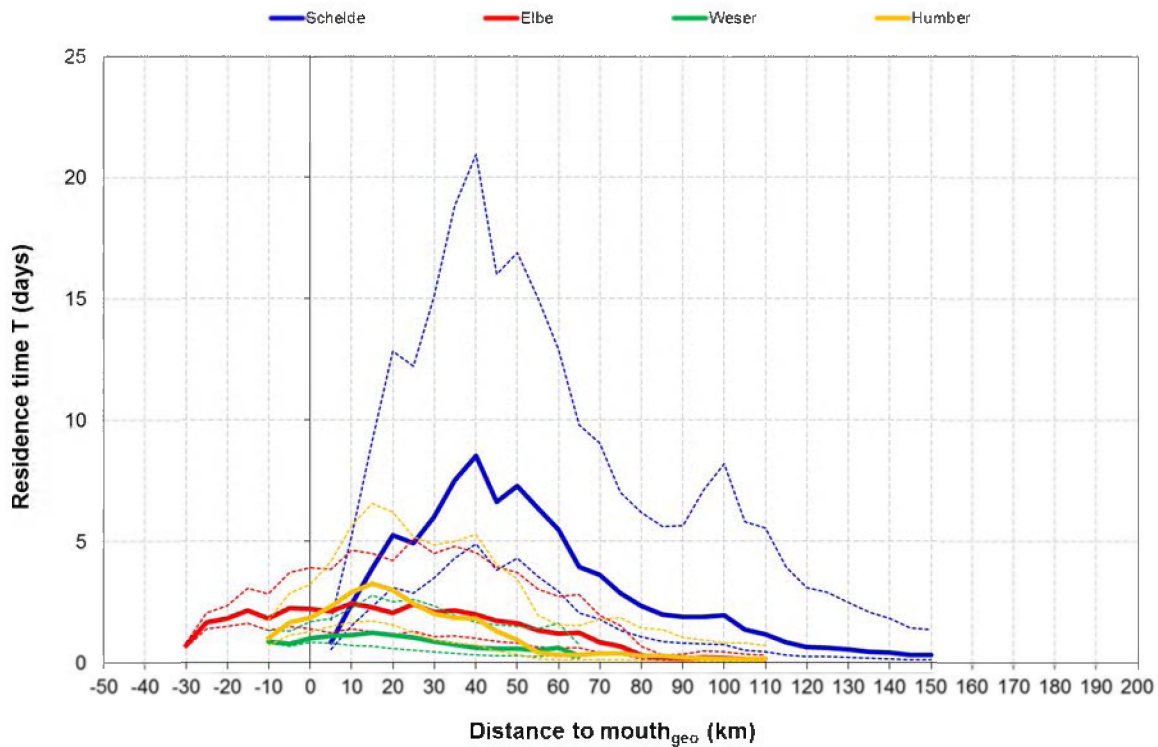


Figure 65 – Residence times for each estuary segment of 5 km along the different estuaries. Solid lines represent the residence time under mean freshwater discharge conditions, envelopes (dashed lines) represent high and low freshwater discharges (respectively P95 and P5 values)

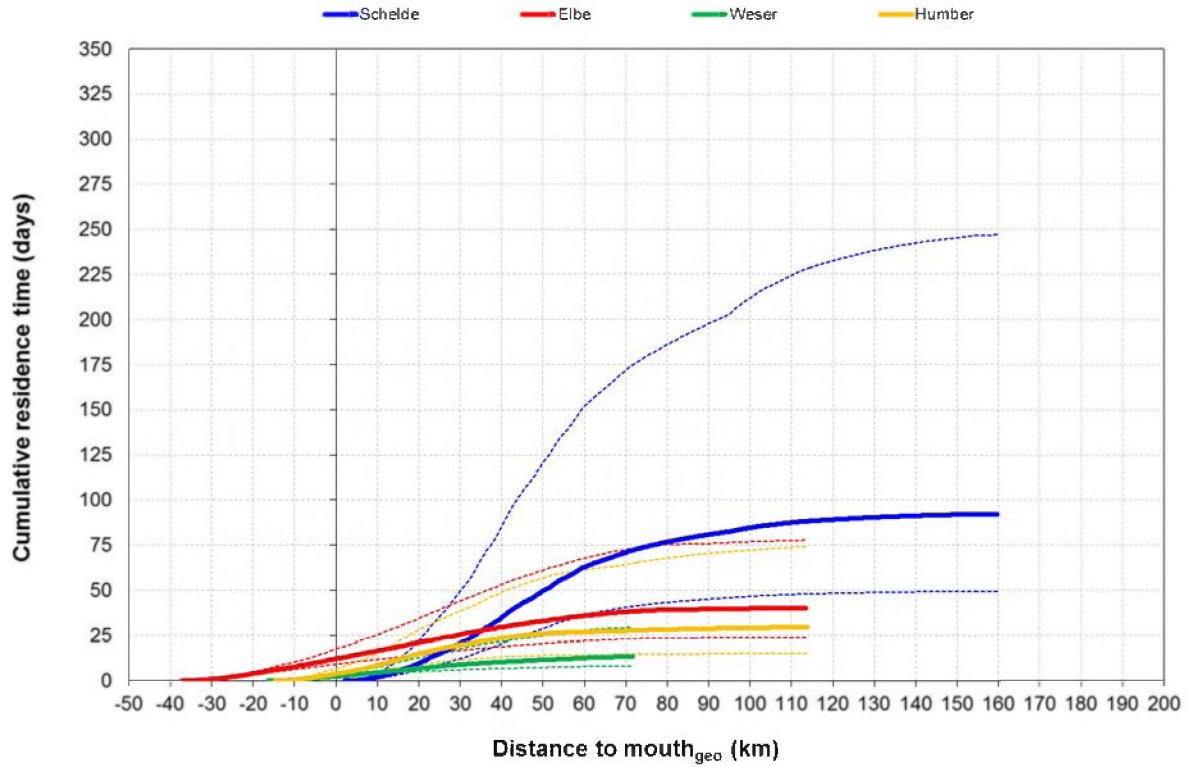


Figure 66 – Cumulative residence times along the different estuaries. Solid lines represent the residence time under mean freshwater discharge conditions, envelopes (dashed lines) represent high and low freshwater discharges (respectively P95 and P5 values)

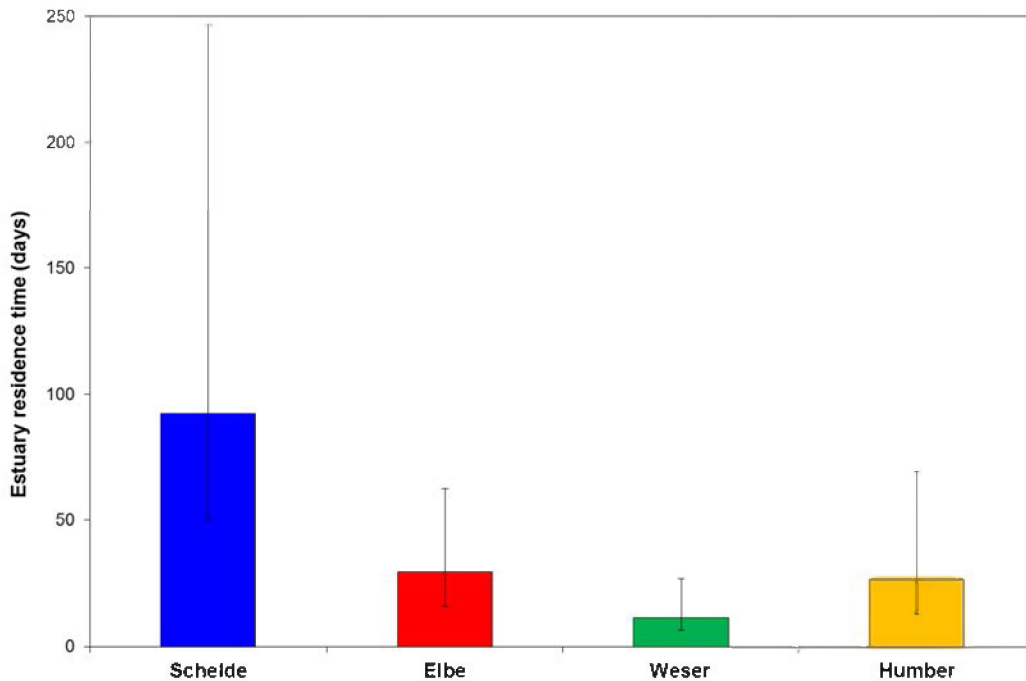


Figure 67 – Total residence time (from up-estuary boundary to mouth_{geo}) under mean freshwater discharge conditions (bar), and for high and low freshwater discharges (P95 and P5)

5.4.3 Conclusions

Within this study residence times were calculated according the fractal freshwater method (§3.2.5). This method incorporates the estuarine volume, the available volume of fresh water in the estuary, and the freshwater discharge (river flow). The calculated residence time for the entire estuary (i.e. from up-estuary boundary to mouth_{geo}) under conditions of mean, low and high freshwater discharge are summarized in Table 8. Estuaries with a high estuarine volume and low freshwater discharges (e.g., Scheldt) will yield high residence time, while estuaries with a low estuarine volume and higher freshwater discharges (e.g., Weser) will yield low residence times. An overview of the residence times per salinity zone is given in Table 9.

Table 8 – Residence time (in days) from up-estuary boundary to mouth_{geo} under conditions of mean, low and high freshwater discharge (river flow), calculated according to the fractal freshwater method

River flow	Scheldt	Elbe	Weser	Humber
High	50	16	7	13
Mean	92	29	11	27
Low	247	63	27	69

Table 9 – Residence time (in days) for each salinity zone (definition of salinity zones see Geerts et al., 2011) under conditions of mean freshwater discharge (= river discharge = R), calculated according to the fractal freshwater method

Salinity zone R = mean	Scheldt	Elbe	Weser	Humber
Freshwater 1	2	1	3	1
Freshwater 2	5	2	2	-
Freshwater 3 ³	-	15	-	-
Oligohaline	13	12	6	2
Mesohaline	29	9	3	11
Polyhaline ⁴	44	-	-	15

³ Freshwater 3 is only defined for the Elbe estuary

⁴ Residence times could not be calculated for the polyhaline zones of the Elbe and Weser because the polyhaline zones were not entirely covered by cross-sections. The most downstream cross-sections are respectively located at TIDE km 151 and 89 while the downstream edge of the polyhaline zone is located at respectively TIDE km 171 and 119 (see also Figure 10 and Figure 11)

5.5 TOPIC 5 – Impact of increasing MHWL on tidal marsh ecosystems

In this topic we look at the impact of increasing MHWL on the tidal marsh ecosystems. Did the increasing high water levels result in increased tidal flooding of the tidal marshes or was vertical sediment accretion in the marshes sufficiently high so that the elevation of the marshes could grow in accordance with the growing high water level? And moreover, if vertical sediment accretion was important, did this result in steepening of the intertidal area and hence in increased landward erosion of the tidal marsh shorelines? The methodology applied for research topic 5 is described in §3.1.6.

5.5.1 Change in marsh platform elevation

For the Scheldt marsh, the mean increase in MHWL over the time period 1931-2010 is 0.53 cm/year (blue line, Figure 68). During this period the marsh evolved from a low elevated marsh in 1931 (platform elevation 0.47 m below MHWL) towards a high elevated marsh in 2010 (platform elevation 0.37 m above MHWL) (brown line, Figure 68). Over a period of 79 year this is an absolute increase in elevation of 1.08 m, which corresponds with a mean rate of 1.4 cm/year. However this rate is not constant in time (orange line, Figure 68), we observe that when the marsh has a low elevation in the tidal frame, the increase in platform elevation is almost 2 cm/year. Once the platform elevation reaches MHWL, the rise in platform elevation decreases towards values of 1-1.2 cm/year. Currently, the platform has an elevation 0.09 m below MHWLS.

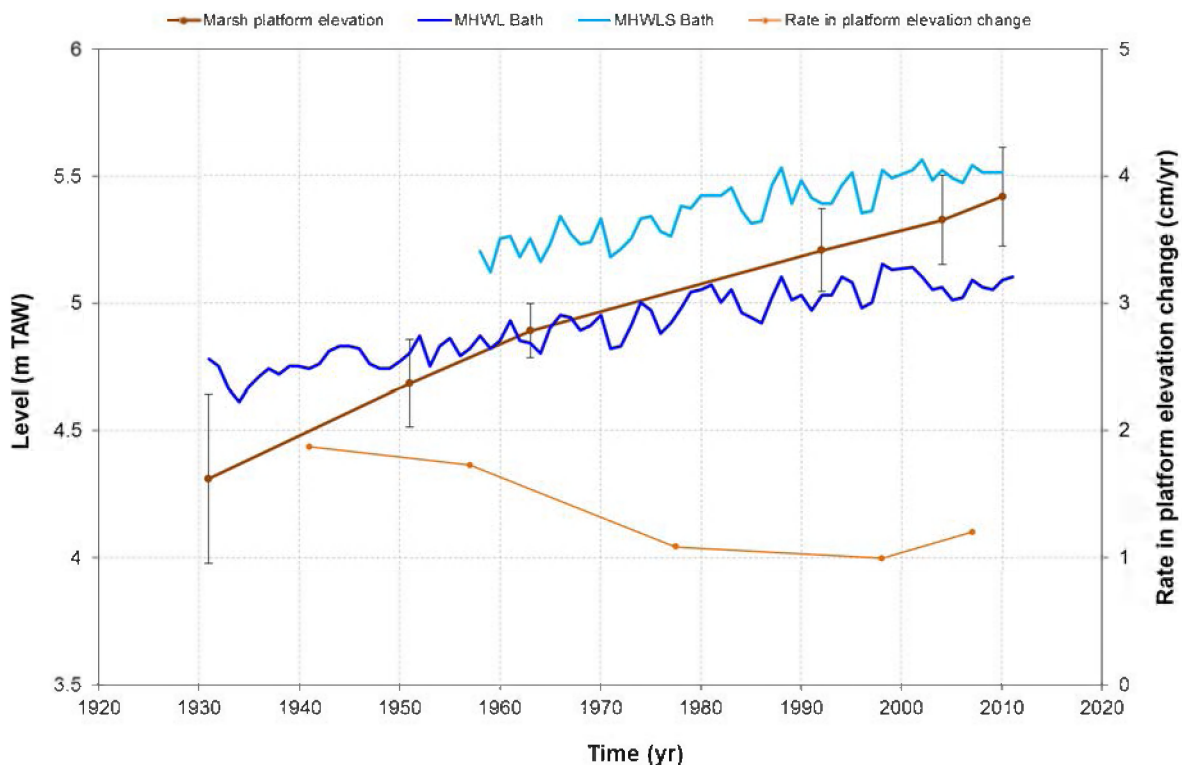


Figure 68 – Change in marsh platform elevation, MHWL, and MHWLS for the Scheldt marsh site (Saeftinghe) (location, see Figure 9 and Figure D 1)

For the Elbe marsh, the mean increase in MHWL over the time period 1958-2008 is 0.4 cm/year (blue line, Figure 69). During this period the marsh evolved from a low elevated marsh in 1958 (platform elevation 0.42 m below MHWL) towards a high elevated marsh in 2008 (platform elevation 0.68 m above MHWL) (brown line, Figure 69). Over a period of 50 year this in an absolute increase in platform elevation of 1.57 m, which corresponds with a mean rate of 3.1 cm/year. However this rate is not constant in time, and ranges between 0.75 and 4.5 cm/year (orange line, Figure 69). As for the Scheldt marsh, we don't observe in time a decrease of the rate in platform elevation change.

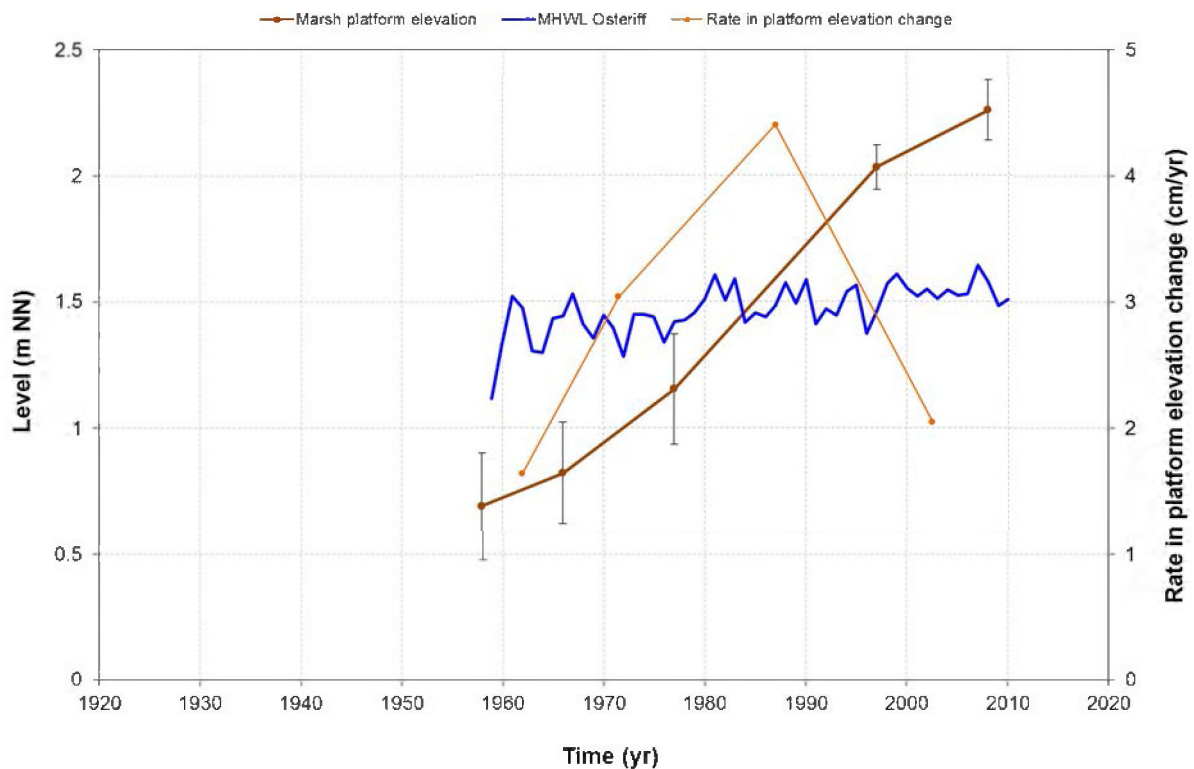


Figure 69 – Change in marsh platform elevation and MHWL for the Elbe marsh site (Kehdingen area) (location, see Figure 10 and Figure D 2)

5.5.2 Conclusions

The platform elevation change of two brackish marsh sites (one in the Scheldt and one in the Elbe) was evaluated in response to an increase in MHWL. Both marsh sites were able to follow up the increase in MHWL (similar for both sites, 0.5 cm/yr for Scheldt, 0.4 cm/yr for Elbe), and evolved from a low elevated marsh (elevation for both sites from about 0.45 below MHWL) towards a high elevated marsh (for the Scheldt site 0.37 m above MHWL, for the Elbe site 0.68 m above MHWL). However, for the Elbe site, the increase in elevation was established in a shorter period of time (50 versus 79 year), and currently the site has a higher position in the tidal frame than the Scheldt site. For the Scheldt marsh, the mean platform elevation increase is 1.4 cm/yr, for the Elbe marsh this is 3.1 cm/yr.

The observation that both marshes are able to follow up the increase in MHWL, suggests that sediment availability at both marsh sites is sufficient. At the Scheldt site, surface SPM values are about 60 mg/l (see Figure 28 and Figure 9), whereas at the Elbe site this is about 150 mg/l (i.e. close to the turbidity maximum, see Figure 28 and Figure 10). The higher SPM values at the Elbe site may explain why the rate in platform elevation increase is about 2 times larger for the Elbe site than for the Scheldt site (3.1 cm/yr versus 1.4 cm/yr). However, we do not know how SPM values evolved historically. For the Scheldt, we observe that the rate in platform increase decreases in time. Thus, as the platform rises in the tidal frame, the increase in platform elevation decreases (asymptotic curve). This is in accordance with earlier findings on long-term changes of marsh platform elevation (Temmerman et al., 2004). However, for the Elbe we do not observe this asymptotic increase. The increase in platform elevation is here much more variable in time, with a peak increase of about 4.5 cm/yr between 1975 and 1995. This could be linked to the deepening of the Elbe fairway in the 1980's, leading to an increase in SPM values. Finally, it should be pointed out that the more rapid increase in platform elevation for the Elbe marsh leads to a faster succession in vegetation types and thus differences in organic accumulation rates. Moreover, vegetation characteristics determine to what extent sediment particles can be captured and accrete on the tidal marsh surface. Currently, the dominant plant species for the Scheldt marsh is *Elymus athericus*, whereas the Elbe marsh is characterized by a higher successive stage dominated by *Phragmites australis*.

Firstly, we may conclude that despite the current differences in SPM values (60 mg/l versus 150 mg/l), both marshes are able to follow up an increase in MHWL. This observation can be considered as favorable for e.g. coastal protection. Secondly, the differences in SPM values have their implications for the ecological state of tidal marshes. For higher SPM values (natural or anthropogenic cause), the increase in platform elevation is faster. This leads to a faster succession of marsh vegetation types, by which a high succession stage with less plant diversity is reached earlier.

6 General conclusions

6.1.1 Geometrical characteristics

Each of the TIDE estuaries is featured by its own morphological signature. Concerning the longitudinal change in width, all four estuaries have a typical funnel shape. The Humber is the most convergent, followed by the Scheldt (intermediate convergence), the Elbe and Weser are the least convergent (Figure 70). In the past the width of the estuaries has been reduced by land reclamation. Although most of the land reclamation took place over a longer period that started in the Middle Ages, morphological changes in the estuaries can still be influenced by these historical activities.

The mean estuary depth is very comparable for the Scheldt, Weser and Elbe and ranges from 7 – 7.5 m (i.e. the cross-section averaged depth at low water, Figure 70). The Humber on the other hand is much more shallow with a mean estuary depth of about 3.3 m. The large estuary depths for the Scheldt, Elbe and Weser are (partly) a consequence of intense dredging activities. As the most important ports are located deep inland, large parts of these 3 estuaries need to be dredged to maintain and occasionally also deepen, the fairway and in this way enable large ships to reach the harbors of Antwerpen, Hamburg and Bremen (Figure 71). In the Humber, the most important port is located near the mouth and limited dredging activities are only necessary in the mouth area.

Deepening of the fairway not only affects the depth, but also the shape of a cross section. Deepened, dredged channels have a typical wide and deep trapezoidal shape, while naturally formed channels (no artificial dredging) have a more rounded profile and generally shallower average depths. These differences in shape are found in the distribution of the subtidal habitats (deep, moderately deep and shallow, see §3.3.1). The Scheldt, Elbe and Weser are dominated by the deep subtidal habitat, whereas the deep, moderately deep and shallow subtidal habitats of the Humber are equally distributed (Figure 41).

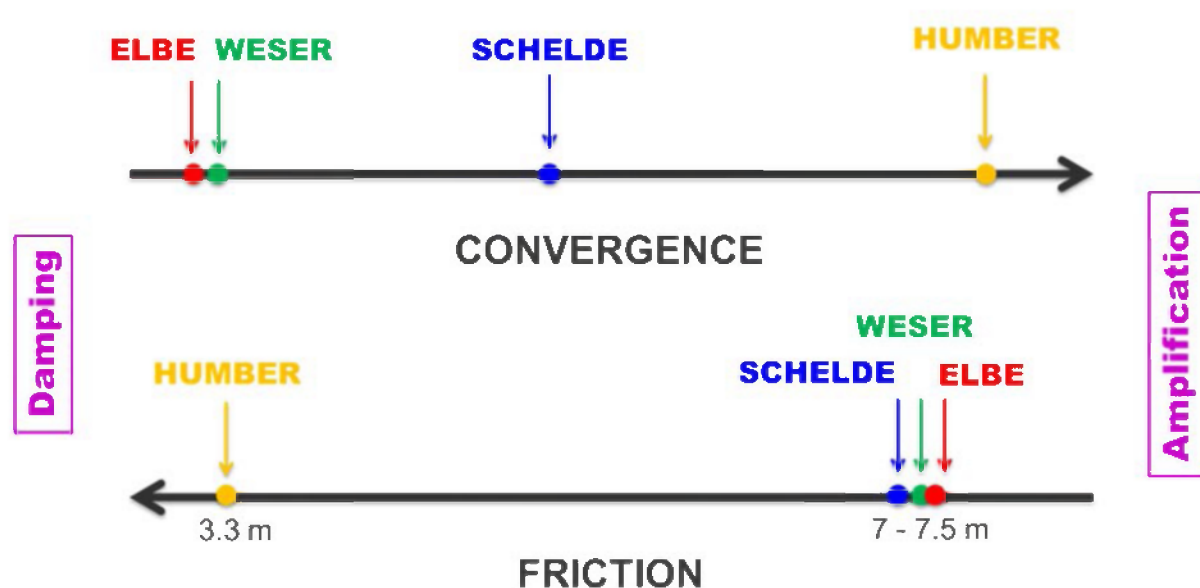


Figure 70 – Convergence (based on $1/b$ value, see estuary convergence in §3.2.2) and friction (based on the cross-section averaged depth at low water) for the four TIDE estuaries.

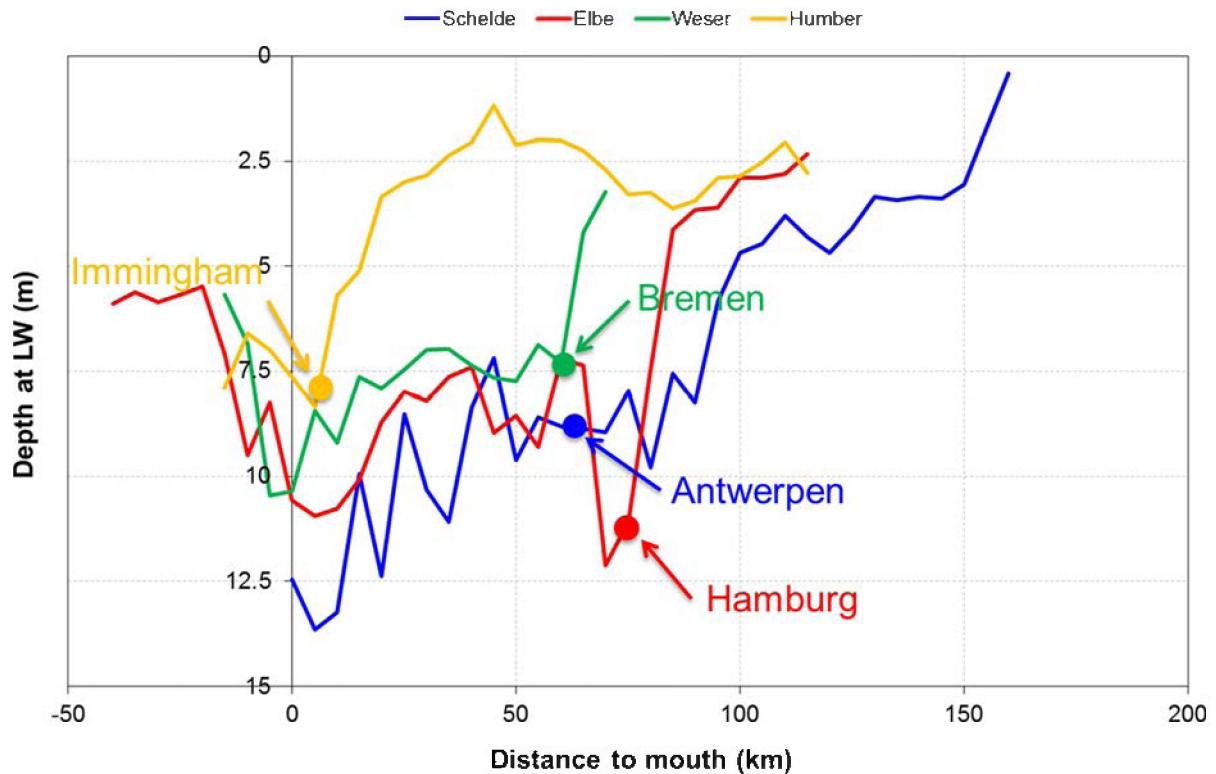


Figure 71 – Cross-section averaged depth at low water along the four TIDE estuaries, with indication of the major ports

6.1.2 The important role of morphology on tidal amplification/damping

The two most important factors that influence tidal amplification and tidal damping in an estuary are: (1) the funneling of the estuary (i.e. estuary convergence) leading to tidal amplification (the more convergent, the more tidal amplification), and (2) the friction in the estuary (controlled by the estuary depth) which leads to tidal damping. So, if an estuary is strongly convergent and is featured by a large estuary depth (thus a limited friction), it makes the estuary more vulnerable to tidal amplification (Figure 70). Based on the geometric and morphological features of the TIDE estuaries (see Figure 70), we may infer that the Scheldt estuary is most vulnerable to tidal amplification since it has an intermediate convergence and a large estuary depth. Indeed, we observe that the tidal range increases up to a maximum TR_x/TR_0 value of 1.4 (the highest of the 4 estuaries, see Figure 30), and that increased tidal range ($TR_x/TR_0 > 1$) occurs over a distance of 130 km, which is 85% of the estuary length (see Figure 31). The Elbe also reaches large TR_x/TR_0 values (up to 1.3), but here tidal amplification starts deeper in the estuary (about 10 km from the mouth, see Figure 32). Although we did not look at the mouth area in particular, the shallow character of the Elbe mouth area (which is friction dominated) may possibly play an important role in the damping of the tidal wave as it enters the estuary ($1/\beta < 0$, Figure 24). Moreover, from km 0 till 40 from the mouth, the Elbe can be considered as a more or less prismatic channel. It is known that in an ideal prismatic channel no tidal amplification occurs (e.g., Savenije, 2001). The Weser has only a limited maximum TR_x/TR_0 value of 1.1, but here an increased tidal range ($TR_x/TR_0 > 1$) occurs over the entire estuary length. It should be pointed out that the Weser is the shortest estuary (65 km) which is not sufficiently long to reduce the tidal range ($TR_x/TR_0 < 1$). The fact that the maximum tidal range only reaches a value of $TR_x/TR_0 = 1.1$ is due to absence of tidal amplification between km 15 and 40 from the mouth (see Figure 32). In this area the subtidal width is relatively small compared to the intertidal width and thus the volume of water stored above the intertidal area (which is affected by friction) is probably relatively large compared to the volume of water which is transported through the deep subtidal channel with limited friction (see also Figure 24, $1/\beta < 0$). A second explanation for the absence of tidal amplification is the fact that the Weser estuary in that area is not a converging channel but a prismatic channel (see Figure A 3). The Humber finally is the most convergent estuary, but has a limited maximum TR_x/TR_0 of 1.15, and the tidal range becomes already damped at 25 km from the mouth (Figure 32). At this point friction becomes strongly dominant in the Humber (no deepened channels), especially in the area between Hull and Trent falls (see also Figure 24, $1/\beta \ll 0$).

Each of the TIDE estuaries has thus an area which can be considered as very important in the protection against flooding, since these areas induce tidal damping or they reduce the tidal amplification. In the Elbe, the mouth area (important friction), and the area in the most downstream part of the estuary between Brunsbüttel and Glückstadt (prismatic channel) prevent an increase in tidal range. For the Weser, no increase in tidal range is observed between Stadland and Elsfleth due to prismatic nature of the Weser channel in combination with an increase in friction. In the Humber, important tidal damping occurs between Hull and the Trent falls due to high friction in that area. The high friction is induced by the shallow character of the subtidal channels (no deepening of the channels by dredging). It should be pointed that this specific area is very important for the safety against flooding along the Humber. No dredging should be carried out in that zone, especially since the Humber is the most convergent (more vulnerable to tidal amplification) of all TIDE estuaries. In the Scheldt estuary we do not observe directly an area which could be considered as important for tidal damping or reduction of the tidal amplification. However, in this study we only looked at mean tidal conditions and consequently the effect of tidal marshes was not evaluated. For the Scheldt, it is known that the Saeftinghe marsh (3000 ha, around TIDE km 110, see Figure 9) stores a large volume of water during spring tides and in this way protects more upstream parts along the estuary.

Despite the important role of the above described areas in reducing or stopping tidal amplification, we cannot consider this as sufficient for a robust protection against flooding, especially along the Scheldt and Elbe where the strongest tidal amplification is observed. Several measures could be introduced to reduce tidal amplification in an estuary. Based on the analysis of all 4 estuaries, we found that tidal damping in estuary becomes important once the estuary depth (i.e. cross-section averaged depth at low water) is smaller than 4.2 - 7.7 m. As analysis were performed over 5 km blocks, this critical estuary depth should be present for at least 5 km along the estuary. The range in critical estuary depth (4.2 – 7.7 m) is a consequence of the estuary convergence: the more convergent the estuary, the smaller the critical estuary depth. However, we are convinced that it is necessary to include more estuaries in the analysis to improve the accuracy of the found threshold values in estuary depth. We also looked at the effect of habitat occurrence on tidal damping/amplification (i.e. vertical tide) and on flow velocities (i.e. horizontal tide). Tidal damping and tidal amplification in estuaries are to a large extent determined by the subtidal habitats, whereas intertidal and marsh habitats have no significant influence based on the observations. Tidal amplification occurs when the relative width in deep subtidal habitat (> 5 m below LW) is larger than 30% ($S_d > 30\%$) and the sum of the moderately deep and shallow subtidal habitats (5 - 0 m below LW) is smaller than 25%. Tidal damping occurs when $S_d < 20\%$ and $S_{ms} > 35\%$. To induce tidal damping in an estuary we thus recommend to have over a distance of 5 km (data were averaged over 5 km blocks), no excessive width in deep subtidal habitat (< 20%) and sufficient width in moderately deep and shallow subtidal habitat (> 35%). It should be pointed out that these analysis were performed only under mean tidal conditions. Possibly, an effect of intertidal and marsh areas on tidal damping/amplification will be observed under spring tide conditions. For the horizontal tide we could not find any relationship between the habitat occurrences and the flow velocity.

6.1.3 Indirect effects of morphology on SPM and tidal marsh evolution

Tidal amplification along estuaries not only affects the flooding risk, but also has a more indirect effect on for example sediment management or ecology. We found that turbidity maxima in estuaries occur at locations where the tidal energy (i.e. common effect of vertical and horizontal tide) is high. For the Scheldt and Elbe also deflocculation/flocculation processes may lead to higher SPM values. Higher amounts of SPM have on their turn an important influence on the ecology, concerning for example primary production or tidal marsh ecology. With regard to tidal marshes, we found that higher SPM values lead to a faster evolution towards a climax vegetation state. At this stage the tidal marsh is from an ecological point of view less valuable due to the limited plant diversity. On the other hand are sufficient high SPM values wanted because it enables tidal marshes to follow up the increase in MHWL which can be considered as favorable for coastal protection.

7 References

Brys, R.; Ysebaert, T.; Escaravage, V.; Van Damme, S.; Van Braeckel, A.; Vandevoorde, B.; Van den Bergh, E. (2005). Afstemmen van referentiecondities en evaluatiesystemen in functie van de KRW: afleiden en beschrijven van typespecifieke referentieomstandigheden en/of MEP in elk Vlaams overgangswatertype vanuit de overeenkomstig de KRW ontwikkelde beoordelingssystemen. Verslag van het Instituut voor Natuurbehoud, IN.O.2005.7. Brussel, 178 pp.

Dalrymple, R. W.; Zaitlin, B.A.; Boyd, R. (1992). "Estuarine Facies Models: Conceptual Basis and Stratigraphic Implications," *Journal of Sedimentary Petrology*, Vol. 62, No. 6, pp. 1130-1146.

Dyer, K.R. (1973). *Estuaries: A physical introduction*. Wiley, New York.

Fofonoff, N.P.; Millard, R.C. (1983). Algorithms for computation of fundamental properties of seawater. UNESCO Technical Papers in Marine Science = Documents techniques de l'Unesco sur les sciences de la mer, 44. UNESCO Division of Marine Science: Paris. 53 pp.

Forch, C.; Knudsen, M.; Sorensen, S.P.L. (1902). Berichte über die Konstanten-bestimmungen zur Anstellung der Hydroginphischen Tabellen Kgl. Kgl. *Danske Videnskab Selskabs, Skifter Naturvidenskab math.* Afdel XII, 1:1–151.

Geerts, L.; Wolfstein, K.; Jacobs, S.; Van Damme, S.; Vandenbruwaene, W. (2012). Zonation of the TIDE estuaries.

Ides, S.; Plancke, Y.; Temmerman S. (2011). Interestuarine comparison: proposal from hydrodynamic & morphological viewpoint.

Plancke, Y.; Taverniers, E.; Mostaert, F. (2011). Kubatuuurberekening voor het Scheldt-estuarium: Karakteristieke getijden uit het decennium 1991 - 2000 en topo-bathymetrische gegevens uit 2001. Versie 1_0. WL Rapporten, 770_54. Waterbouwkundig Laboratorium: Antwerpen, België

Plancke, Y.; Schramkowski, G.; Vandenbruwaene, W.; Mostaert, F. (2012a). TIDE - WP3 task 4: Interestuarine comparison: "Cubage" calculation for the Weser estuary. Version 2.0. WL Rapporten, 770/62b. Flanders Hydraulics Research; Antwerp, Belgium

Plancke, Y.; Vandenbruwaene, W.; Schramkowski, G.; Mostaert, F. (2012b). TIDE - WP3 task 4: Interestuarine comparison: "Cubage" calculation for the Elbe estuary. Version 2.0. WL Rapporten, 770/62b. Flanders Hydraulics Research; Antwerp, Belgium

Plancke, Y.; Vandenbruwaene, W.; Schramkowski, G.; Mostaert, F. (2012c). TIDE - WP3 task 4: Interestuarine comparison: "Cubage" calculation for the Humber estuary. Version 2.0. WL Rapporten, 770/62b. Flanders Hydraulics Research; Antwerp, Belgium

Savenije, H.H.G. (2001). A simple analytical expression to describe tidal damping or amplification *J. Hydrol.* (Amst.) 243(3-4): 205-215

Savenije, H.H.G. (2005). *Salinity and tides in alluvial estuaries*. Elsevier: Amsterdam. ISBN 0-444-52108-9. xiv, 194 pp.

Smets, E. (1996). Getij-en kubatuuurberekeningen voor het Scheldtbekken: het gemiddeld getij over het decennium 1971-1980, een gemiddeld getij typisch voor het jaar 1980. WL Rapporten, 405_2. Waterbouwkundig Laboratorium: Antwerpen. Vol. 1 (Verslag); Vol. 2 (resultatenbundel, tabellen en grafieken) pp.

Temmerman, S.; Govers, G.; Wartel, S.; Meire, P. (2004). Modelling estuarine variations in tidal marsh sedimentation: response to changing sea level and suspended sediment concentrations. *Mar. Geol.* 212(1-4): 1-19. [dx.doi.org/10.1016/j.margeo.2004.10.021](https://doi.org/10.1016/j.margeo.2004.10.021)

Uncles, R.J.; Stephens, J.A.; Smith, R.E. (2002). The dependence of estuarine turbidity on tidal intrusion length, tidal range and residence time. *Continental Shelf Research* 22: 1835-1856.

van Rijn, L.C. (2011). Comparison hydrodynamics and salinity of tide estuaries; Elbe, Humber, Scheldt and Weser. *Deltares: Delft*. 97 pp.

Winterwerp, J.C. (2012). On the response of tidal curves to deepening and narrowing – risks for a regime shift towards hyper-turbid conditions.

Appendix A – Estuary convergence

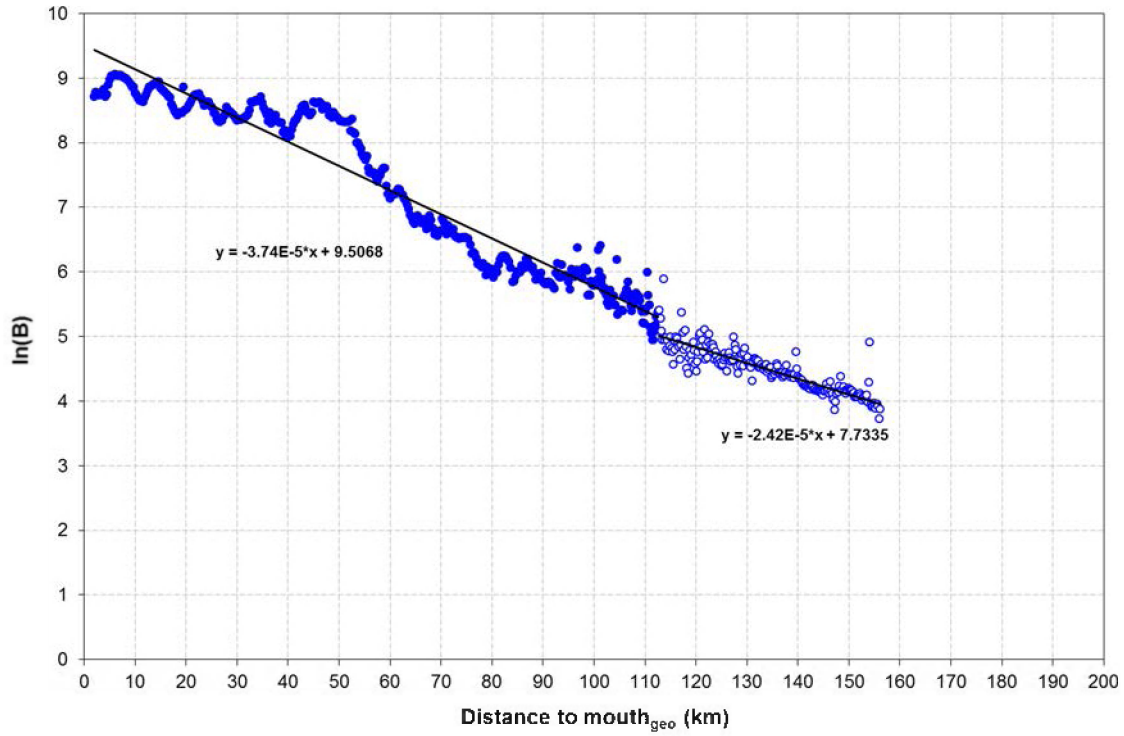


Figure A 1 – Convergence for the Scheldt estuary. 1/b values are given in Table 4

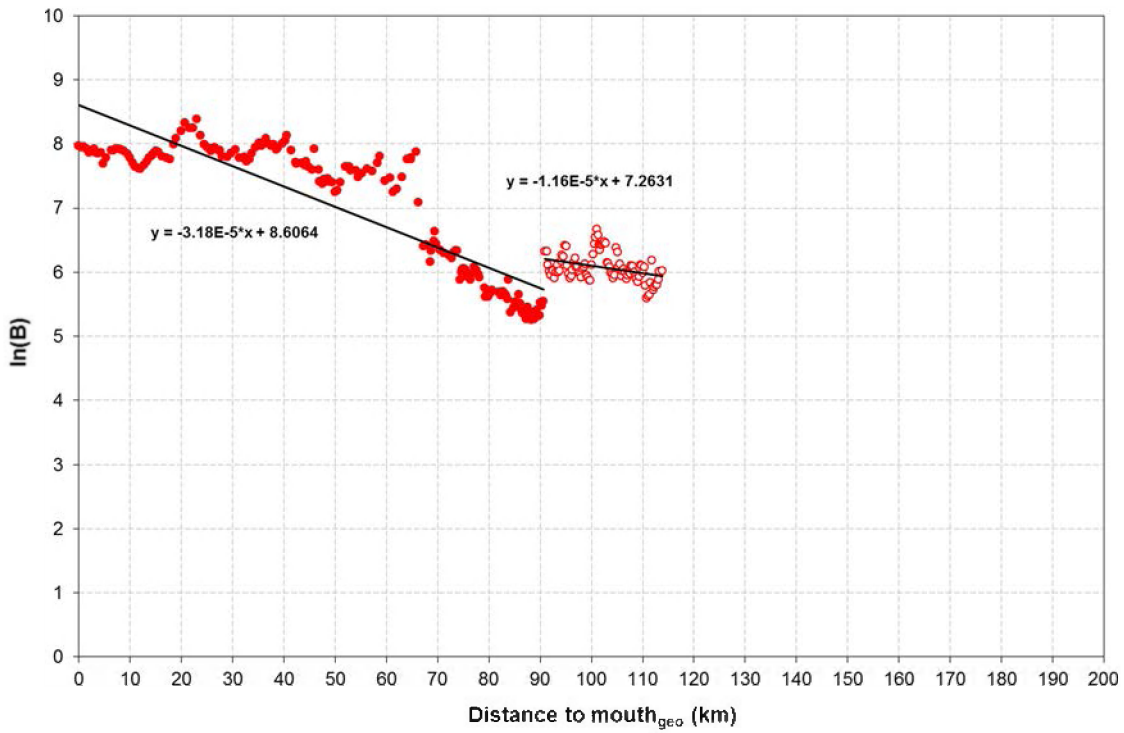


Figure A 2 – Convergence for the Elbe estuary. 1/b values are given in Table 4

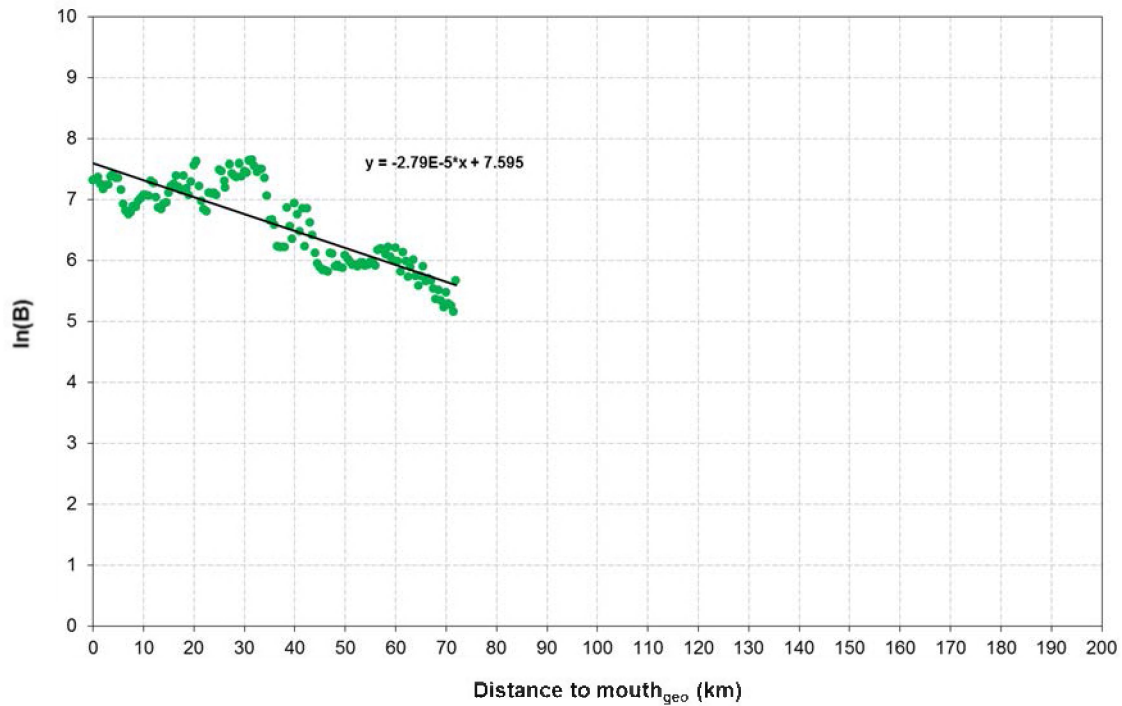


Figure A 3 – Convergence for the Weser estuary. $1/b$ values are given in Table 4

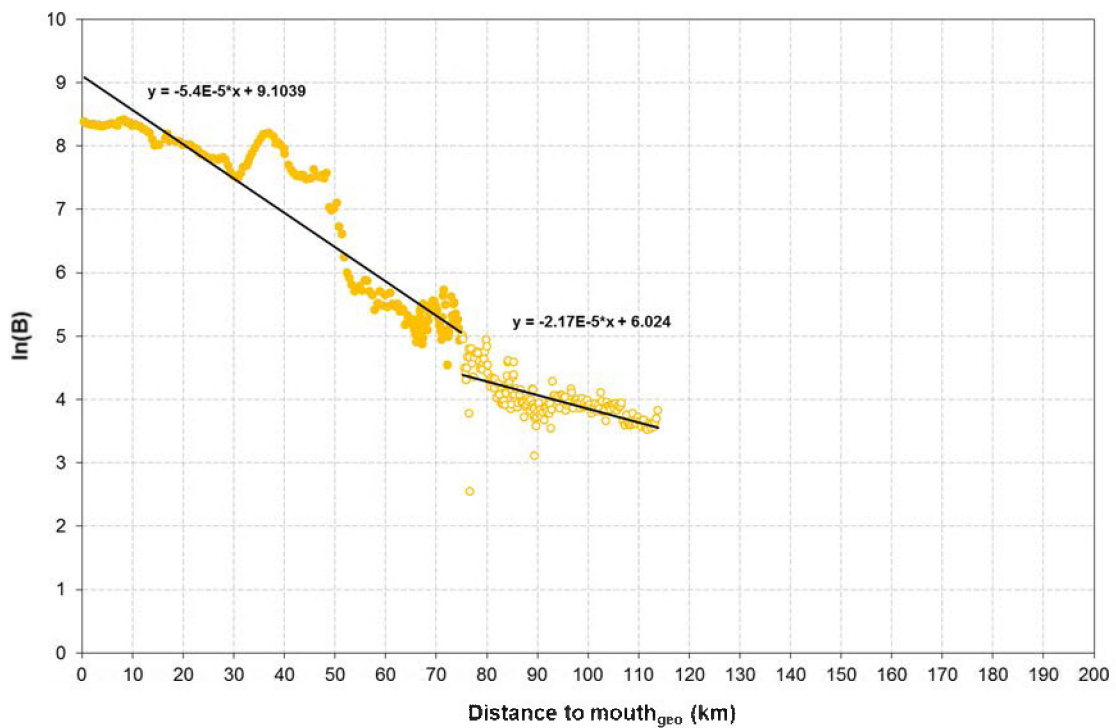


Figure A 4 – Convergence for the Humber-Ouse estuary. $1/b$ values are given in Table 4

Appendix B – Habitat maps

- Subtidal deep (Sd): > 5 m below MLWL
- Subtidal moderately deep (Sm): 5 – 2 m below MLWL
- Subtidal shallow (Ss): 2 m below MLWL – MLWL
- Intertidal flat (If): MLWL – MHWL; slope < 2.5%
- Intertidal steep (Is): MLWL – MHWL; slope > 2.5%
- Marsh (M): > MHWL

Figure B 1 – Legend for the habitat maps

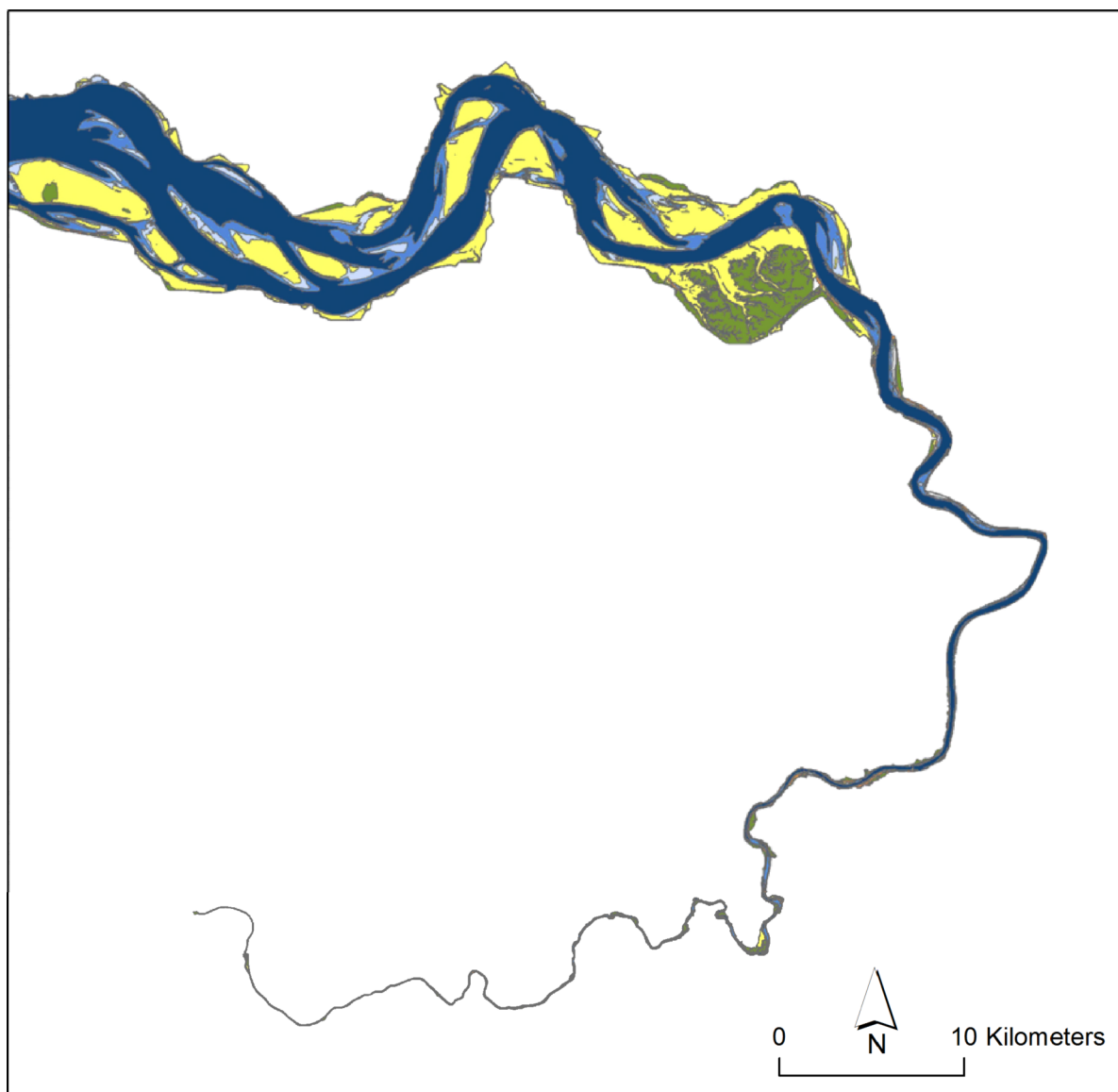


Figure B 2 - Habitat map for the Scheldt estuary (2007-2009, 20 x 20 m grid)

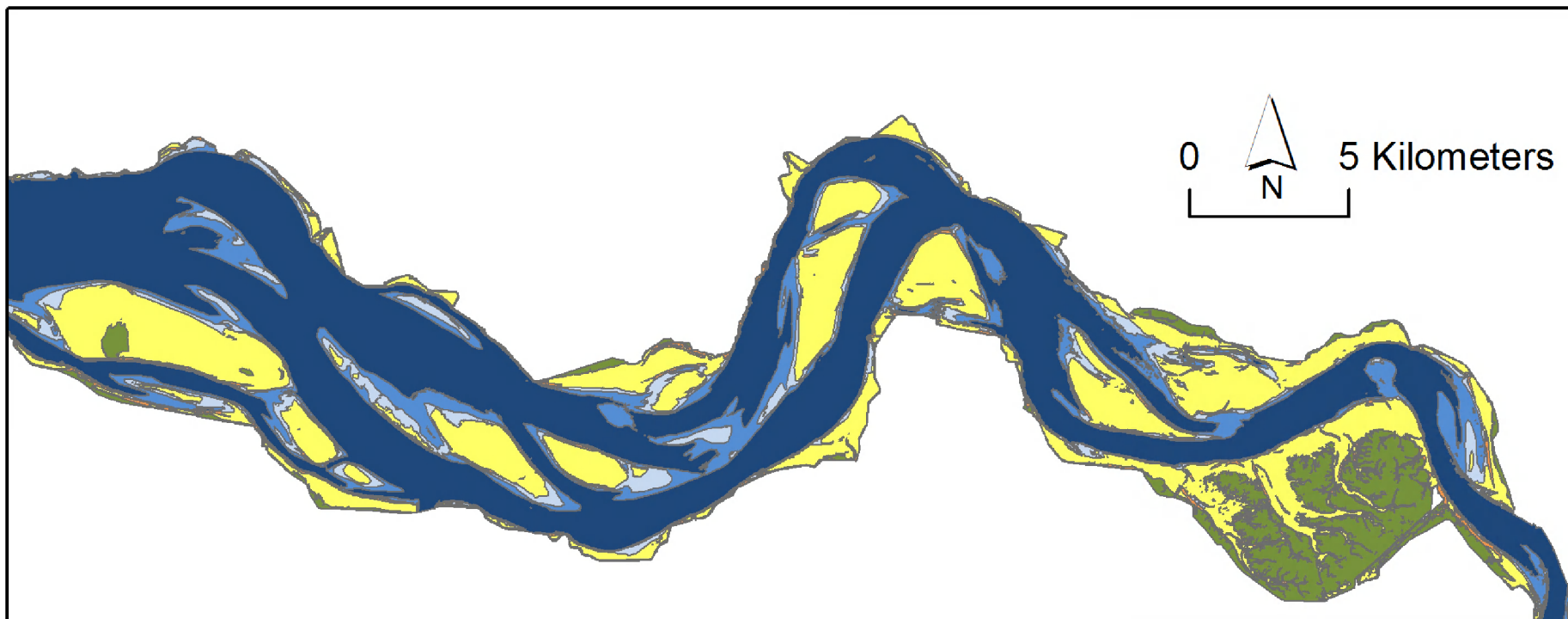


Figure B 3 – Habitat map for the WesterScheldt (2007-2009, 20 x 20 m grid)

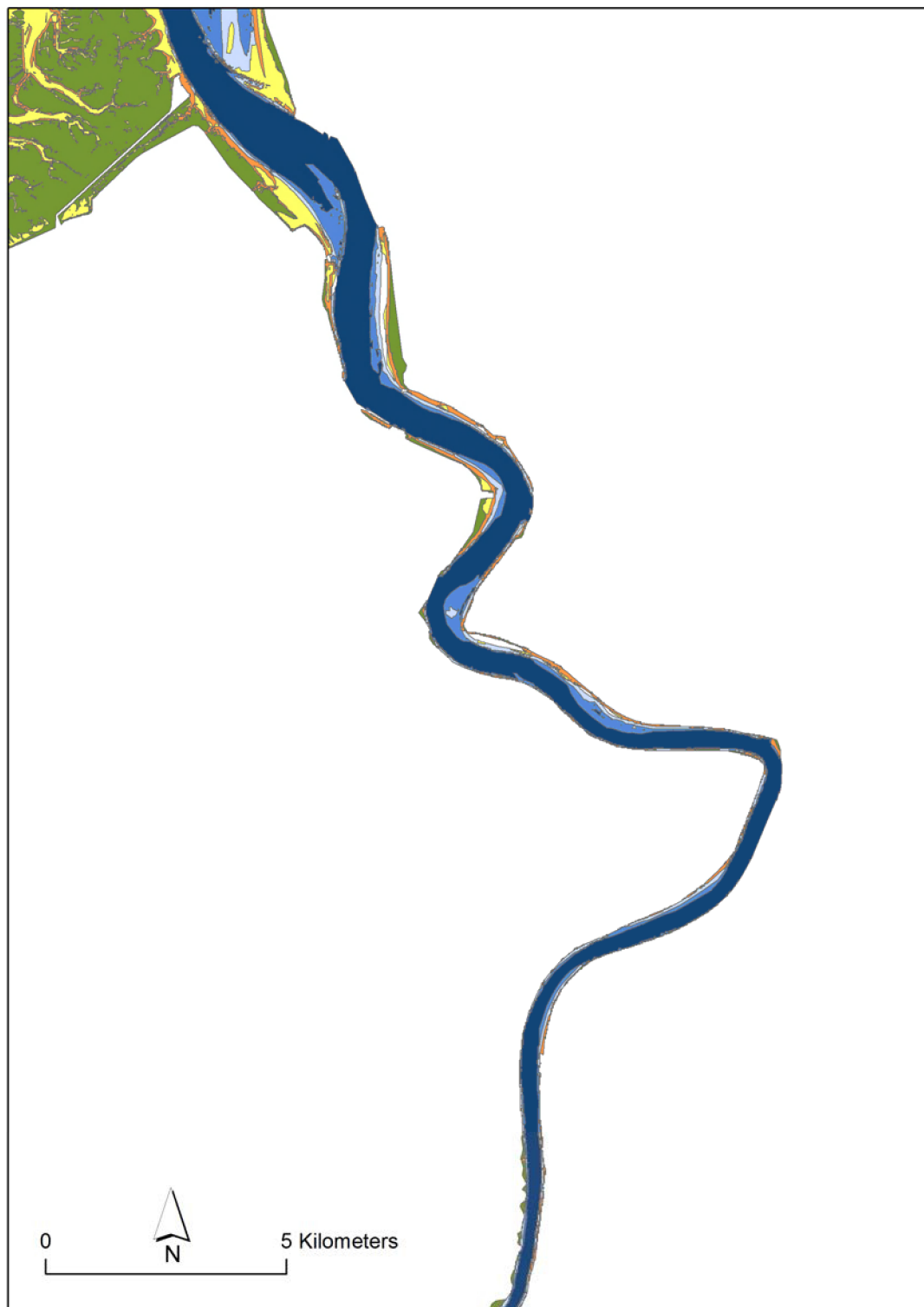


Figure B 4 – Habitat map for the Beneden ZeeScheldt (2007-2009, 20 x 20 m grid)

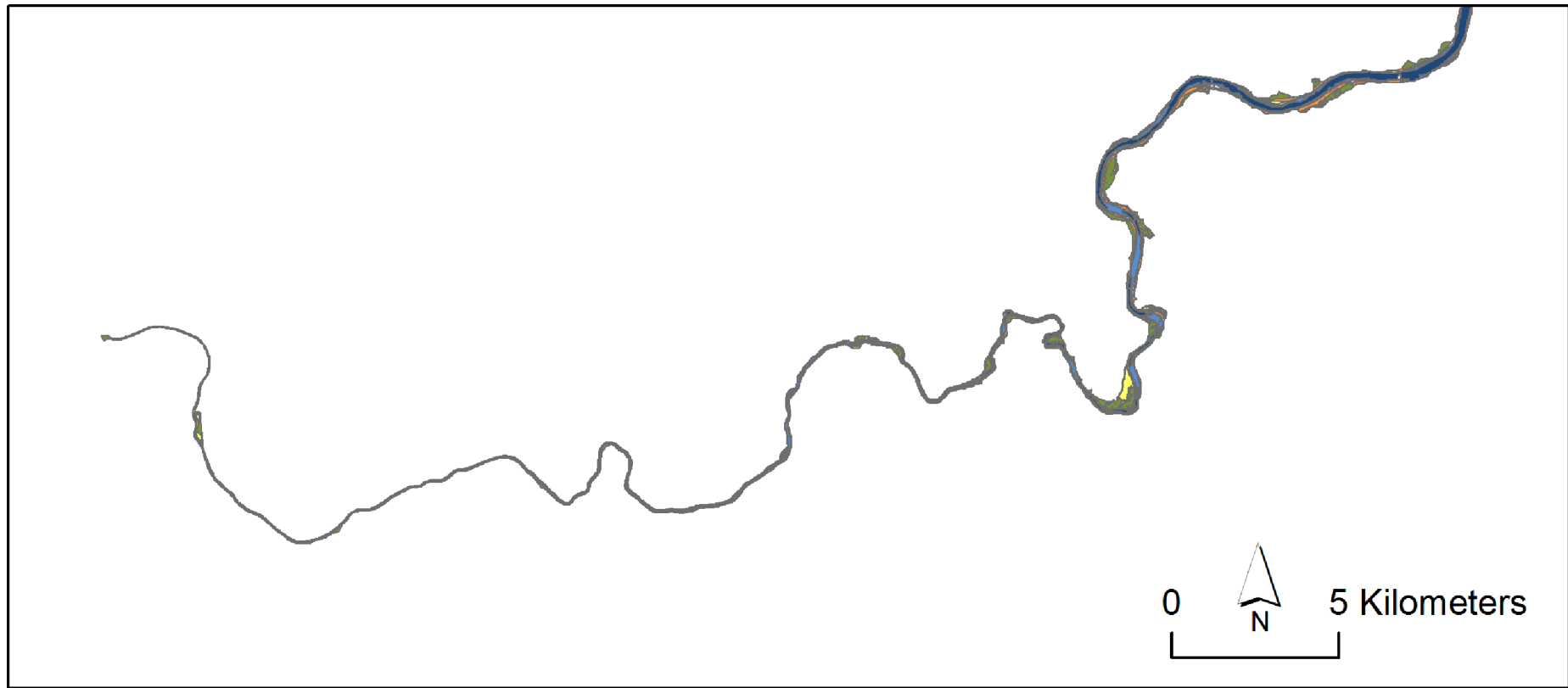


Figure B 5 – Habitat map for the Boven ZeeScheldt (2007-2009, 20 x 20 m grid)

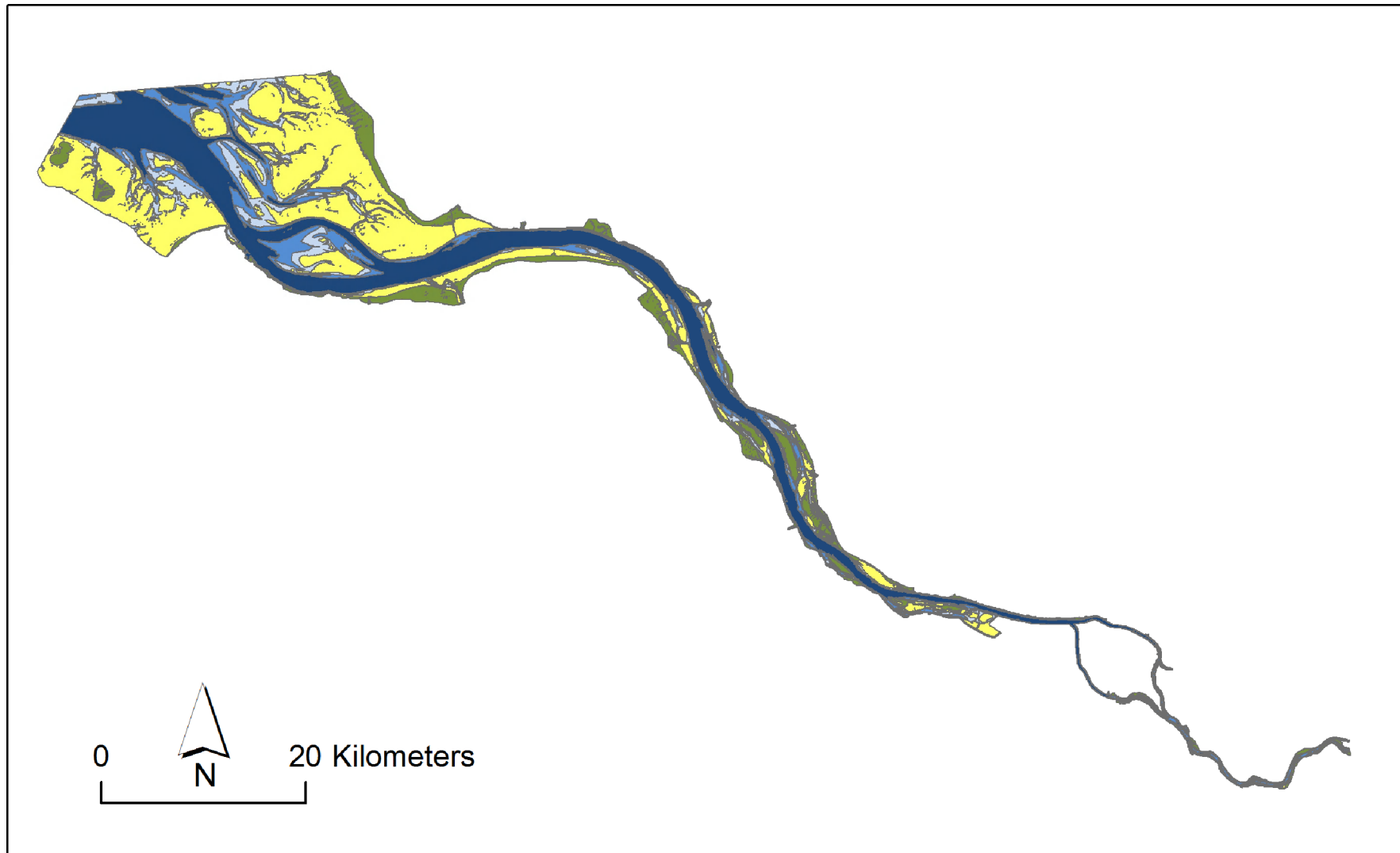


Figure B 6 – Habitat map for the Elbe estuary (2006, 10 x 10 m grid)

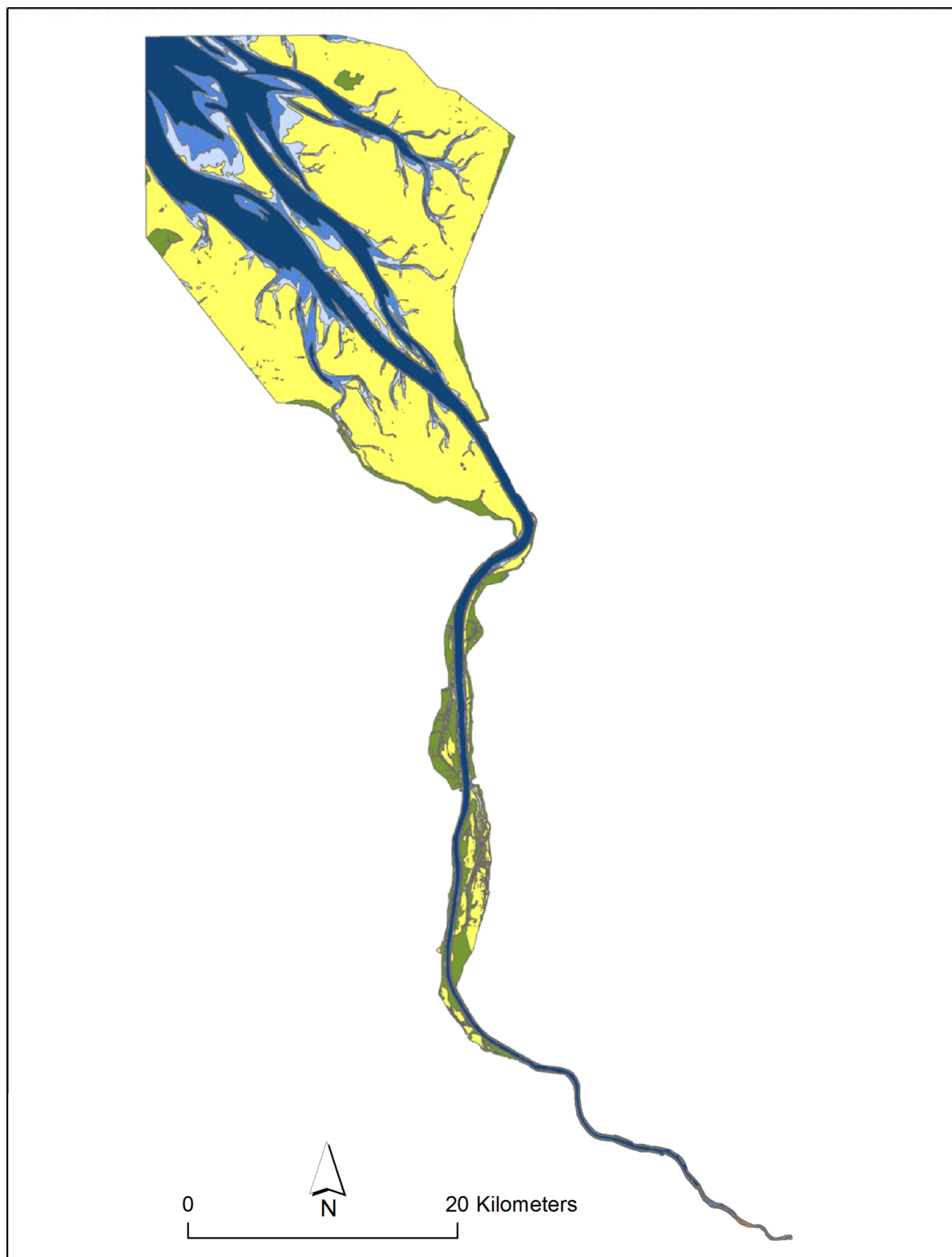


Figure B 7 – Habitat map for the Weser estuary (2009, 20 x 20 m grid)

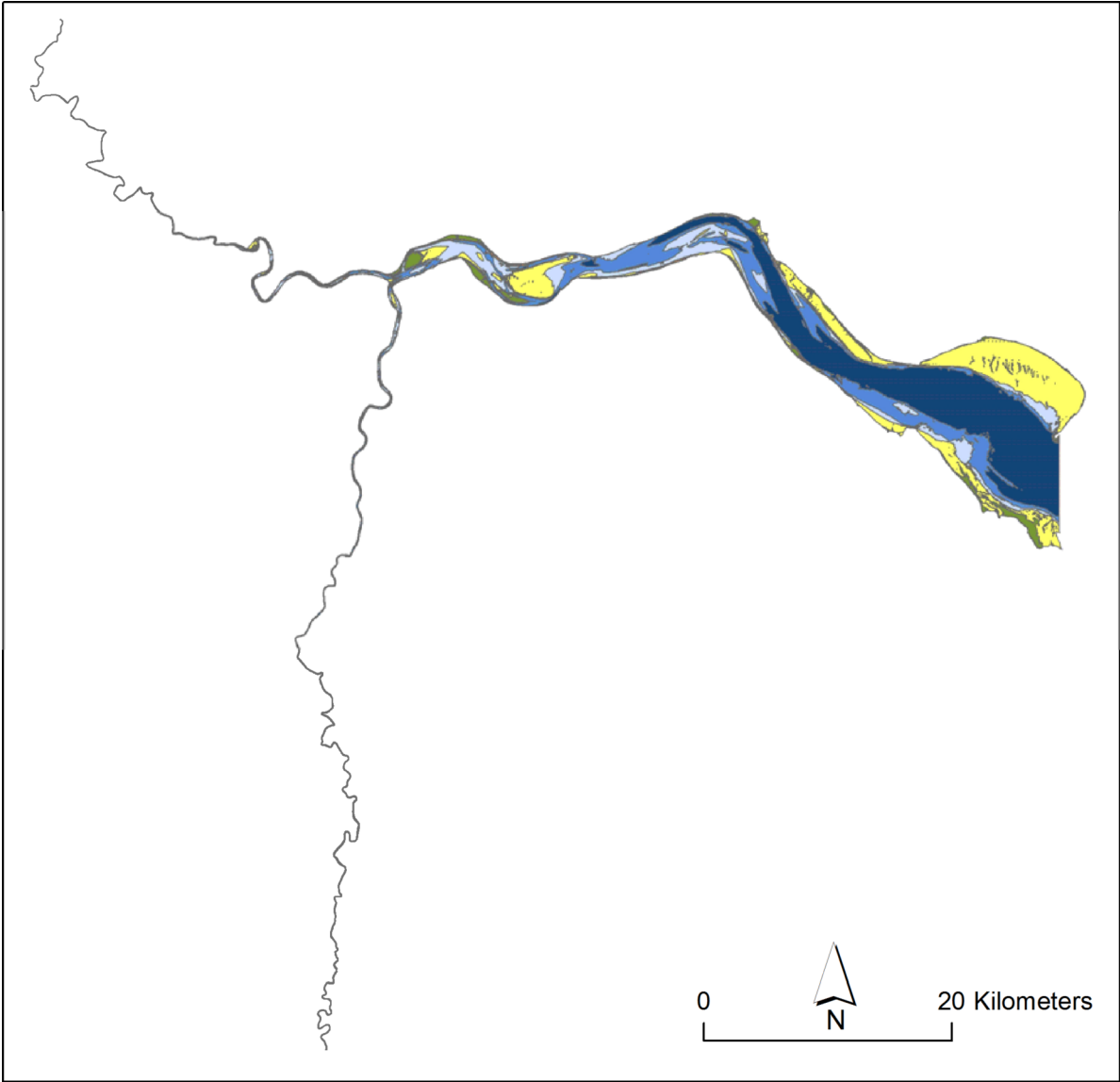


Figure B 8 – Habitat map for the Humber estuary (2005, 10 x 10 m grid)

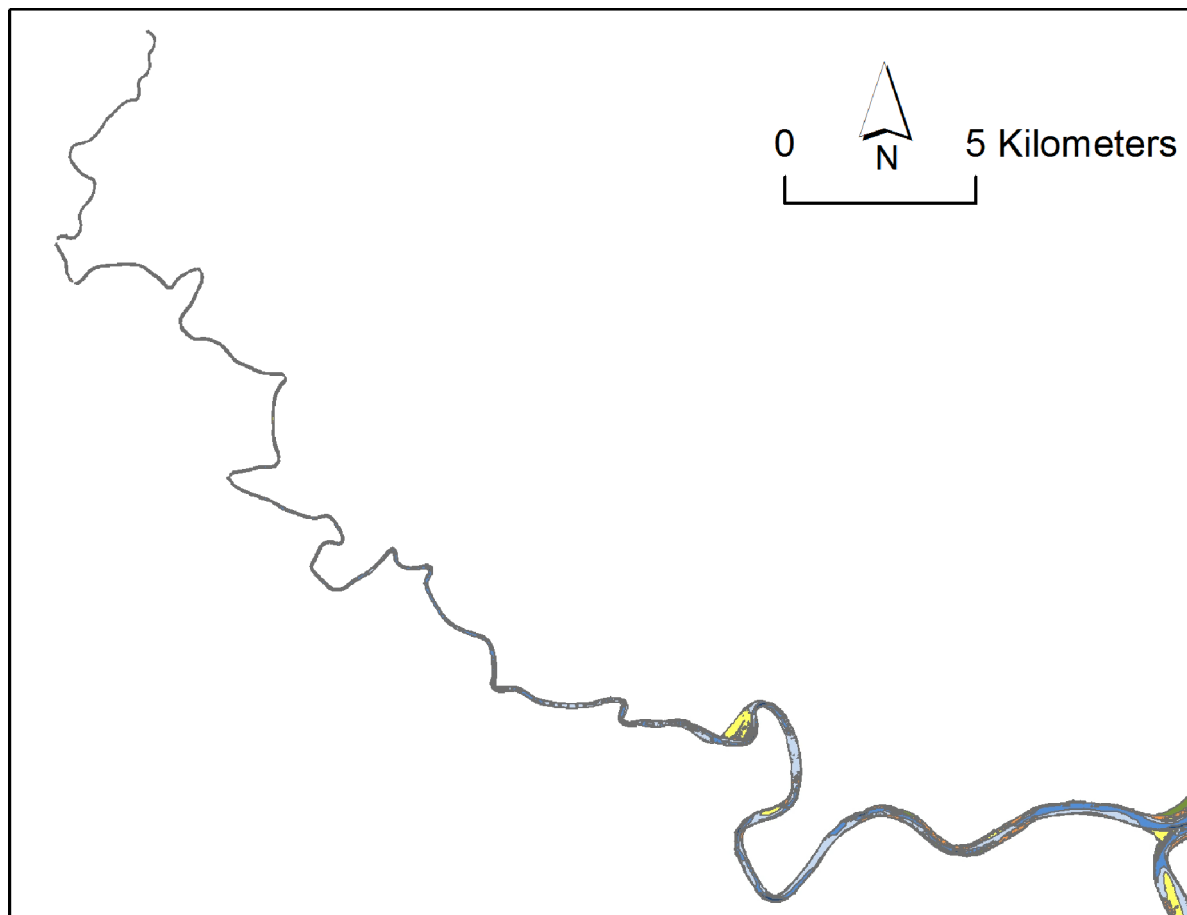


Figure B 9 – Habitat map for the Ouse (2005, 10 x 10 m grid)

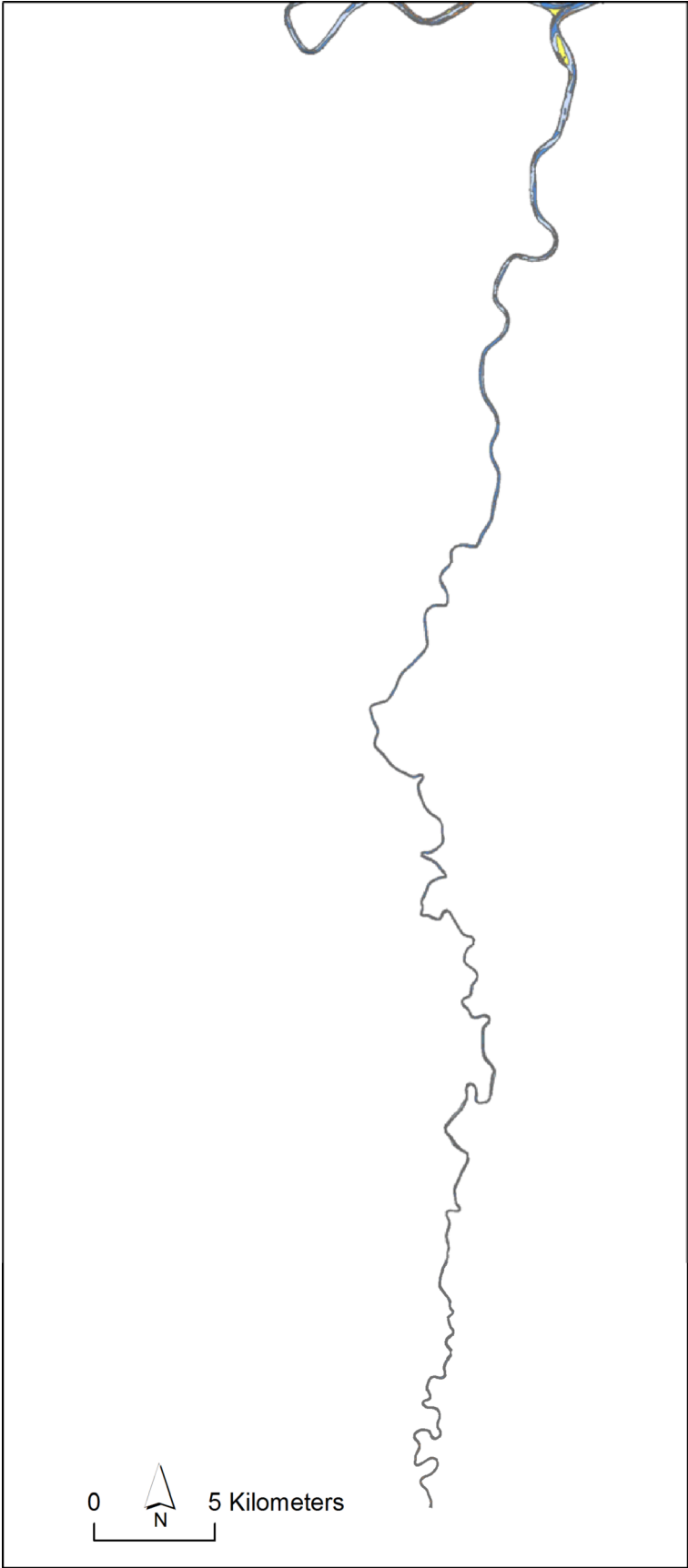


Figure B 10 – Habitat map for the Trent (2005, 10 x 10 m grid)

Appendix C – Habitat widths

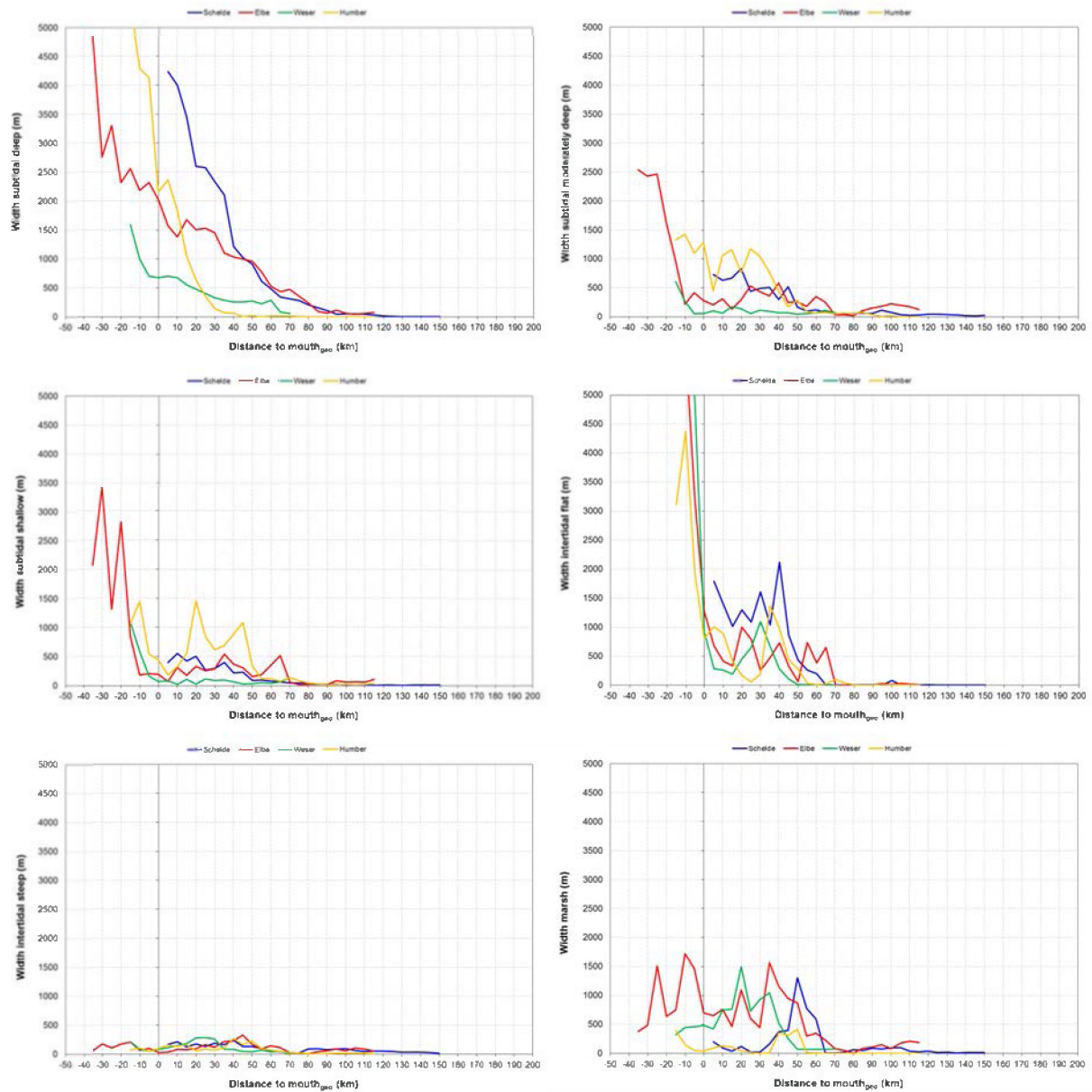


Figure C 1– Absolute width of each habitat compared for the 4 estuaries

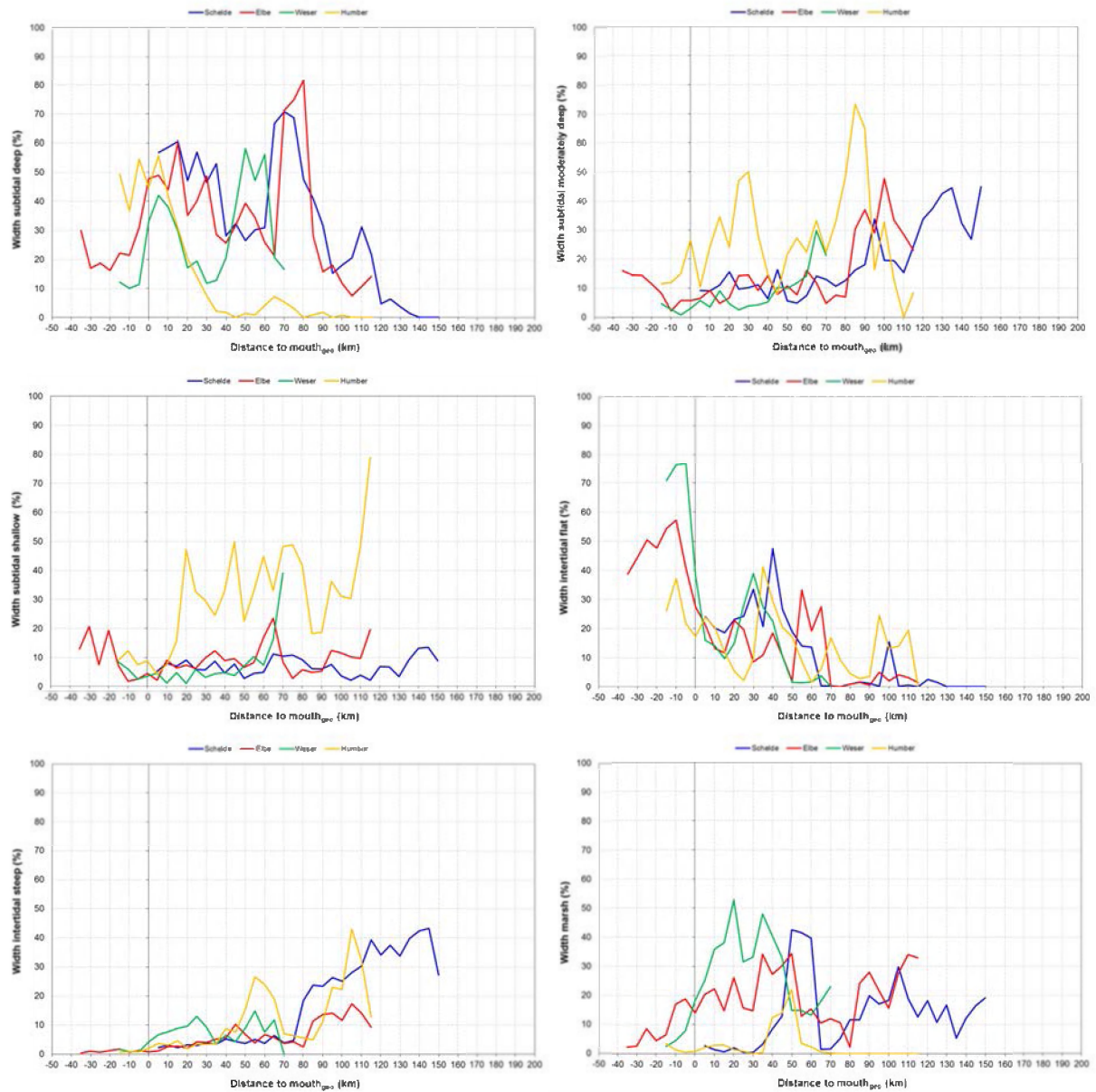


Figure C 2– Width of each habitat (in %) compared for the 4 estuaries

Appendix D – Tidal marsh sites

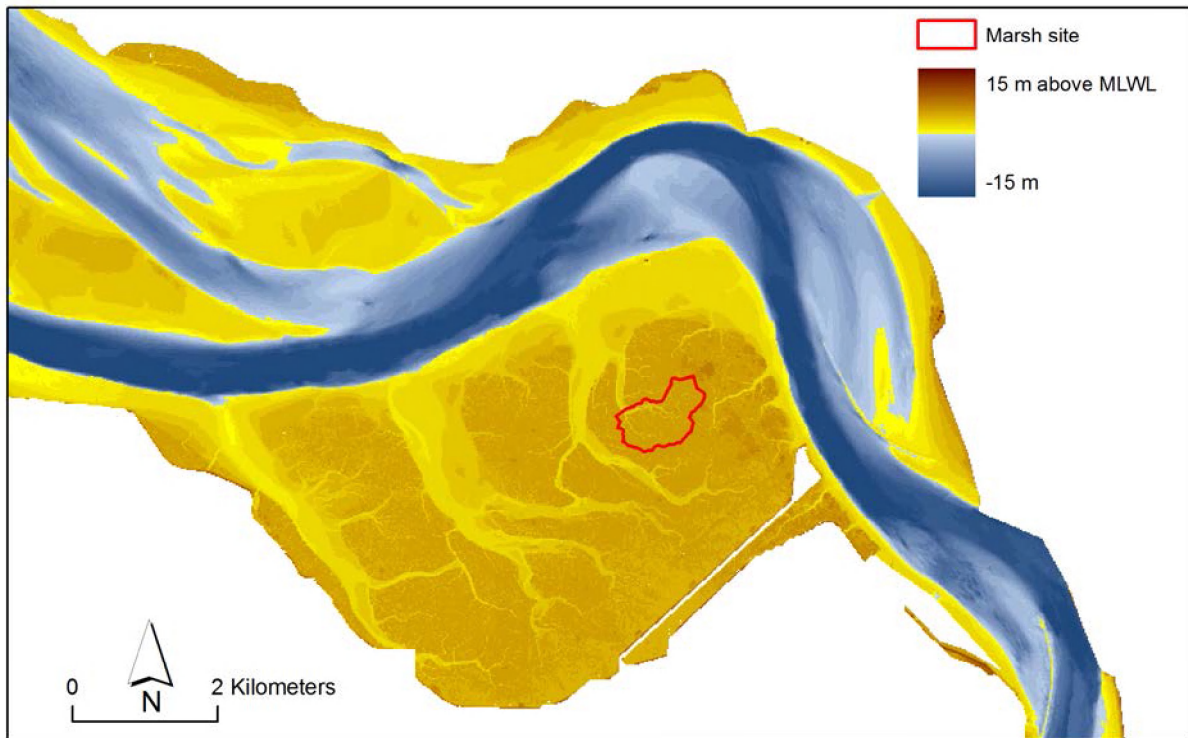


Figure D 1 – Analysed marsh site (Saeftinghe) plotted against the present topo-bathymetry (2001) of the Scheldt

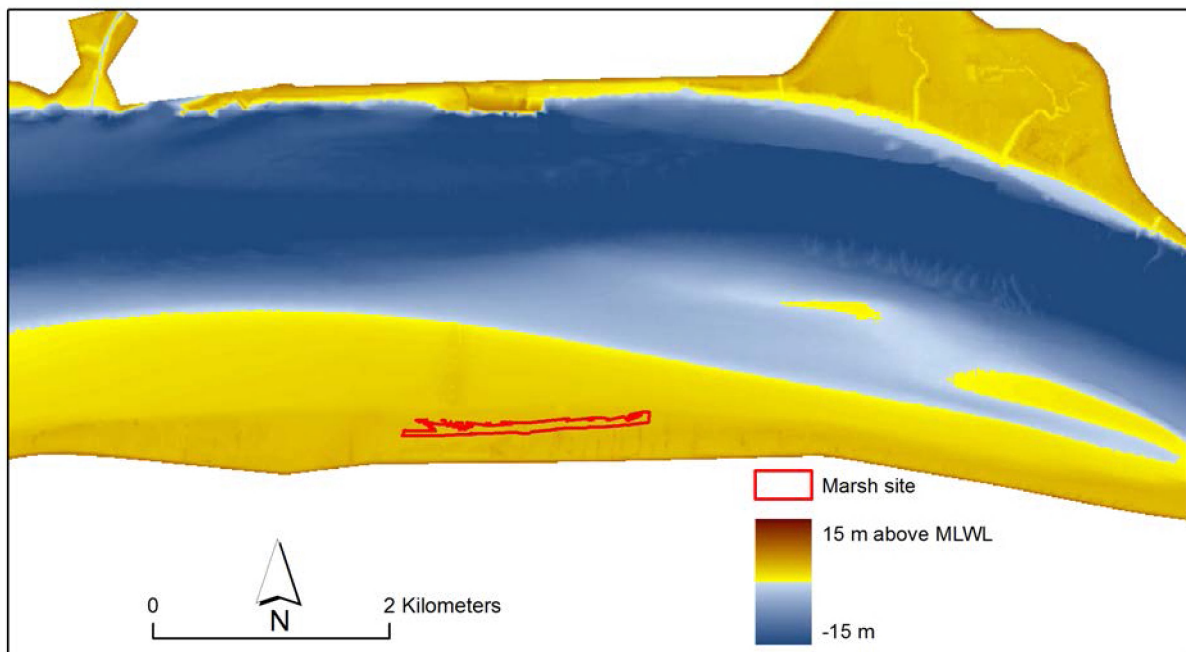


Figure D 2 – Analysed marsh site (Kehdingen area) plotted against the present topo-bathymetry (2006) of the Elbe



Waterbouwkundig Laboratorium

Flanders Hydraulics Research

B-2140 Antwerp

Tel. +32 (0)3 224 60 35

Fax +32 (0)3 224 60 36

E-mail: waterbouwkundiglabo@vlaanderen.be

www.watlab.be